AD_____

Award Number: DAMD17-03-1-0024

TITLE: Activation of Polymine Catabolism as a Novel Strategy for Treating and/or Preventing Human Prostate Cancer

PRINCIPLE INVESTIGATOR: Carl W. Porter, Ph.D.

CONTRACTING ORGANIZATION: Health Research, Incorporated
Buffalo, NY 14263

REPORT DATE: March 2006

TYPE OF REPORT: Final

PREPARED FOR: U.S. Army Medical Research and Materiel Command
Fort Detrick, Maryland 21702-5012

REPORT DOCUMENTATION PAGE

Form Approved
OMB No. 0704-0188

1. REPORT DATE	2. REPORT TYPE	3. DATES COVERED
01-03-2006	Final	1 Mar 2003 – 28 Feb 2006

4. TITLE AND SUBTITLE

Activation of Polymine Catabolism as a Novel Strategy for Treating and/or Preventing Human Prostate Cancer

5a. CONTRACT NUMBER

5b. GRANT NUMBER
DAMD17-03-1-0024

5c. PROGRAM ELEMENT NUMBER

6. AUTHOR(S)

Carl W. Porter, Ph.D.

5d. PROJECT NUMBER

5e. TASK NUMBER

5f. WORK UNIT NUMBER

7. PERFORMING ORGANIZATION NAME(S) AND ADDRESS(ES)

Health Research, Incorporated
Buffalo, NY 14263

8. PERFORMING ORGANIZATION REPORT NUMBER

9. SPONSORING / MONITORING AGENCY NAME(S) AND ADDRESS(ES)
U.S. Army Medical Research and Materiel Command
Fort Detrick, Maryland 21702-5012

10. SPONSOR/MONITOR'S ACRONYM(S)

11. SPONSOR/MONITOR'S REPORT NUMBER(S)

12. DISTRIBUTION / AVAILABILITY STATEMENT
Approved for Public Release; Distribution Unlimited

13. SUPPLEMENTARY NOTES
Original contains colored plates: ALL DTIC reproductions will be in black and white.

14. ABSTRACT

We proposed that activation of polyamine catabolism as opposed to inhibition of polyamine biosynthesis will have a therapeutic effect against prostate carcinoma. Thus, we found that (a) conditional overexpression of the polyamine catabolic enzyme spermidine /spermine N1-acetyltransferase (SSAT) causes growth inhibition in LNCaP prostate carcinoma cells via a unique mechanism and (b) transgenic overexpression of SSAT in TRAMP mice markedly suppresses prostate tumor development. Both effects were found to occur via SSAT mediated metabolic flux through the polyamine pathway leading to depletion of the critical SSAT cofactor acetyl-CoA and interference with fat metabolism. Genetic deletion of SSAT had no effect on tumor development in the TRAMP mouse while heterozygous expression of the polyamine biosynthetic enzyme ornithine decarboxylase unexpectedly enhanced tumor growth while reducing tumor invasion into the seminal vesicles. Taken together, the findings suggest that a specific small molecule inducer of SSAT will suppress the development of prostate cancer.

15. SUBJECT TERMS
Prostate Cancer

16. SECURITY CLASSIFICATION OF:				18. NUMBER OF PAGES	19a. NAME OF RESPONSIBLE PERSON
a. REPORT	b. ABSTRACT	c. THIS PAGE			USAMRMC
U	U	U	UU	59	19b. TELEPHONE NUMBER *(include area code)*

Standard Form 298 (Rev. 8-98)
Prescribed by ANSI Std. Z39.18

Table of Contents

Cover……1

SF 298……2

Introduction……4

Body……4

Key Research Accomplishments……9

Reportable Outcomes……10

Conclusions……11

Salaried Personnel……11

References……12

Appendices……14

DAMD17-03-1-0024

I. REPORT BODY *(Tables & Figures located in Appendix 1)*

A. Introduction:

Polyamines are organic cations found in all cells and known to be essential for the initiation and maintenance of cell growth. As such, polyamine biosynthesis has been targeted as an anticancer strategy. The relationship of polyamines to the prostate is unique among all tissues since in addition to synthesizing these molecules for cell growth, the gland produces massive quantities for export into semen. It might, therefore, be expected that prostatic tumors could exhibit atypical polyamine-related regulatory responses (1). In recognition of the unique physiology of the prostate gland, Heston and collaborators proposed that targeting polyamine biosynthesis may be particularly effective against prostate cancer (2). Although most of these efforts have focused on inhibition of polyamine biosynthesis, we propose that activation of polyamine catabolism may have unique therapeutic potential against prostate carcinoma. The concept derives from our studies with polyamine analogs where, for example, we have shown that polyamine analogs such as N^1,N^{11}-diethylnorspermine (DENSPM) down-regulate polyamine biosynthesis at the level of ornithine decarboxylase (ODC) and S-adenosylmethionine decarboxylase (SAMDC) and at the same time, potently (i.e. >200-fold) up-regulate polyamine catabolism at the level of spermidine/spermine N^1-acetyltransferase (SSAT, 3). Several lines of evidence support the idea that analog induction of SSAT and hence, activation of polyamine catabolism, is critically responsible for DENSPM drug action (4-10). These various studies relate to SSAT induction in the context of analog treatment but they do not address what happens when SSAT is selectively induced in cells. In the absence of a specific SSAT inducer, this could only be evaluated using genetic systems such as conditional overexpression as a means to mimic small molecule induction of the enzyme. We have previously shown that conditional overexpression of SSAT leads to polyamine pool depletion and growth inhibition in MCF-7 breast carcinoma cells (11). On the basis of rationale suggesting that prostate carcinoma may be more sensitive to perturbations in polyamine homeostasis, we proposed in this project to investigate the metabolic and antiproliferative consequences of conditional SSAT overexpression in *in vitro* and transgenic overexpression in *in vivo* systems. *The bottom-line goal of these studies was to genetically validate the concept that small molecule induction of SSAT will be a useful anticancer strategy against prostate cancer and thus, worthy of small molecule discovery and development.* On the basis of findings obtained over the past 3 years as reviewed below, it now seems apparent that activation of polyamine catabolism, as opposed to inhibition of polyamine biosynthesis, represents a viable polyamine-directed anticancer strategy for prostate cancer. The findings also revealed a previously unknown metabolic relationship between polyamine metabolism and fat metabolism. In fact, it would appear that unique and unforeseen metabolic mechanisms initiated and sustained by SSAT account for the antitumor and antiproliferative effects enzyme over-expression.

B. *Originally Proposed Tasks*

Task 1. To evaluate the cellular and metabolic consequences of conditional SSAT over-expression in cultured LNCaP cells as a means to genetically validate the antiproliferative potential of this strategy .

Task 2. To determine the generality of cellular and metabolic consequences seen in Task 1 on representative prostate cancer cell lines in which SSAT has been adenovirally transduced.

Task 3. To confirm that responses to SSAT over-expression seen *in vitro* (as determined in Tasks 1 and 2) are translatable to antitumor activity using three novel *in vivo* approaches. These include (**a**) conditional regulation of SSAT in LNCaP tumors to evaluate therapeutic potential, (**b**) adenoviral based SSAT therapy of human prostate tumor xenografts to test therapeutic generality and (**c**) cross-breeding SSAT over-expressing transgenic mice (12) with prostate carcinoma prone (TRAMP, 13) mice to evaluate chemopreventive potential.

C. *Progress according to task:*

Task 1. *To evaluate the cellular and metabolic consequences of conditional SSAT over-expression in cultured LNCaP cells as a means to genetically validate the antiproliferative potential of this strategy .*

On the basis of findings with polyamine analogs, we hypothesized that activation of the polyamine catabolism at the level of SSAT will also inhibit cell growth and this Task set out to genetically validate that hypothesis in prostate cancer cells. Previously, this laboratory, did so in breast cancer cells where SSAT-induced polyamine pool depletion correlated nicely with growth inhibition (11). As noted above, the expectation was that prostate cancer cells would be more sensitive to such metabolic perturbations. To summarize this work, SSAT was conditionally over-expressed in LNCaP prostate carcinoma cells via a tetracycline-regulatable (Tet-off) system. Tetracycline removal resulted in a rapid ~10-fold increase in SSAT mRNA and a ~20-fold increase in enzyme activity. Consistent with this response, high levels of the SSAT products N^1-acetylspermidine, N^1-acetylspermine and N^1,N^{12}-diacetylspermine were found to accumulate both intracellularly and extracellularly. SSAT induction led to significant growth inhibition which in contrast to MCF-7 cells (11), was not accompanied by polyamine pool depletion. Rather, intracellular spermidine and spermine pools were elevated or maintained at control levels by a robust compensatory increase in biosynthesis at the levels of ODC and SAMDC activities. This, in turn, gave rise to a high rate of metabolic flux through both the biosynthetic and catabolic pathways—a new concept in polyamine biology (Figure 1). Interruption of that flux with α-difluoromethylornithine (DFMO), an inhibitor of ODC and well-known antiproliferative agent, unexpectedly prevented growth inhibition during Tet removal. As diagramed in our newly revised figure for metabolic flux, it appears that flux-induced growth inhibition may derive from excess product accumulation (i.e. acetylated polyamines) and/or to metabolite depletion such as a ~50% reduction in *S*-adenosylmethionine (SAM) pools or a ~50% decrease in the SSAT cofactor acetyl-CoA. In summary, the results demonstrate that activation of polyamine catabolism by conditional SSAT overexpression leads to: (a) altered polyamine pool homeostasis (b) a compensatory increase in polyamine biosynthesis, (c) heightened metabolic flux through both the biosynthetic and catabolic pathways, (d) depletion of metabolite pools such as the polyamine precursor SAM and the SSAT cofactor, acetyl-coenzyme A (acetyl-CoA) and (e) rapid and sustained growth inhibition. Whether these responses are unique to prostate derived tumor cells remains to be demonstrated. Overall, this important study shows that activation of polyamine catabolism gives rise to growth inhibition and thereby provides genetic validation of the idea that small molecule induction of SSAT may be effective as an anticancer strategy for treating prostate cancer. The above work is fully summarized in Kee *et al*., (14, Appendix).

Task 2. *To determine the generality of cellular and metabolic consequences seen in Task 1 on representative prostate cancer cell lines in which SSAT has been adenovirally transduced.*

As shown in Figure 2, we have successfully prepared and purified a SSAT expressing adenovirus in which human SSAT cDNA was cloned into a replication-deficient adenoviral system containing an internal ribosomal entry site (IRES) for GFP. Thus, both SSAT and GFP were under the control of a CMV promoter for maximum expression. The virus was prepared in human 293 cells which seemed to be immune to adverse effects on cell growth. The goal of these studies was to use the adenovirus to transduce SSAT into a number of prostate cancer cell lines and examine the effects on polyamine metabolism and cell growth. The expectation was that findings would be similar to those with LNCaP cells in Task 1, namely, that growth would be inhibited. An unexpected complication was that while the SSAT adenovirus could be used to transduce SSAT into 293 cells in the absence of toxicity, it could not be similarly used in transducing LNCaP or PC-3 cells which were cytotoxically affected. In these prostate carcinoma cells, the MOI for SSAT-bearing adenovirus was the same as that of the vector-bearing adenovirus. Northern blots indicated that SSAT was not effectively transduced presumably because it had aged for nearly one year after being purified. In view of these unforeseen difficulties and in consideration of the success of Task 3, we submitted in 2004 a shift of work (SOW) request in which we proposed to abandon Task 2 and focus on additional cross-breeding opportunities under Task 3. These include making use of genetically altered mice currently that are now under development in the Porter laboratory. *The SOW to do this work was approved and we are expanding our efforts in Task 3 to include genetic crosses with these new mice as they become available.* In the past cycle, we began crossing TRAMP mice with SSAT knock-out mice and ODC heterozygous mice (see Task 3).

Task 3. *To confirm that responses to SSAT over-expression seen in vitro (as determined in Tasks 1 and 2) are translatable to antitumor activity in vivo.*

As noted in Task 1, we have found that activation of polyamine catabolism via conditional overexpression of SSAT has antiproliferative consequences in LNCaP prostate carcinoma cells growing in culture (14). In this Task, we sought to examine the *in vivo* consequences of SSAT over-expression in a mouse model for prostate cancer termed TRAMP (TRansgenic Adenocarcinoma of the Mouse Prostate, 13). Although the overall effect was established relatively quickly, considerable effort was expended accumulating the ancillary data necessary for publication in the Journal of Biological Chemistry (15, see Appendix). This included quantitation of prostate and liver SSAT gene expression in mouse cohorts of the SSAT / TRAMP cross, confirming that the tumor suppressive effect of SSAT extended beyond 30 wks, investigating the effects of SSAT-induced metabolic flux on acetyl-CoA and S-adenosylmethionine pools, and documenting the loss of abdominal and subdermal fat in SSAT transgenic mice as support for the effects of metabolic flux on acetyl-CoA pools. The overall effect can be summarized as follows. TRAMP female C57BL/6 mice that express the SV40 early genes (T/t antigens) under an androgen-driven probasin promoter (12) were cross-bred with male C57BL/6 transgenic mice that systemically over-express SSAT (13). Experiments were staged by small animal nuclear magnetic resonance image (MRI) tracking of tumor appearance and growth (i.e. Fig. 5). At 30 wks of age (Fig. 3), the average genitourinary tract weights for TRAMP mice were 1,417 ± 181 mg compared to 344 ± 52 mg for TRAMP/SSAT mice. Thus, transgenic overexpression of SSAT suppressed outgrowth of prostate tumors. Since this could represent a delay in tumor development, we examined the effects at a later age. By 36 wk, the average TRAMP genitourinary tract increased by ~2-fold relative to the 30 wk data while those of TRAMP/SSAT actually decreased by 33% as

opposed to growing larger (Fig. 3). Since the differential effect increased between groups, we conclude that the tumor suppressive effect was not temporary but rather progressive. Immunohistochemistry revealed that SV40 large T-antigen expression in the prostate epithelium was similar in TRAMP versus TRAMP/SSAT mice indicating that the driving oncogene was intact and unaffected. Consistent with the 18-fold increase in SSAT activity in the TRAMP/SSAT transgenics, intracellular N^1-acetylspermidine and putrescine pools were markedly increased (i.e. 35-fold and 16-fold, respectively) relative to the TRAMP mice while spermidine and spermine pools were largely unaffected due to a compensatory 5- to 7-fold increase in the biosynthetic enzyme activities of ODC and SAMDC. The latter led to heightened metabolic flux through the polyamine pathway and an associated ~70% reduction in the SSAT cofactor acetyl-CoA and a ~40% reduction in the polyamine aminopropyl donor S-adenosylmethionine in TRAMP/SSAT compared to TRAMP prostatic tissue (Fig. 4). In addition to elucidating the antiproliferative and metabolic consequences of SSAT overexpression in a prostate cancer model, these findings provide genetic support for the discovery and development of specific small molecule inducers of SSAT as a novel therapeutic strategy targeting prostate cancer. This work is summarized in the J. Biological Chemistry publication by Kee *et al*. (15, see Appendix). On the basis of the above findings, Dr. Porter was recently awarded a NCI RAND grant to search by high throughput screening of the NCI compound library for specific small molecule inducers of SSAT as an anticancer agent leads. Given the fact that transgenic overexpression of SSAT affected normal prostates of mice as well as neoplastic prostates, such compounds may find usefulness in treating prostatic hyperplasia.

In addition to the antitumor implications, the findings of Task 1 and 3 provide the first definitive linkage between polyamine catabolism and fat metabolism via the SSAT coenzyme acetyl-CoA. The finding is strongly supported by the observations that SSAT-transgenic mice lack fat (Fig. 5) and a significant proportion (i.e. ~33%) of SSAT-knock-out mice accumulate fat (see Fig 6). The latter finding has important implications for a possible role of SSAT in fat homeostasis, *a lead that is being explored under separate funding mechanisms*. At a minimum, it is consistent with recent strategies by other groups to use interference with fat biosynthesis [i.e. fatty acid synthase (FAS) inhibitors] as an anticancer approach to prostate cancer (16).

To compliment the above findings, we initiated studies in which SSAT-null mice were crossed with TRAMP mice (17) and observed that null expression of the enzyme had no effect on prostate tumor growth (Fig. 6). Preliminary biochemical analysis of various tissues including prostate and prostate tumors mice failed to show any major perturbations of polyamine metabolism (data not shown). Taken together, the findings are consistent with the SSAT transgenic studies and further, imply that there is no therapeutic merit for SSAT-inhibition as an anticancer strategy in prostate. While waiting for additional genetically altered mice to be developed (see below), we have also examined the effects of ODC heterozygosity on tumorigenesis in the TRAMP mouse since a decrease in biosynthesis might mimic an increase in catabolism via SSAT (18). These are relatively difficult crosses but on the basis of animals obtained thus far, it appears that ODC haploinsufficiency actually enhances prostate tumorigenesis in the TRAMP mouse (Fig. 8). Further, the tumors tend to be more restricted to the prostate gland and they do not move out into the seminal vesicles as is typical of tumors in the C57 Bl/6 TRAMP background. Preliminary biochemical findings on various tissues including prostate tumors from TRAMP and TRAMP/ODC$^{+/-}$ show no major perturbations in polyamine metabolism despite a reduction in ODC gene dose (data not shown). The promoting effect of ODC heterozygosity on tumorigenesis is highly unexpected based on the known role of this enzyme in carcinogenesis and

tumor growth and the finding may reflect something unique about the context of prostate cells and tissue. Accumulation of significant numbers of TRAMP/ODC$^{+/-}$ mice is time consuming but will be continued over the next year in the absence of DOD funding since we believe that this is an important and somewhat unexpected finding.

Based on our success with SSAT and consistent with our earlier SOW for Task 2, projected plan was to cross-breed TRAMP mice with mice having altered expression of other polyamine catabolic enzymes (19-20). Our laboratory was first to report on the genomic identification and biochemical characterization of two such enzymes, polyamine oxidase (PAO) and a previously unknown enzyme, spermine oxidase (SMO; 19). Originating such mice was not proposed under the original grant but it represents a natural progression to the SSAT findings. Thus, we have attempted to derive a SMO knock-out mouse over the past year without success; none of 280 microinjected embryonic stem cell clones screened gave enzyme of enzyme deletion. This effort is continuing with a new construct targeting a different region of the SMO gene. A SMO knock-out mouse will then be used to extend studies in Task 3 as described in the SOW for Task 2; namely to cross the TRAMP mice with a SMO knock-out mouse with the expectation that it will suppress tumorigenesis since SMO has the potential to be a major source of H_20_2 production and hence of genetic instability. We have also attempted to derive a PAO transgenic mouse for similar purposes. Offspring from the transgenic PAO founder mice have been analyzed and found to selectively over-express the enzyme protein in the muscle and kidney which is of no use for our prostate cancer studies.

Lastly, we have also undertaken to determine whether the antitumor effect of activated polyamine catabolism as seen in the TRAMP mouse model can be applied to other tumor types. Stated otherwise, we sought to determine if the tumor suppression seen in the TRAMP mouse was unique to prostate cancer or whether it could be generalized to other tumor models. Thus, we have begun a collaboration with Dr. Frank Berger (University of South Carolina) studying the *APC^{min}* mice which are genetically predisposed to develop intestinal tumors. Since the animal studies were performed by Dr. Berger, we did not feel that an extension of animal work was necessary. The study can be summarized as follows. The effects of differential SSAT expression on intestinal tumorigenesis was investigated in the Apc$^{Min/+}$ (MIN) mouse. When MIN mice were crossed with SSAT-overproducing transgenic mice, they developed 3- and 6-fold more adenomas in the small intestine and colon, respectively, than normal MIN mice. Despite accumulation of the SSAT product N^1-acetylspermidine, spermidine and spermine pools were only slightly decreased due to a huge compensatory increase in polyamine biosynthetic enzyme activities that gave rise to enhanced metabolic flux. When MIN mice were crossed with SSAT knock-out mice, they developed 75% fewer adenomas in the small intestine suggesting that under basal conditions, SSAT contributes significantly to the MIN phenotype. Despite the loss in catabolic capability, tumor spermidine and spermine pools failed to increase significantly due to a compensatory decrease in biosynthetic enzyme activity giving rise to a reduced metabolic flux. Loss of heterozygosity (LOH) at the *Apc* locus was observed in tumors from both SSAT-transgenic and -deficient MIN mice, indicating that LOH remained the predominant oncogenic mechanism. In similarity to our conclusions in the TRAMP mouse for prostate cancer, we propose a model in which SSAT expression alters flux through the polyamine pathway giving rise to metabolic events that promote tumorigenesis. The difference relative to the findings in the prostate suggests that tissue and metabolic contexts may play a major role in determining the nature of the tumor response to activated polyamine catabolism. It also raises considerations relating to the therapeutic potential of this approach. At a minimum, however, these findings strongly implicate

an important if not differential role for SSAT in tumorigenesis. The findings of that study were recently published in Cancer Research by Tucker *et al*., (21, see Appendix; note that Dr. Porter was the corresponding author for this manuscript).

D. Unscheduled Findings.

Findings under Tasks 1 and 3 provided genetic evidence for the discovery and development of small molecule inducers of SSAT as potential anticancer agents. Although this process has not yet begun, we have hit upon a relevant lead involving a widely used anticancer agent (14). The finding could have important implications in understanding drug action and in designing new anticancer drug combinations. The lead derives from an Affymetrix Oligonucleotide array analysis of >10,000 genes of A2780 ovarian carcinoma cells exposed to oxaliplatin or cisplatin. Unexpectedly, SSAT was among the top 20 up-regulated genes. We went on to confirm by Northern blot that SSAT gene expression increased in a dose-dependent manner, with oxaliplatin being twice as effective as cisplatin. The 15-fold increase in oxaliplatin-induced SSAT mRNA was accompanied by only a 2-fold increase in enzyme activity. In cells treated 2 h with oxaliplatin and then exposed for 24 h to the polyamine analogue, N^1,N^{11}-diethylnorspermine (DENSPM), a synergistic >200-fold increase in SSAT activity was observed together with markedly reduced polyamine pools. Cytotoxicity analysis of oxaliplatin treatment followed by low dose DENSPM suggests a distinctly greater than additive drug interaction. Although these studies were conducted under conditions selected for microarray analysis (i.e. short exposures/high dose) we have since deployed oxaliplatin at pharmacologically attainable (i.e. 5 μM for 20 h) and found an even greater increase in SSAT mRNA which during cotreatment with DENSPM, increased synergistically to even greater SSAT levels than described above. These results reveal a mechanistic synergy whereby oxaliplatin potently induces SSAT mRNA and DENSPM facilitates its translation to enzymatically active protein. These findings are described in detail in Molecular Cancer Therapeutics article by Hector *et al.*, (22, see Appendix) and subsequently used to obtain NCI funding with Dr. L. Pendyala which began in 2005. With appropriate *in vitro* and *in vivo* optimization, these findings could lead to an effective therapeutic strategy. While oxaliplatin is not usually used in treating prostatic cancer, there have been some reports that it is quite active against this disease.

II. KEY RESEARCH ACCOMPLISHMENTS:

- Conditional expression of SSAT in LNCaP prostate carcinoma cells leads to disturbances in polyamine homeostasis and a compensatory increase in metabolic flux through both the biosynthetic and export arms of the polyamine pathway. Inhibition of ODC prevents growth inhibition, and thereby validates a causal linkage between flux and growth inhibition. The role of flux in growth inhibition is a novel concept that differs from the original expectation that growth inhibition would be due to SSAT-induced polyamine pool depletion. Published in Kee *et al.*, (2004a, Appendix).

- We showed for the first time that overexpression of SSAT impacts on other aspects of cellular metabolism including SAM pools and acetyl-CoA pools. The former may affect methylation and the latter can affect such processes as fatty acid synthesis, intermediate metabolism and histone acetylation. On the basis of *in vivo* studies with SSAT-altered mice

it now appears that reduction in acetyl-CoA pools is a major contributor to cell growth inhibition. Published in Kee *et al*., (2004a, 2004b, Appendix).

- Cross-breeding SSAT transgenic mice with TRAMP mice that are genetically predisposed to prostate cancer, markedly suppresses tumor development and this effect correlates closely with very signficant reductions in prostatic acetylCoA pools. The extent of the antitumor effect is greater than seen with any previously reported cross-breeding of TRAMP mice and the linkage between SSAT and acetyl-CoA (i.e. fat metabolism) is entirely novel. This also leads to the possible linkage between SSAT and regulation of fat accumulation (i.e. obesity). Published in Kee et al., (2004b, Appendix).

- Taken together, the data provide *in vitro* and *in vivo* genetic validation of the concept that pharmacological induction of SSAT could represent an effective therapeutic strategy for prostate cancer. Recent recognition that oxaliplatin and cisplatin drugs potently induce SSAT may be relevant to this idea as well. The latter is published in Hector *et al*., (2004, Appendix).

- We are now able to detect and quantitate acetyl-CoA as well as malonyl-CoA (a major regulator of fat oxidation) by capillary electrophoresis, which will be used to study the downstream consequences of SSAT-induced metabolic flux (unpublished) and how it relates to growth inhibition in the LNCaP cell system. We were the first to assay acetyl-CoA and malonyl-CoA in this manner. Published in Kee *et al*., (2004a, Appendix).
- Cross-breeding of TRAMP mice with SSAT null mice appears to have minimal effect on prostate tumorigenesis while cross-breeding to achieve ODC heterozygosity appears to promote TRAMP tumorigenesis (unpublished finding).
- In collaborative studies with Dr. Frank Berger, we found that cross-breeding of SSAT transgenic mice with APC^{min} mice promotes intestinal tumorigenesis which is opposite to the effect seen in the TRAMP model. Interestingly crossing the SSAT-knock out mice had the opposite effect, increasing intestinal tumorigenesis. The findings demonstrate the apparent importance of genetic and/or metabolic context in determining the outcome of SSAT-induced metabolic flux. The findings also reinforce the importance of the SSAT gene in tumor biology. Published in Tucker *et al*., (2005, Appendix).

III. REPORTABLE OUTCOMES: (Reprints of articles attached in Appendix)

- Kee, K., Vujcic, S., Kisiel, N., Diegelman, P., Kramer, D.L., and Porter, C.W. Activation of polyamine catabolism as a novel strategy for treating and/or preventing prostate cancer. Proc. Am Assoc. Cancer Res. 44:1277, 2003.
- Hector, S., Porter, C.W., Kramer, D.L., Clark, K., Pendyala, Activation of polyamine catabolism by oxaliplatin in A2780 ovarian carcinoma cells. Activation of polyamine catabolism by oxaliplatin in A2780 ovarian carcinoma cells. Proc AACR, 2004.
- Kee, K., Vujcic, S., Merali, S., Diegelman, P., Kisiel, N., Powell, C.T., Kramer, D.L. and Porter, C.W. Metabolic and antiproliferative consequences of activated polyamine catabolism in LNCaP prostate carcinoma cells. J. Biol. Chem. 279:27050-27058, 2004.

- Kee, K., Foster, B.A., Merali, S., Vujcic, S., Mazurchuk, R., Hensen, M.L., Diegelman, P., Kisiel, N., Kramer, D.L., and Porter, C.W. Activated polyamine catabolism depletes acetyl-CoA and suppresses prostate tumor growth in the TRAMP mouse. J. Biol. Chem. 279:40076-40083, 2004.
- Hector, S., Porter, C.W., Kramer, D.L., Clark, K. Chen, Y. and Pendyala, L. Polyamine catabolism in platinum drug action: Interactions between oxaliplatin and the polyamine analogue N^1, N^{11}-diethylnorspermine at the level of spermidine/spermine N^1-acetyltransferase. Molec. Cancer Therap. 3:813-822, 2004.
- Tucker JM, Murphy JT, Kisiel N, Diegelman P, Barbour KW, Davis C, Medda M, Alhonen L, Janne J, Kramer DL, Porter CW, Berger FG. Potent modulation of intestinal tumorigenesis in $Apc^{Min/+}$ mice by the polyamine catabolic enzyme spermidine/spermind N^1-acetyltransferase. Cancer Res. 65:5390-5398, 2005. *(CWP Corresponding Author)*

IV. CONCLUSIONS

We have genetically validated the hypothesis that activated polyamine catabolism at the level of SSAT has profound antitumor effects against prostate cancer at both the *in vitro* and *in vivo* levels. These finding provide genetic evidence for the concept that selective small molecule induction of SSAT may be effective in treating prostate hyperplasia and cancer. The findings further defines the downstream metabolic consequences of this strategy include marked reduction of acetyl-CoA pools in a manner that correlates very closely with suppression of tumor growth. This is the first recognition of a biological consequence deriving from altered flux through the polyamine pathway. Since this seems to occur selectively in both the normal and neoplastic prostate and since the phenotypic consequences of sustained transgenic overexpression of SSAT include only hair loss and female infertility, a small molecule induction of SSAT would appear to be selectively directed at prostate disease. Lastly, we have clearly shown that the *in vivo* antitumor responses to perturbations in SSAT activity are highly dependent on tissue and metabolic context with prostate tumors being suppressed by induction of SSAT and intestinal tumors being augmented by induction of SSAT. While clearly indicating the importance of SSAT in tumorigenesis, these findings provide cautionary guidance in the pharmacological use of an SSAT modulating agent.

V. PERSONNEL WHO RECEIVED SALARY.

Mary Hensen	Animal Technician
Jason Jell	Predoctoral Student
Kristin Kee	Predoctoral Student
Nicholas Kisiel	Biochemistry Technican
Lihui Ou	Predoctoral Student
Carl W. Porter, Ph.D.	Principal Investigator

VI. REFERENCES

1. Mi, Z., Kramer, D. L., Miller, J. T., Bergeron, R. J., Bernacki, R., and Porter, C. W. Human prostatic carcinoma cell lines display altered regulation of polyamine transport in response to polyamine analogs and inhibitors. Prostate, 34*:* 51-60, 1998.
2. Heston, W. D. Prostatic polyamines and polyamine targeting as a new approach to therapy of prostatic cancer. Cancer Surveys, 11*:* 217-238, 1991.
3. Porter, C. W., Regenass, U., and Bergeron, R. J. Polyamine inhibitors and analogs as potential anticancer agents. *In:* R. H. Dowling, U. R. Folsch, and C. Loser (eds.), Falk Symposium on Polyamines in the Gastrointestinal Tract, pp. 301-322. Dordrecht, Netherlands: Kluwer Academic Publishers Group, 1992.
4. Casero, R. A., Jr., Celano, P., Ervin, S. J., Porter, C. W., Bergeron, R. J., and Libby, P. R. Differential induction of spermidine/spermine N^1-acetyltransferase in human lung cancer cells by the bis(ethyl)polyamine analogues. Cancer Res, 49*:* 3829-3833, 1989.
5. Shappell, N. W., Miller, J. T., Bergeron, R. J., and Porter, C. W. Differential effects of the spermine analog, N^1,N^{12}-bis(ethyl)-spermine, on polyamine metabolism and cell growth in human melanoma cell lines and melanocytes. Anticancer Res, 12*:* 1083-1089, 1992.
6. Pegg, A. E., Wechter, R., Pakala, R., and Bergeron, R. J. Effect of N^1,N^{12}-bis(ethyl)spermine and related compounds on growth and polyamine acetylation, content, and excretion in human colon tumor cells. J Biol Chem, 264: 11744-11749, 1989.
7. Porter, C. W., Ganis, B., Libby, P. R., and Bergeron, R. J. Correlations between polyamine analogue-induced increases in spermidine/spermine N^1-acetyltransferase activity, polyamine pool depletion, and growth inhibition in human melanoma cell lines. Cancer Res, 51: 3715-3720, 1991.
8. McCloskey, D. E. and Pegg, A. E. Altered spermidine/spermine N^1-acetyltransferase activity as a mechanism of cellular resistance to bis(ethyl)polyamine analogues. J Biol Chem, 275: 28708-28714, 2000.
9. Chen, Y., Kramer, D. L., Li, F., and Porter, C. W. Loss of inhibitor of apoptosis proteins as a determinant of polyamine analog-induced apoptosis in human melanoma cells. Oncogene, 22: 4964-4972, 2003.
10. Chen, Y., Kramer, D. L., Jell, J., Vujcic, S., and Porter, C. W. Small interfering RNA suppression of polyamine analog-induced spermidine/spermine N^1-acetyltransferase. Mol Pharmacol, 64: 1153-1159, 2003.
11. Vujcic, S., Halmekyto, M., Diegelman, P., Gan, G., Kramer, D. L., Janne, J., and Porter, C. W. Effects of conditional overexpression of spermidine/spermine N^1-acetyltransferase on polyamine pool dynamics, cell growth, and sensitivity to polyamine analogs. J Biol Chem, 275: 38319-38328, 2000.
12. Pietilä, M., Alhonen, L., Halmekytö, M., Kanter, P., Jänne, J. and Porter, C.W., Activation of polyamine catabolism profoundly alters tissue polyamine pools and affects hair growth and female fertility in transgenic mice overexpressing spermidine/spermine N^1-acetyltransferase. J. Biol. Chem. 272:18746-18751, 1997.

13. Greenberg, N.M., DeMayo, F., Finegold, M.J., Medina, D., Tilley, W.D., Aspinal, J.O., Cunha, G.R., Donjacour, A.A., Matusik, R.J., Rosen, J.M., Proc. Nat'l. Acad. Sci. USA 92:3439-43, 1995.

14. Kee, K., Vujcic, S., Merali, S., Diegelman, P., Kisiel, N., Powell, C.T., Kramer, D.L. and Porter, C.W. Metabolic and antiproliferative consequences of activated polyamine catabolism in LNCaP prostate carcinoma cells. J. Biol. Chem. 279:27050-27058, 2004. (see Appendix)

15. Kee, K., Foster, B.A., Merali, S., Vujcic, S.,, Mazurchuk, R., Hensen, M.L., Diegelman, P., Kisiel, N., Kramer, D.L., and Porter, C.W. Activated polyamine catabolism depletes acetyl-CoA and suppresses prostate tumor growth in the TRAMP mouse. J. Biol. Chem. 279:40076-40083, 2004. (see Appendix).

16. Ali, P.M., Pinn, M.L., Jaffe, E.M., McFadden, J.M., Kuhajda, F.P., Fatty acid synthase inhibitors are chemopreventive for mammary cancer in neu-N transgenic mice. Oncogene 24:39-46, 2005.

17. Niiranen, K., Pietila, M., Pirttila, T.J., Jarvinen, A., Halmekyto, M., Korhonen, V.P., Alhonen, L., Janne, J. Targeted disruption of spermidine/spermine N1-acetyltrasferase gene in mouse embryonic stem cells. J. Biol. Chem. 277:25323-8, 2002.

18. Nilsson, J.A., Keller, U.B., Baudino, T.A., Yang, C., Norton, S., Brennan, J.A., Neale, G., Porter, C.W., Kramer, D.L., and Cleveland, J.L., Targeting ornithine decarboxylase in Myc-induced lymphomagenesis prevents tumor formation. Cancer Cell 7:1-12, 2005.

19. Vujcic, S., Liang, P., Diegelman, P., Kramer, D.L. and Porter, C.W. Genomic identification and biochemical characterization of the mammalian polyamine oxidase involved in polyamine back-conversion. Biochem J. 370:19-28, 2003.

20. Vujcic, S., Diegelman, P., Bacchi, C.J., Kramer, D.L., and Porter, C.W., Identification and characterization of a novel flavin-containing spermine oxidase of mammalian cell origin. Biochem. J. 367:665-675, 2002.

21. Hector, S., Porter, C.W., Kramer, D.L., Clark, K. Chen, Y. and Pendyala, L. Polyamine catabolism in platinum drug action: Interactions between oxaliplatin and the polyamine analogue N^1, N^{11}-diethylnorspermine at the level of spermidine/spermine N^1-acetyltransferase. Molec. Cancer Therap. 3:813-822, 2004.

22. Tucker JM, Murphy JT, Kisiel N, Diegelman P, Barbour KW, Davis C, Medda M, Alhonen L, Janne J, Kramer DL, Porter CW, Berger FG. Potent modulation of intestinal tumorigenesis in $Apc^{Min/+}$ mice by the polyamine catabolic enzyme spermidine/spermind N^1-acetyltransferase. Cancer Res. 65:5390-5398, 2005.

23. Janne, J., Alhonen, L., Pietila, M., Keinanen, T.A., Uimari, A., Hyvonen, M.T., Pirinene, E., and Jarvinen, A., Genetic manipulation of polyamine catabolism in rodents. J. Biochem. (In Press).

DAMD17-03-1-0024

APPENDICES

TEXT FIGURES

Figures 1-9 plus legends.

REPRINTS OF ARTICLES

- Kee, K., Vujcic, S., Merali, S., Diegelman, P., Kisiel, N., Powell, C.T., Kramer, D.L. and Porter, C.W. Metabolic and antiproliferative consequences of activated polyamine catabolism in LNCaP prostate carcinoma cells. J. Biol. Chem. 279:27050-27058, 2004.
- Kee, K., Foster, B.A., Merali, S., Vujcic, S.,, Mazurchuk, R., Hensen, M.L., Diegelman, P., Kisiel, N., Kramer, D.L., and Porter, C.W. Activated polyamine catabolism depletes acetyl-CoA and suppresses prostate tumor growth in the TRAMP mouse. J. Biol. Chem. 279:40076-40083, 2004.
- Hector, S., Porter, C.W., Kramer, D.L., Clark, K. Chen, Y. and Pendyala, L. Polyamine catabolism in platinum drug action: Interactions between oxaliplatin and the polyamine analogue N^1, N^{11}-diethylnorspermine at the level of spermidine/spermine N^1-acetyltransferase. Molec. Cancer Therap. 3:813-822, 2004.
- Tucker JM, Murphy JT, Kisiel N, Diegelman P, Barbour KW, Davis C, Medda M, Alhonen L, Janne J, Kramer DL, Porter CW, Berger FG. Potent modulation of intestinal tumorigenesis in $Apc^{Min/+}$ mice by the polyamine catabolic enzyme spermidine/spermind N^1-acetyltransferase. Cancer Res. 65:5390-5398, 2005. *(CWP Corresponding Author)*

REPORTS

Summary of Animal Use

Invention Report

Figure 1

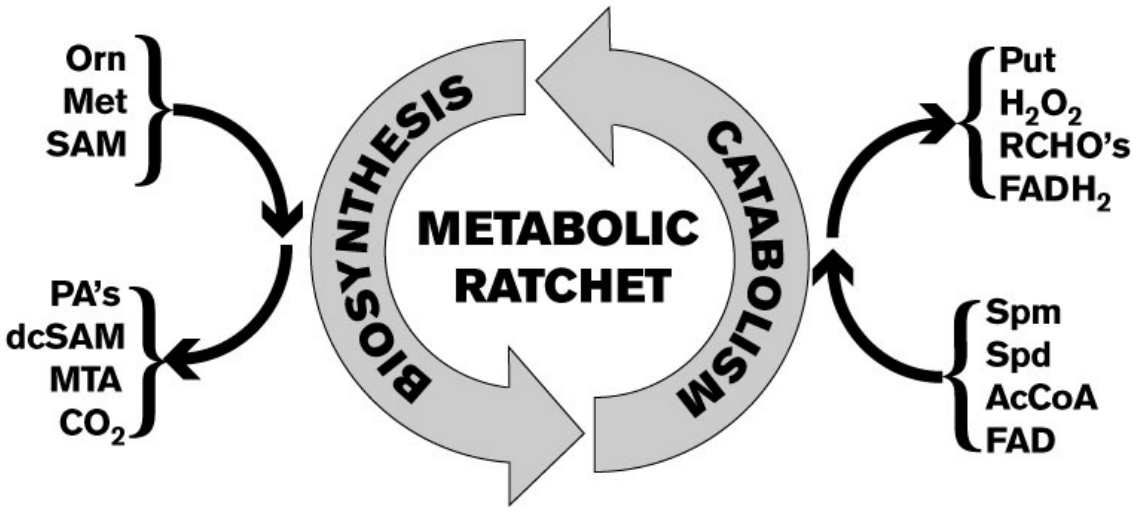

Figure 1. Metabolic ratchet model for polyamine homeostasis. Large arrows represent the primary pathways for polyamine biosynthesis (left) and catabolism (right). Various metabolites are shown which are either substrates or products of these pathways. Substrates and precursors utilized in polyamine biosynthesis include ornithine (Orn), methionine (Met) and the SAMDC aminopropyl donor, S-adenosylmethionine (SAM) while substrates utilized in polyamine catabolism include spermidine (Spd), spermine (Spm), acetyl-CoA (AcCoA), and FAD. Compounds produced during polyamine biosynthesis include the natural polyamines (PA's), the SAMDC by-product decarboxylated S-adenosylmethionine (dcSAM), the Spd and Spm synthase by-product, 5'methylthioadenosine (MTA) and the decarboxylase by-product, CO_2. Compounds produced during catabolism include the PAO product putrescine (Put) and the by-products hydrogen peroxide (H_2O_2), the aliphatic aldehyde 3-acetamidopropanal (RCHO's), and $FADH_2$. In response to SSAT-induced decreases in Spd and Spm, polyamine biosynthesis increases, giving rise to a sustained rise in metabolic flux. As flux through the pathway increases (such as that occurring in SSAT-over-expressing LNCaP cells or in SSAT-transgenic mice), substrate utilization and product accumulation increase; conversely, as flux decreases (such as that occurring in SSAT-knockout mice), substrate utilization and product accumulation decrease. The cellular response to alterations in flux depend upon the particular metabolites that change and how effectively the cell or tissue can react to that change. This Figure appears in publication by Tucker *et al*., (2005) as Figure 6. We note that an authority in the field J. Jänne has embraced our novel concept of polyamine metabolic flux in a recent review (Janne *et al.*, 23)

Figure 2

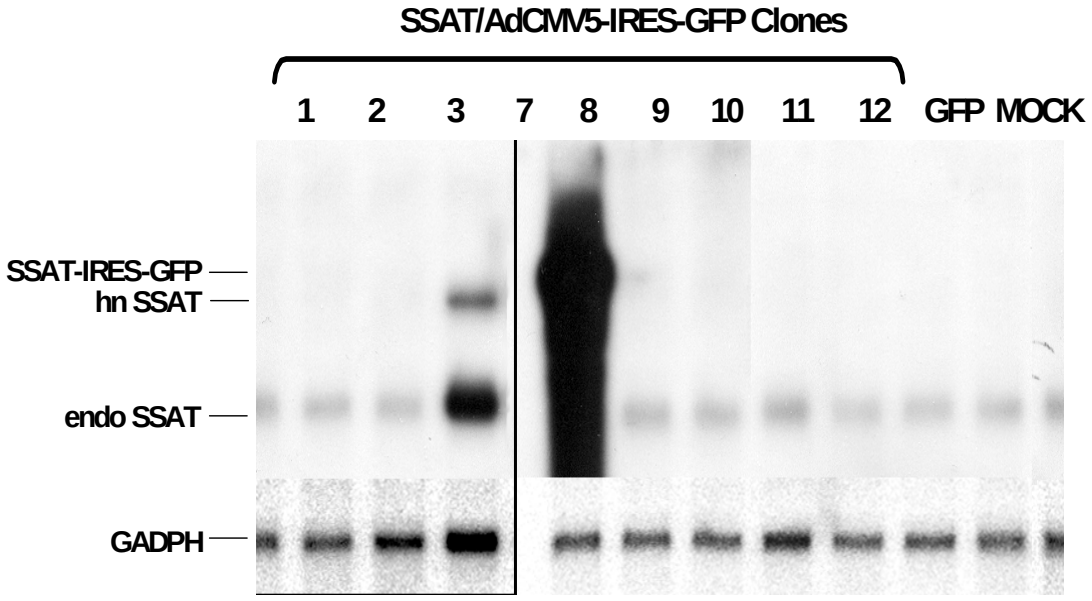

Figure 2. SSAT mRNA expression in adenovirally transduced 293 cells. The highest expressing clone (lane 1) was selected for further amplification and purification. The finding also indicates that the SSAT adenovirus can be raised in human cells.

Figure 3

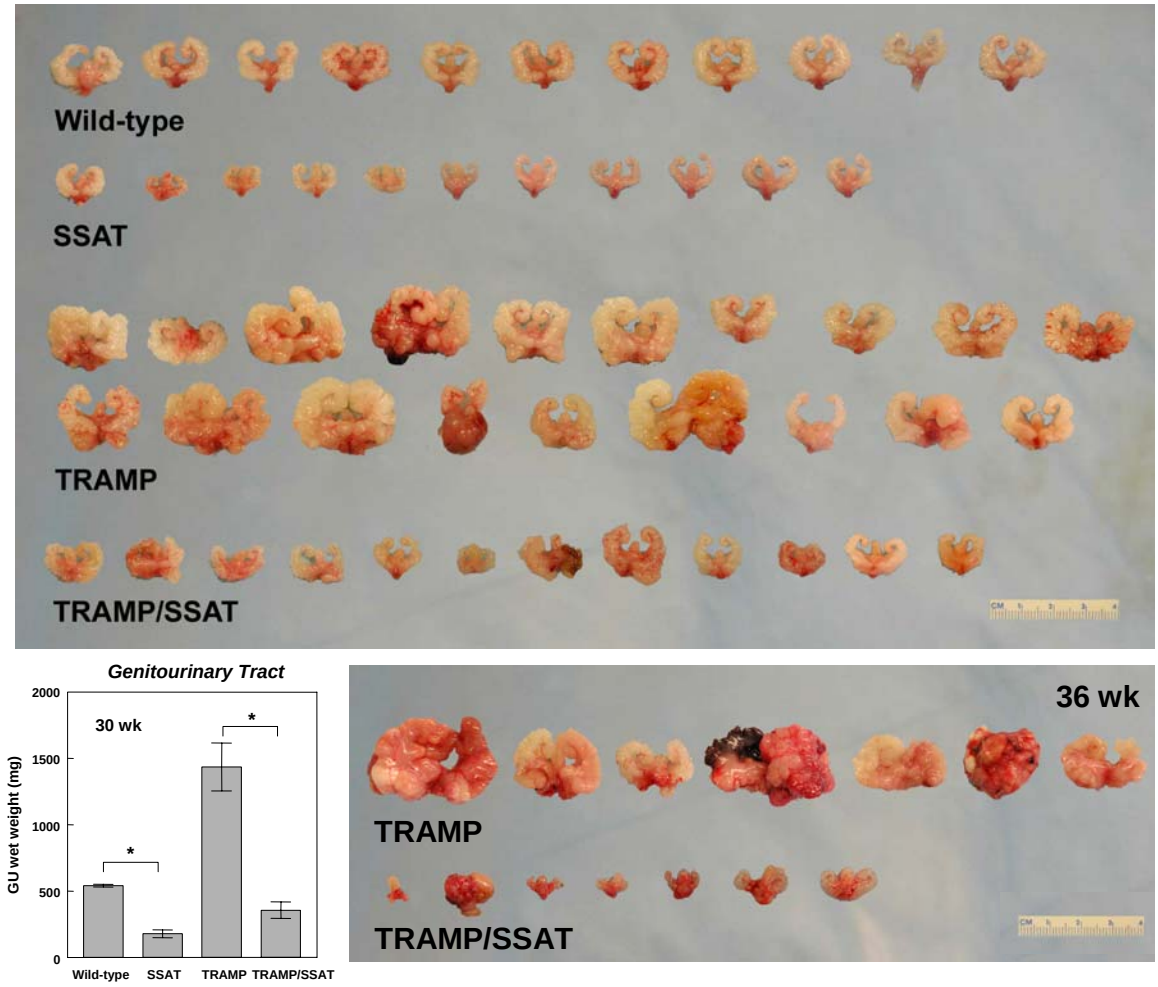

Figure 3. Comparison of GU tracts. (A) GU tracts of the four genetic cohorts deriving from the TRAMP x SSAT cross at 30 wk. Note that the GU tracts of SSAT mice were smaller than those of wild-type mice and that the GU tracts of TRAMP/SSAT mice were much smaller and less variable in size and shape than those of TRAMP mice. (B) GU tract weights at 30-wk of four genetic cohorts deriving from the TRAMP x SSAT cross. The GU tracts of TRAMP/SSAT animals weighed less than TRAMP mice (*$p < 0.0001$), and GU tracts of SSAT mice were also different from wild-type (*$p < 0.0001$) as determined by Student's unpaired t-test. (C) Comparison of GU tracts for TRAMP and TRAMP/SSAT mice at 36 wk of age. During the period 30 to 36 wk period, the average TRAMP GU tract increased by 200% while the average TRAMP/SSAT GU tract remained statistically the same.

Figure 4

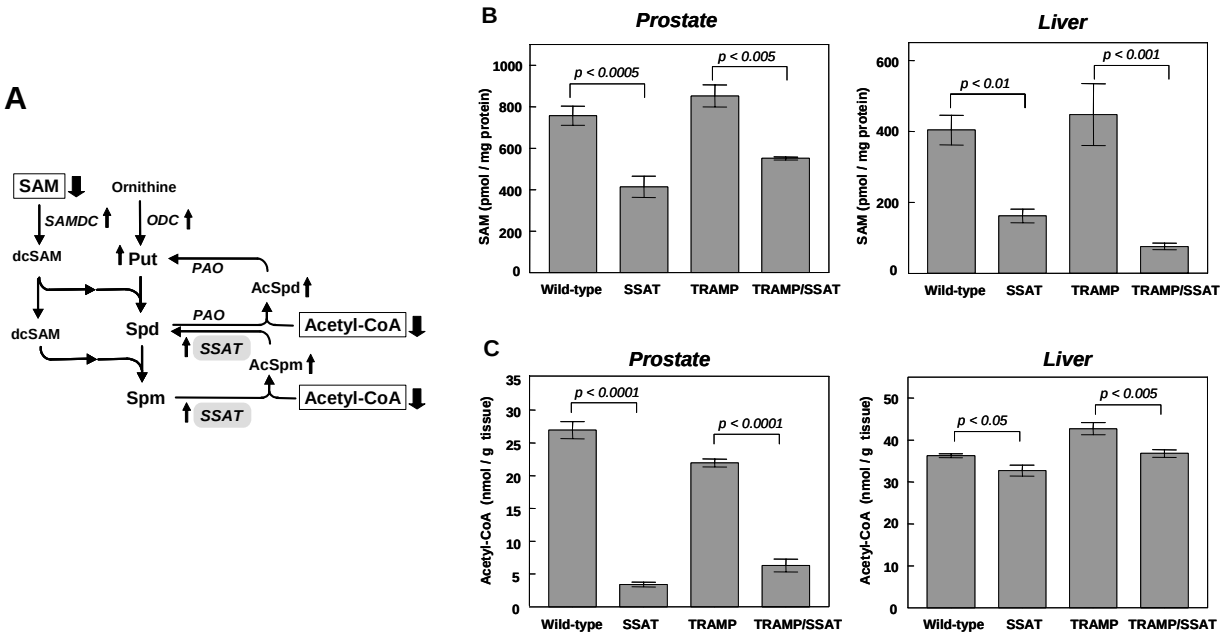

Figure 4. Downstream effects of SSAT overexpression. (A) Metabolic consequences to SSAT overexpression. Activation of polyamine catabolism at the level of SSAT results in a compensatory increase in the activities of the polyamine biosynthetic enzymes ODC and SAMDC. This activated polyamine synthesis minimizes polyamine pool depletion despite massive production of AcSpd. At the same time, it gives rise to heightened metabolic flux through the biosynthetic and catabolic pathways (not shown). The possible downstream consequences connecting heightened metabolic flux to growth inhibition include over-production of pathway products such as Put and AcSpd and/or depletion of critical metabolic precursors such as the aminopropyl donor SAM and the SSAT cofactor acetyl-CoA, both of which are markedly decreased in SSAT transgenic and TRAMP/SSAT bigenic animals. (B) SAM levels in prostate and liver tissues of TRAMP/SSAT littermates as determined on tissue extracts by HPLC. Note that SAM pools were much lower (>40%) in the prostate and liver of SSAT and TRAMP/SSAT mice. (C) Acetyl-CoA levels in prostate and liver tissues of TRAMP x SSAT littermates as detected by HPCE. Note that during SSAT overexpression, there was significant reduction (~70%) of acetyl-CoA in the prostates of SSAT and TRAMP/SSAT mice but not in the livers. Data represents mean ± standard error, where n = 3 animals per group. Statistical significance (*p*-value) was determined by ANOVA with Fisher's PLSD test for pair-wise comparisons.

Figure 5

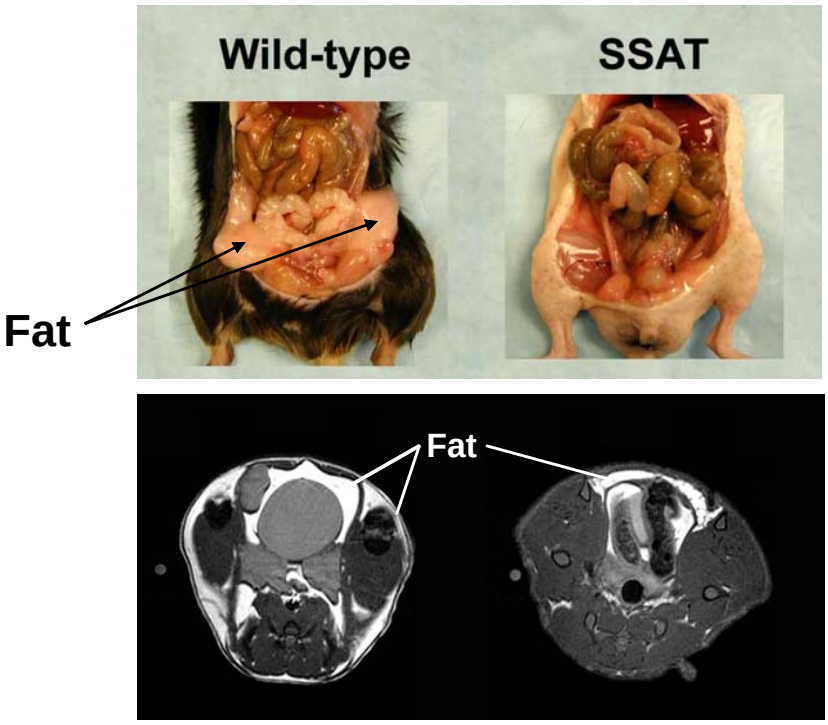

Figure 5. Abdominal fat stores in wild-type and SSAT transgenic mice at 30 wk. A Comparison of dissected mice (upper panel) shows the presence of large abdominal/mesenteric fat deposits in wild-type animals (left) and the absence of similar deposits in the SSAT transgenic animals (right). Representative high resolution transaxial MR images (lower panels) of wild type (left) and SSAT (right) mice. Note the presence of abdominal and sub-dermal fat (seen as bright areas) in wild-type mice and the absence of similar deposits in SSAT transgenic mice.

Figure 6

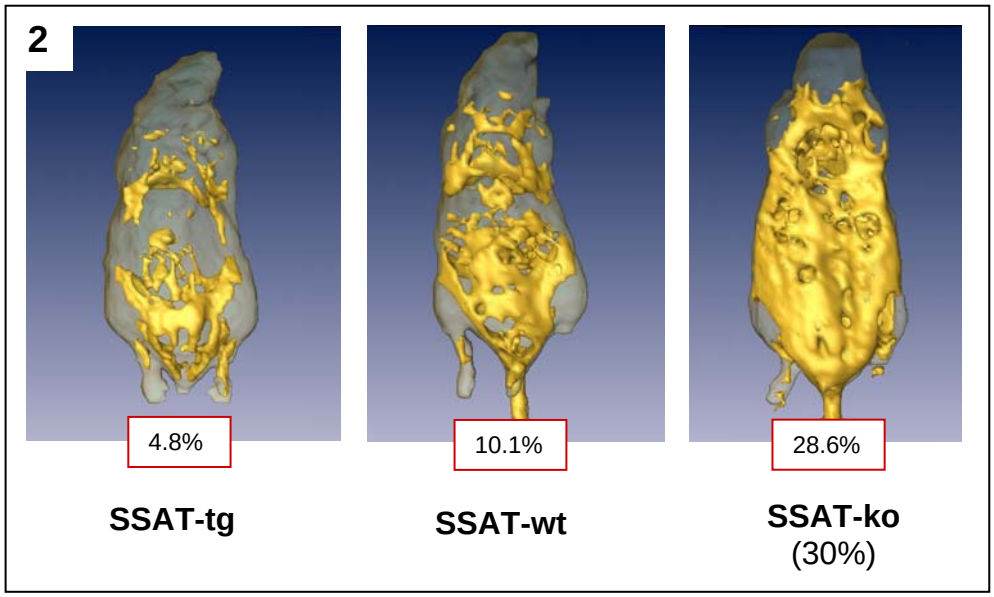

Figure 6. MRI quantitation of body fat composition according to SSAT status of mice. Representative whole animal MRI ventral views of SSAT-transgenic mouse (left), SSAT-wild-type mouse (center) and SSAT-knockout mouse (right). The numbers indicate the percent body fat composition as quantified by MRI. Approximately 30% of the SSAT-ko mice (Fig. 3A) are significantly heavier than SSAT-wt mice. These findings support an association between SSAT, acetyl-CoA and fat accumulation.

Figure 7

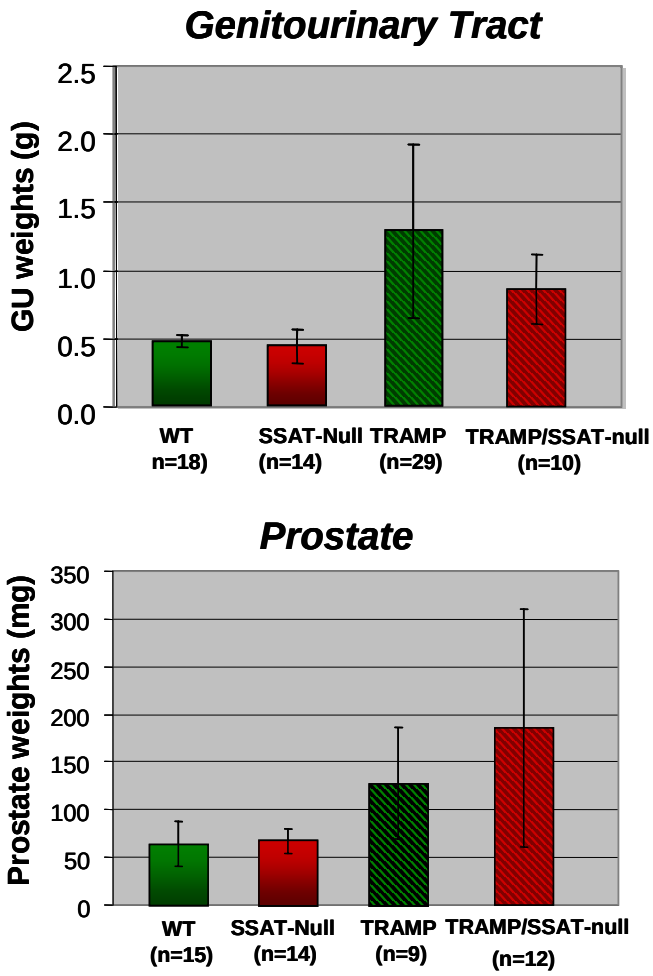

Figure 7. Effect of SSAT deletion on prostatic tumorigenesis in the TRAMP mouse. TRAMP mice were cross bred with SSAT null mice (both in the C57 Bl/6 background). Prostate glands and genitourinary tract (GU) weights were obtained at 30 wks. Observations thus far suggest that in both TRAMP and TRAMP/SSAT null, tumors originate in the prostate and rapidly spread to the seminal vesicles (as per GU weights). Note the difference in scale for the two tissues. Thus, the majority of the GU weight derives from the prostate and the difference between the two mouse cohorts was not found to be significant ($p < 0.05$). Additional mice are being accumulated for these studies.

Figure 8

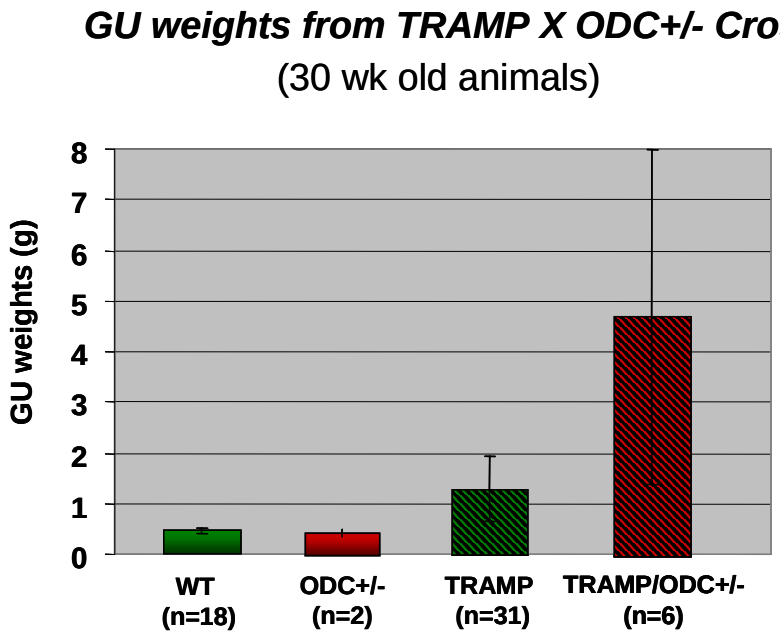

Figure 8. Effect of ODC haploinsufficiency on prostatic tumorigenesis in the TRAMP mouse. *TRAMP* mice were cross bred with heterozygous ODC mice (both in the C57 Bl/6 background). Genitourinary tract (GU) weights were obtained at 30 wks. Unlike TRAMP mice that typically show tumor invasion of the seminal vesicles, the majority of the TRAMP/ODC+/- tumors remained confined to the prostate. Despite large variation in tumor size, there is clear indication among individual animals that ODC heterogeneity promotes tumorigenesis within the prostate gland. Additional animals will be analyzed during the next year in order to counter the experimental variability.

Figure 9

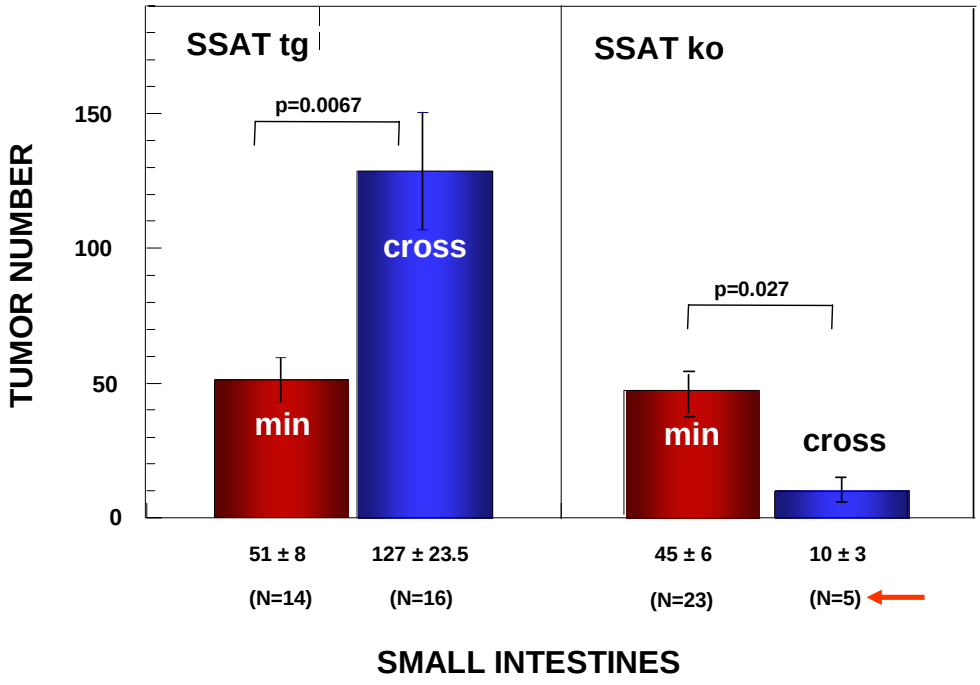

Figure 9. Effect of SSAT overexpression on intestinal tumorigenesis. *APC*^{min} mice were crossed with SSAT transgenic (SSAT-tg, (left) or SSAT knock-out (SSAT-ko, right) mice (all in the C57 Bl/6 background). Tumor counts were determined over the entire length of small intestine. At 40 days, tumor counts were much higher in the *APC*^{min} x SSAT transgenic (127 ± 23.5) than in the *APC*^{min} mice (51 ± 8). Thus, *SSAT over- expression markedly increased the number of tumors in both the intestine relative to the APC*^{min} *mice. In contrast, SSAT deletion markedly decreased the number of intestinal tumors (i.e. 10* ± 3 vs 45 ± 6). Similar trends were also seen in the colon which typically contains fewer tumors than the small intestine. Overall, the trend is opposite that seen for prostate tumor size in the TRAMP model; an effect attributed to metabolic context responses to SSAT modulation.

THE JOURNAL OF BIOLOGICAL CHEMISTRY
Vol. 279, No. 26, Issue of June 25, pp. 27050–27058, 2004

Printed in U.S.A.

Metabolic and Antiproliferative Consequences of Activated Polyamine Catabolism in LNCaP Prostate Carcinoma Cells*

Received for publication, March 25, 2004, and in revised form, April 9, 2004
Published, JBC Papers in Press, April 19, 2004, DOI 10.1074/jbc.M403323200

Kristin Kee‡, Slavoljub Vujcic‡, Salim Merali§, Paula Diegelman‡, Nicholas Kisiel‡, C. Thomas Powell¶, Debora L. Kramer‡, and Carl W. Porter‡‖

From the ‡Grace Cancer Drug Center, Roswell Park Cancer Institute, Buffalo, New York 14263, the §Department of Medical and Molecular Parasitology, New York University School of Medicine, New York, New York 10010, and the ¶Cleveland Clinic Foundation, Lerner Research Institute, Cleveland, Ohio 44195

Depletion of intracellular polyamine pools invariably inhibits cell growth. Although this is usually accomplished by inhibiting polyamine biosynthesis, we reasoned that this might be more effectively achieved by activation of polyamine catabolism at the level of spermidine/spermine N^1-acetyltransferase (SSAT); a strategy first validated in MCF-7 breast carcinoma cells. We now examine the possibility that, due to unique aspects of polyamine homeostasis in the prostate gland, tumor cells derived from it may be particularly sensitive to activated polyamine catabolism. Thus, SSAT was conditionally overexpressed in LNCaP prostate carcinoma cells via a tetracycline-regulatable (Tet-off) system. Tetracycline removal resulted in a rapid ~10-fold increase in SSAT mRNA and an increase of ~20-fold in enzyme activity. SSAT products N^1-acetylspermidine, N^1-acetylspermine, and N^1,N^{12}-diacetylspermine accumulated intracellularly and extracellularly. SSAT induction also led to a growth inhibition that was not accompanied by polyamine pool depletion as it was in MCF-7 cells. Rather, intracellular spermidine and spermine pools were maintained at or above control levels by a robust compensatory increase in ornithine decarboxylase and *S*-adenosylmethionine decarboxylase activities. This, in turn, gave rise to a high rate of metabolic flux through both the biosynthetic and catabolic arms of polyamine metabolism. Treatment with the biosynthesis inhibitor α-difluoromethylornithine during tetracycline removal interrupted flux and prevented growth inhibition. Thus, flux-induced growth inhibition appears to derive from overaccumulation of metabolic products and/or from depletion of metabolic precursors. Metabolic effects that were not excluded as possible contributing factors include high levels of putrescine and acetylated polyamines, a 50% reduction in *S*-adenosylmethionine, and a 45% decline in the SSAT cofactor acetyl-CoA. Overall, the study demonstrates that activation of polyamine catabolism in LNCaP cells elicits a compensatory increase in polyamine biosynthesis and downstream metabolic events that culminate in growth inhibition.

Cell growth is dependent on a sustained supply of polyamines, which is typically met by the integrated contributions of biosynthesis, catabolism, uptake, and export, each of which is sensitively regulated by effector molecules that, in turn, are controlled by intracellular polyamine pools (1). Thus, ornithine decarboxylase (ODC)[1] and *S*-adenosylmethionine decarboxylase (SAMDC) control biosynthesis, a polyamine transport system modulates uptake, and spermidine/spermine N^1-acetyltransferase (SSAT) regulates polyamine catabolism and export out of the cell. Neoplastic cell growth is associated with elevated polyamine biosynthetic activity, even when the surrounding normal tissue itself is rapidly proliferating, such as the intestinal mucosa (2–4). Thus, the rationale for targeting polyamines in antitumor strategies relates to their critical role in supporting neoplastic cell growth and to the overexpression of biosynthetic enzymes in tumor *versus* normal tissues (3, 5, 6).

The biology and metabolism of polyamines in the prostate is distinctly different from that of other tissues. In addition to synthesizing these molecules for epithelial cell replacement, the gland produces massive quantities of spermine (Spm) for export into reproductive fluids (7–10). The only major tissue that synthesizes polyamines for export, the prostate, and presumably tumors derived from it, may be dependent on novel and therapeutically exploitable homeostatic mechanisms. For example, we have observed that, in contrast to other cell lines, two of three prostate carcinoma lines failed to regulate polyamine transport in response to polyamine analogues or inhibitors (11). Very recently, Rhodes *et al.* (12) performed a meta-analysis of four independent microarray datasets comparing gene expression profiles of benign *versus* malignant patient prostate samples (12). Their study showed that polyamine biosynthesis was the most consistently and significantly affected metabolic, signaling, or apoptotic pathway. More particularly, the study revealed a synchronous network of genes contributing to polyamine biosynthesis was up-regulated while genes detracting from polyamine biosynthesis were down-regulated. In support of these findings, clinical studies by Bettuzzi *et al.* (13) indicate a significant increase in transcripts of the polyamine biosynthetic enzymes, ODC and SAMDC, in human prostatic cancer relative to benign hyperplasia.

* This work was supported by NCI National Institutes of Health Grants CA-72648, CA-22153, CA-09072-30 and CA-16056 and by Department of Defense Award PC020638. The costs of publication of this article were defrayed in part by the payment of page charges. This article must therefore be hereby marked "*advertisement*" in accordance with 18 U.S.C. Section 1734 solely to indicate this fact.

‖ To whom correspondence should be addressed. Tel.: 716-845-3002; Fax: 716-845-2353; E-mail: carl.porter@roswellpark.org.

[1] The abbreviations used are: ODC, ornithine decarboxylase; CoA, coenzyme A; AcSpd, N^1-acetylspermidine; AcSpm, N^1-acetylspermine; dcSAM, decarboxylated *S*-adenosylmethionine, DiAcSpm, N^1,N^{12}-diacetylspermine; DENSPM, N^1,N^{11}-diethylnorspermine; DFMO, α-difluoromethylornithine; HPCE, high performance capillary electrophoresis; HPLC, high performance liquid chromatography; MTA, 5′-methylthioadenosine; PAO, polyamine oxidase; Put, putrescine; SAM, *S*-adenosylmethionine; SAMDC, *S*-adenosylmethionine decarboxylase; Spd, spermidine; Spm, spermine; SSAT, spermidine/spermine N^1-acetyltransferase; Tet, tetracycline; TRAMP, transgenic adenocarcinoma of mouse prostate; tTA, tetracycline-repressible transactivator; dansyl, 5-dimethylaminona-phthalene-1-sulfonyl.

In recognition of the unique physiology of the prostate gland, Heston and collaborators (14, 15) were among the first to propose that targeting polyamine biosynthesis may be particularly effective against prostate cancer. Most of these efforts have made use of known inhibitors of ODC or SAMDC (16–19). Gupta *et al.* (20) showed that the ODC inhibitor, α-difluoromethylornithine (DFMO) effectively suppressed development of prostate cancer in the TRAMP mouse model. As an alternative approach to the use of enzyme inhibition, we propose that disruption of polyamine homeostasis at the level of polyamine catabolism may have unique therapeutic potential against prostate carcinoma. It has been demonstrated, for example, that polyamine analogues such as N^1,N^{11}-diethylnorspermine (DENSPM) down-regulate polyamine biosynthesis at the level of ODC and SAMDC and, at the same time, potently (*i.e.* >200-fold) up-regulate polyamine catabolism at the level of spermidine/spermine N^1-acetyltransferase (SSAT) (1, 21–27). Several lines of evidence support the idea that analogue induction of SSAT and hence, activation of polyamine catabolism, is a critical determinant of DENSPM drug action. For example, DENSPM growth inhibition among tumor cell lines correlates with the extent to which SSAT is induced (23–25), and analogues that differentially induce SSAT inhibit cell growth in a correlative manner (22, 26, 27). As more direct evidence for this relationship, McCloskey *et al.* (28) showed that DENSPM-resistant Chinese hamster ovary cells are unable to induce SSAT. Recently, Chen *et al.* (29, 30) reported that small interference RNA interference with DENSPM induction of SSAT prevented polyamine pool depletion while blocking analogue-induced apoptosis in human melanoma cells.

The studies cited above relate to SSAT induction in the context of analogue treatment, but they do not address what happens when SSAT is selectively induced in cells. In an earlier report (31), we showed that conditional overexpression of SSAT leads to polyamine pool depletion and growth inhibition in MCF-7 breast carcinoma cells. On the basis of rationale suggesting that prostate carcinoma may react differently to perturbations in polyamine homeostasis, we investigated the consequences of conditional SSAT overexpression in LNCaP prostate carcinoma cells.

EXPERIMENTAL PROCEDURES

Materials—The inhibitor of polyamine oxidase (PAO), N^1-methyl-N^2-(2,3-butadienyl)butane-1,4-diamine (MDL-72527) was generously provided by Aventis Pharmaceuticals Inc. (Bridgewater, NJ). The ODC inhibitor DFMO was obtained from Ilex, Inc. (San Antonio, TX). Tetracycline (Tet), aminoguanidine, polyamines, and the acetylated polyamines N^1-acetylspermidine (AcSpd) and N^1-acetylspermine (AcSpm) were purchased from Sigma-Aldrich, whereas N^1,N^{12}-diacetylspermine (DiAcSpm) was provided as a gift from Dr. Nikolaus Seiler (Laboratory of Nutritional Oncology, Institut de Recherche Contre les Cancers, Strasbourg, France). SAM was purchased from Sigma-Aldrich, and the SAM metabolites, decarboxylated *S*-adenosylmethionine (dcSAM) and 5-methylthioadenosine (MTA), were synthesized and kindly provided by Drs. Canio Marasco and Janice Sufrin (Roswell Park Cancer Institute). Radioactive compounds L-[1-^{14}C]ornithine, [acetyl-1-^{14}C] coenzyme A, [α-^{32}P]dCTP were purchased from PerkinElmer Life Sciences, and *S*-adenosyl-L-[*carboxyl*-^{14}C]methionine was obtained Amersham Biosciences. Acetyl-coenzyme A (acetyl-CoA) was purchased from Sigma-Aldrich and solubilized as described by Liu *et al.* (32). Geneticin (G418) and hygromycin B were obtained from Clontech Laboratories, Inc. (Palo Alto, CA) and Invitrogen, respectively.

Cell Culture—LNCaP prostate carcinoma cells engineered to constitutively express the tetracycline-repressible transactivator (tTA) (33), designated LNGK9 (34), were cultured in RPMI 1640 media supplemented with 2 mM glutamine (Invitrogen), 10% Tet-approved fetal bovine serum (Clontech Laboratories, Inc.), penicillin at 100 units/ml, streptomycin at 100 units/ml (Invitrogen), and 150 μg/ml hygromycin B at 37 °C in the presence of humidified 5% CO_2. Aminoguanidine (at 1 mM) was routinely included in the media as an inhibitor of copper-dependent bovine serum amino oxidases to prevent conversion of extracellular polyamines to toxic products. Cells were harvested by trypsinization and counted electronically (Coulter Model ZM, Coulter Electronics, Hialeah, FL).

Transfections—LNGK9 cells expressing the tTA were seeded at 2×10^6 cells per 100-mm culture dishes in the absence of hygromycin B and Tet. The following day, fresh media were replaced and cells were co-transfected with the tTA-responsive pTRE-SSAT plasmid (31) and a G418-resistance selection plasmid pcDNA3 (Invitrogen) at a ratio of 20:1 using FuGENE 6 (Roche Applied Science) according to manufacturer's protocol. Stably transfected clones were selected in medium containing 500 μg/ml antibiotic G418, 150 μg/ml hygromycin B, and 1 μg/ml Tet. Healthy G418-resistant clones were selected and tested for SSAT mRNA by Northern blot analysis in the presence or absence of 1 μg/ml Tet. With the Tet-off system, SSAT transcription is induced in the absence of Tet (−Tet) but not in its presence (+Tet). A Tet concentration of 1 μg/ml was found to fully and consistently suppress SSAT gene expression during routine cell culture passage. Clones that expressed low basal level of SSAT mRNA under +Tet conditions and high induced levels of SSAT mRNA under −Tet conditions were selected for further study. Clones were maintained continuously under 1 μg/ml +Tet until experiments were initiated.

Northern Blot Analysis—Northern blot analysis was carried out as described by Fogel-Petrovic *et al.* (35) with modifications. Briefly, total RNA was extracted with an RNeasy® Mini kit (Qiagen Inc., Valencia, CA), and its concentration was determined by UV spectrophotometry. RNA samples (5 μg/lane) were separated on 1.5% agarose/formaldehyde gels and transferred to a Duralon-UV membrane (Stratagene, La Jolla, CA). The membrane was cross-linked in a Stratalinker™ 1800, hybridized to [^{32}P]dCTP random-labeled cDNA probes (Stratagene) for detection of SSAT mRNA (36), and exposed for autoradiography. A glyceraldehyde-3-phosphate dehydrogenase signal was used as a loading control.

Polyamine Enzymes and Polyamine Pools—SSAT, ODC, and SAMDC activities were assayed as described previously (27, 37). Polyamine enzyme activities were expressed as picomoles of AcSpd generated per minute/mg of protein for SSAT and as nanomoles of CO_2/h/mg of protein for ODC and SAMDC. Intracellular polyamines, including acetylated derivatives of spermidine (Spd) and Spm were extracted from cell pellets with 0.6 N perchloric acid, dansylated, measured by reverse phase high-performance liquid chromatography (HPLC) as described by Kramer *et al.* (38), and expressed as picomoles/10^6 cells. Extracellular polyamines and acetylated polyamines were extracted from media as described by Kramer *et al.* (39), containing fetal bovine serum, Tet, and L-glutamine but not G418 or hygromycin B. A total of 50 μl of dansylated sample was injected for HPLC, and data were collected and analyzed as noted above. Extracellular polyamine pools were expressed as nanomoles/equivalent volume (ml)/10^6 cells.

S-Adenosylmethionine and Metabolite Pools—Intracellular SAM and its metabolites, dcSAM and MTA, were extracted from cell pellets with 0.6 N perchloric acid and measured by HPLC according to chromatographic conditions reported by Yarlett and Bacchi (40) with modifications as described by Kramer *et al.* (38). Briefly, samples (50 μl) were eluted from a C18 column (40 °C) at a flow rate of 0.8 ml/min with a linear gradient starting with solvent A (0.1 M NaH_2PO_4, 8 mM octane sulfonic acid, 0.05 mM EDTA, 2% acetonitrile) at 80% and solvent B (0.15 mM NaH_2PO_4, 8 mM octane sulfonic acid, 26% acetonitrile) at 20%. Over the course of 30 min, the gradient increased to 100% solvent B for 10 min. Effluent was monitored with a Waters 2487 dual wavelength UV detector, and data were processed using instrumentation described for polyamine pool analysis and expressed as picomoles/10^6 cells.

Measurement of Acetyl-CoA—High performance capillary electrophoresis (HPCE) separation and quantitation of acetyl-CoA in biological samples followed the method of Liu *et al.* (32). Cells were lysed and processed by using a solid-phase extraction. Extracts were then analyzed on a Beckman P/ACE MDQ capillary electrophoresis system equipped with a photodiode array detector and an uncoated fused silica CE column of 75-μm inner diameter and 60 cm in length with 50 cm from inlet to the detection window (Polymicro Technologies, Phoenix, AZ). Electrophoretic conditions were according to Liu *et al.* (32) with modifications. Briefly, the capillary was preconditioned with 1 M NaOH and Milli-Q water for 10 min each at 20 p.s.i. and then equilibrated with 100 mM NaH_2PO_4 running buffer containing 0.1% β-cyclodextrin (pH 6.0) for 10 min. After each run, the capillary was rinsed with 1 M NaOH, Milli-Q water, and running buffer for 2 min each. The injection was done hydrodynamically at a pressure of 0.5 p.s.i. for 10 s. Injection volume was calculated using CE Expert Lite software from Beckman. Separation voltage was 15 kV at a constant capillary temperature of 15 °C. To establish the standard calibration curves, solutions contain-

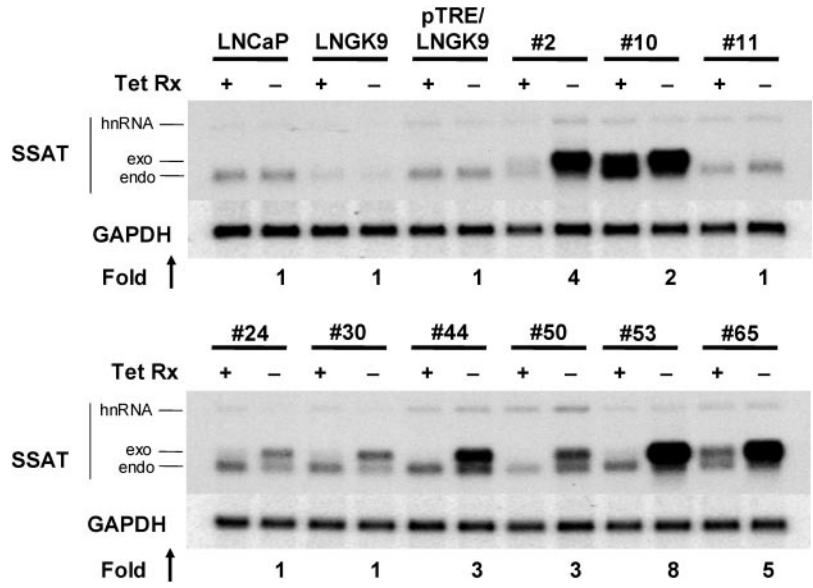

FIG. 1. **Conditional overexpression of SSAT mRNA in LNCaP clones transfected with Tet-regulatable human SSAT cDNA. LNGK9 cells, a subline of LNCaP, were transfected with the Tet-repressible human SSAT plasmid.** Stably transfected clones resistant to neomycin were selected and tested for their responsiveness to Tet by Northern blot analysis. Representative examples from over 100 selected clones were cultured for 48 h in the presence (+) or absence (−) of 1 μg/ml Tet. Note the endogenous (*endo*) and exogenous (*exo*, *i.e.* plasmid transcript) mature SSAT mRNA can be distinguished on the basis of size (*i.e.* ~1.3 *versus* ~1.5 kb, respectively). For quantitation, the exogenous and endogenous SSAT mRNA bands were scanned fluorometrically, normalized to the glyceraldehyde-3-phosphate dehydrogenase (*GAPDH*) signal, and expressed as -fold increase (*Fold* ↑) in −Tet relative to +Tet. Blots are representative of findings from three separate experiments. *hnRNA*, heteronuclear RNA.

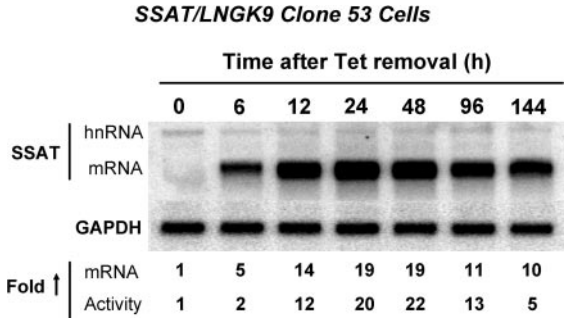

FIG. 2. **Time-dependent increases in SSAT mRNA and activity in SSAT/LNGK9 clone 53 following Tet removal.** Tet was removed for the indicated time, and cells were harvested for total RNA isolation and SSAT enzyme activity. An amount of 5 μg of total RNA was loaded onto each Northern blot lane. Note that following removal of 1 μg/ml Tet, both SSAT mRNA and activity increased rapidly before reaching a plateau between 24 and 48 h. For quantitation, SSAT mRNA bands were scanned fluorometrically, normalized to the glyceraldehyde-3-phosphate dehydrogenase (*GAPDH*) signal, and expressed as -fold increase (*Fold* ↑) relative to +Tet at 0 h (*lane 1*). As expressed by -fold increase, SSAT activity increased in parallel to SSAT mRNA. This blot is representative of findings from three separate experiments. *hnRNA*, heteronuclear RNA.

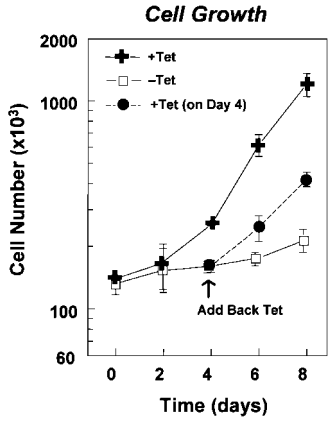

FIG. 3. **Effects of conditional SSAT overexpression on growth kinetics of LNCaP prostate carcinoma cells.** SSAT/LNGK9-clone 53 cells were cultured in the presence (+*Tet*, ⊕) or absence (−*Tet*, □) of 1 μg/ml Tet for the indicated time and collected for growth analysis. Removal of Tet (□) resulted in an inhibition of cell growth over the course of 8 days. Note that addition of 1 μg/ml Tet at 96 h (●) leads to a resumption of cell growth. Data represent means ± S.E., where *n* is 3.

ing the acetyl-CoA and the internal standard (isobutyryl-CoA, 41 nmol) were prepared at concentrations ranging from 1 to 200 nmol. Standards were processed as described above for cell lysates and resuspended in 10 μl of water. The detector response was ($r > 0.99$) for all acetyl-CoA species over the above concentration range. Coenzyme As were monitored with a photodiode array detector at the maximum absorbance wavelength (253.5 nm). Data were collected and processed by using Beckman P/ACE 32 Karat software version 4.0. Cellular acetyl-CoA levels were expressed as nanomoles/10^6 cells.

RESULTS

Derivation of Transfected Cells—Cells transfected with the human SSAT cDNA were selected in neomycin and grown as clones in the presence of 1 μg/ml Tet. Of the 100 SSAT/LNGK9 clones screened (data not shown), those most sensitive to Tet regulation were selected according to the differential expression between SSAT mRNA in +Tet (SSAT-off) *versus* mRNA in −Tet (SSAT-on) (Fig. 1). Based on these criteria, clone 53 was selected for further study, because it displayed low SSAT mRNA in +Tet and an 8-fold increase in total SSAT mRNA (exogenous and endogenous) under −Tet conditions for 48 h. Nearly identical responses were also obtained with several other clones. Transfected human SSAT cDNA (~1.5 kb) was distinguishable from the smaller endogenous transcript (~1.3 kb) by differences in polyadenylation, which became apparent during enzyme induction (35). Although the exogenous 1.5-kb transcript levels increased with Tet removal, the endogenous 1.3-kb transcript levels remained at basal levels, indicating that the presence or absence of the antibiotic did not affect endogenous gene expression. Tet-regulated expression of SSAT mRNA and activity was characterized from 0 to 144 h in clone 53 (Fig. 2). Following Tet removal, SSAT mRNA increased significantly by 6 h and plateaued by 24 h at levels ranging between 10- and 20-fold greater than the 0-h sample. Induction of mRNA was closely paralleled by increases in SSAT activity, which reached a maximum of ~20-fold by 24 h (see Figs. 2 and 4).

Effects of SSAT Overexpression on Cell Growth and Polyamine Metabolism—As shown in Fig. 3, SSAT overexpression caused significant inhibition of cell growth at ~2 days following Tet removal, which was sustained through the 6-day experiment. Growth inhibition appeared to be cytostatic rather than cytotoxic, because there was no obvious decline in cell number as would be expected with apoptosis and because addition of

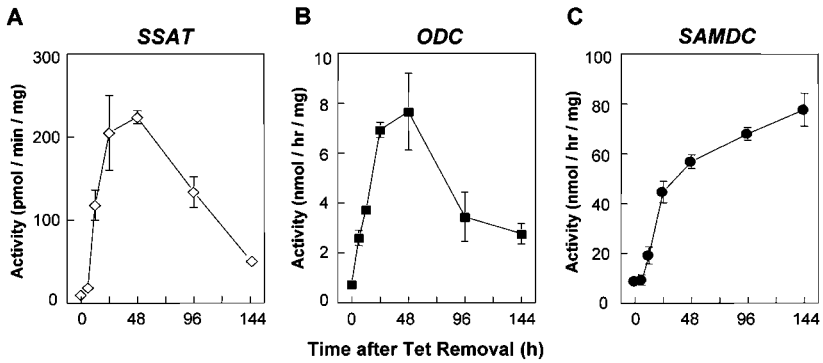

FIG. 4. **Time-dependent effects of conditional SSAT overexpression on polyamine biosynthetic enzyme activities.** Tet was removed from SSAT/LNGK9-clone 53 cells for the indicated time after which cells were harvested for polyamine enzyme activities for SSAT, ODC, and SAMDC. Following Tet removal, both SSAT activity (◇) increased sharply to a maximum of ~20-fold (*A*), and ODC activity (■) increased sharply to ~10-fold (*B*) at 48 h before undergoing a steady decline. By contrast, SAMDC activity (●) increased steadily over the course of 144 h to a maximum of ~18-fold that of basal levels (*C*). Enzyme activities of SSAT/LNGK9-clone 53 cells grown continuously in the presence of Tet remained relatively unchanged from 0 h (data not shown). Data represents mean values ± S.E., where *n* is 3.

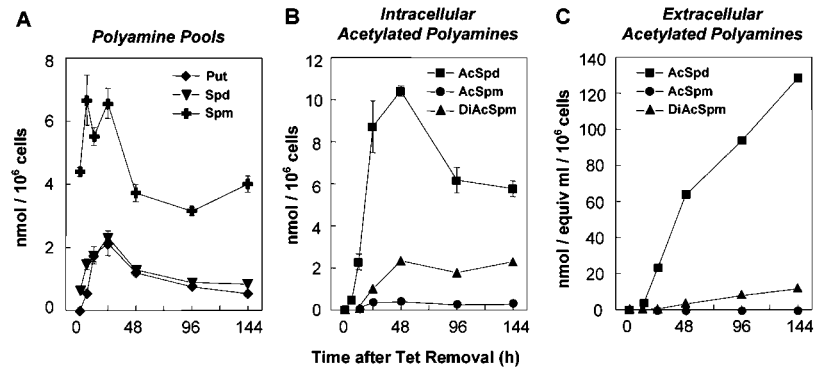

FIG. 5. **Time-dependent effects of conditional SSAT overexpression on intracellular and extracellular polyamines.** Similar to the experiment as described in Fig. 4, SSAT/LNGK9-clone 53 cells were grown in the absence of Tet for the indicated time and then harvested for polyamine pool analysis by HPLC. Intracellular polyamines pools increased transiently for 24 h following Tet removal and then decreased steadily. Note that, even at 144 h, Put, Spd, and Spm pools remained similar to or slightly above basal levels (0 h) (*A*). Intracellular AcSpd and AcSpm increased markedly following Tet removal (*B*). At the same time, huge amounts of AcSpd accumulated in the media (*C*) indicating that acetylated products are readily exported. Significant levels of DiAcSpm were detected intracellularly and extracellularly (*B* and *C*). (*AcSpd*, N^1-acetylspermidine; *AcSpm*, N^1-acetylspermine; *DiAcSpm*, N^1,N^{12}-diacetylspermine; *Put*, putrescine; *Spd*, spermidine; *Spm*, spermine). Data represent means ± S.E., where *n* is 3.

Tet at 96 h resulted in a rapid resumption of cell growth (Fig. 3). The time-dependent effects of Tet removal on enzyme activities and polyamine pools are shown in Figs. 4 and 5. SSAT increased steadily to 22-fold by 48 h before declining slowly from 48 to 144 h (Figs. 2 and 4). This steady decrease in SSAT activity and mRNA may be due to a homeostatic adjustment of gene expression and/or to a time-dependent selection of cells that express lower levels of SSAT. Consistent with the observed rise in enzyme activity, acetylated polyamines increased under −Tet conditions (Fig. 5). Intracellular AcSpd increased remarkably from undetectable levels (<10 pmol/10^6 cells) to 10,420 pmol/10^6 cells by 48 h. Other SSAT products, AcSpm and DiAcSpm, which are rarely seen in cells (31), accumulated to 390 pmol/10^6 cells and 2,340 pmol/10^6 cells, respectively, by 48 h and remained elevated during the course of the 144-h experiment. Putrescine (Put) pools also rose remarkably due presumably to back-conversion of Put from Spd via AcSpd (Fig. 5) and to forward synthesis due to increased ODC activity (described below). Despite the massive accumulation of acetylated polyamines, intracellular levels of Spd and Spm failed to decrease. In fact, the levels of Put, Spd, and Spm increased substantially during the first 24 h following SSAT induction, after which they declined slowly to levels that were above (*i.e.* Put and Spd) or close to (*i.e.* Spm) 0 h levels. Enzyme activity data in Fig. 4 (*B* and *C*) strongly suggest that these pools were sustained by compensatory increases in ODC and SAMDC activities, which rose ~10-fold and ~8-fold, respectively, during the first 48 h of SSAT overexpression (Fig. 4*A*).

Analysis of cell culture media revealed huge amounts of acetylated polyamines following SSAT overexpression (Fig. 5*C*). In particular, AcSpd and DiAcSpm, which were barely detectable in +Tet culture media, were as high as 128,210 pmol/equivalent ml/10^6 cells and 11,500 pmol/equivalent ml/10^6 cells, respectively, 144 h following Tet removal. These extracellular levels were actually 10-fold higher than intracellular levels on the basis of 10^6 cells. The finding is consistent with the tenet that acetylation by SSAT facilitates export of polyamines out of the cell (41–43). Taken together, the above findings indicate that SSAT induction leads to a strong metabolic flux through both the biosynthetic and catabolic arms of the polyamine pathway. As additional indication for this interpretation, we observed increased conversion of SAM to dcSAM via the SAMDC reaction and increased intracellular accumulation MTA, a well known by-product of dcSAM that is stoichiometrically released during the Spd and Spm synthase reactions (Fig. 6).

Effects of PAO and ODC Inhibition on SSAT-induced Growth Inhibition and Pool Dynamics—Data in Figs. 4 and 5 indicate that SSAT overexpression and inhibition of cell growth in LNCaP cells were *not* due to depletion of intracellular Spd and Spm pools. Thus, our next experiments were designed to investigate the basis for SSAT-induced growth inhibition in LNCaP

cells. Because polyamine oxidase (PAO) is functionally located downstream of SSAT, and because the enzyme liberates toxic by-products (hydrogen peroxide and reactive aldehydes) having clear cytotoxic potential (44), we first examined whether the PAO inhibitor MDL-72527 might prevent growth inhibition during SSAT-mediated deregulation of polyamine catabolism. As shown in Fig. 7*A*, the presence of 10 μM MDL-72527 during −Tet failed to abrogate growth inhibition. The substantial increase in acetylated polyamines during inhibitor treatment relative to −Tet alone confirms that PAO was effectively blocked (Table I). We next considered that growth inhibition might be due to metabolic flux resulting from up-regulation of ODC and polyamine biosynthesis. To test this hypothesis, the specific ODC inhibitor DFMO was added to the media during Tet removal to interrupt metabolic flux. As others have reported (45), wild-type LNCaP cells are inherently resistant to DFMO. SSAT-off (+Tet) cells treated with 1 mM DFMO grew similarly to cells not treated with DFMO (Fig. 7). The more unexpected finding was that DFMO treatment of SSAT-on (−Tet) cells effectively prevented growth inhibition. Thus, by inhibiting ODC, a relationship between metabolic flux and the antiproliferative effect was established. Importantly, ODC inhibition fully prevented accumulation of acetylated polyamines (Table I) and thereby provided direct evidence for interruption of polyamine flow from biosynthesis to catabolism. In experiments to be discussed below (see Fig. 10*D*), interference with flux by DFMO is further confirmed by the fact that there is no accumulation of MTA, the by-product of Spd and Spm synthesis.

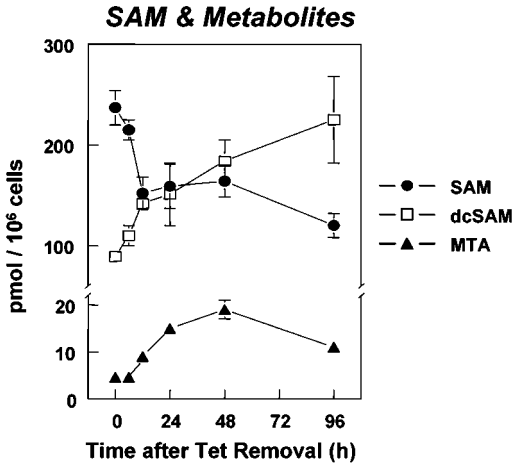

FIG. 6. **Effects of SSAT overexpression on SAM, dcSAM and MTA pools.** Tet was removed from SSAT/LNGK9-clone 53 cells for the indicated times after which cells were harvested and extracted for SAM pool analysis by HPLC. Note that upon Tet removal (−Tet), intracellular levels of the SAMDC substrate SAM (●) declined steadily to ~50% at 96 h while the SAMDC product dcSAM (□) increased steadily to a maximum of 250% at 96 h. At the same time, the biosynthetic by-product of dcSAM metabolism MTA (▲) increased to a maximum of ~400% at 48 h. The findings are consistent with accelerated polyamine metabolic flux due to increased polyamine biosynthesis and acetylation in −Tet cells. The limit of detection for MTA is <5 pmol/10^6 cells. Data represent means ± S.E., where *n* is 3.

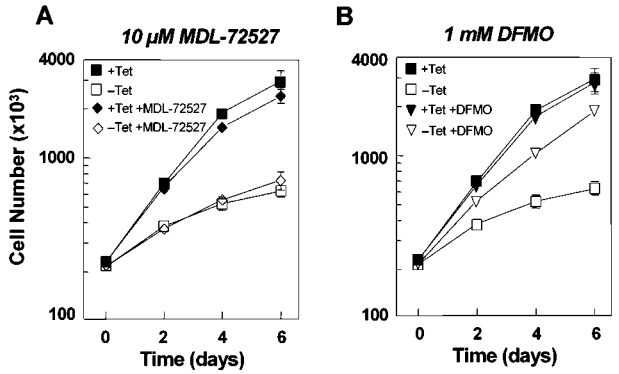

FIG. 7. **Effects of PAO or ODC inhibition on SSAT-induced cell growth inhibition.** SSAT/LNGK9-clone 53 cells were grown in the presence and absence of Tet and treated with either a PAO inhibitor (10 μM MDL-72527 (*A*)) or an ODC inhibitor (1 mM DFMO (*B*)) for the indicated time and then analyzed for prevention of cell growth inhibition. When included during Tet removal, the PAO inhibitor MDL-72527 failed to prevent growth inhibition by SSAT (*A*), whereas the ODC inhibitor DFMO was very effective in preventing SSAT-induced growth inhibition (*B*). Data represent means ± S.E., where *n* is 3.

The basis for sustained cell growth in the presence of DFMO is not clear by the polyamine analysis shown in Table I. At 48 h, Put and Spd pools are very low and Spm pools remain as high as those seen in the growth-inhibited −Tet cells. It is possible that, although most cells seem to rely on Spd for cell growth (18), LNCaP cells may grow under conditions of severe Put and Spd limitation by relying on Spm pools and a small amount of Spd back-converted from Spm via the SSAT/PAO pathway. Consistent with this idea, Spm pools were maintained at near to control levels for more than 96 h (data not shown).

Metabolic Flux and Depletion of Polyamine Precursor Stores—Enhanced metabolic flux may deplete metabolites and polyamine precursors and thereby limit their availability for cell growth. Such molecules include the biosynthetic precursors ornithine, methionine, SAM, and the SSAT cofactor acetyl-CoA. As shown in Fig. 8, the inclusion of 1 mM ornithine or methionine in the −Tet media failed to prevent SSAT-induced growth inhibition indicating that the amino acids were not limiting to cell growth.

The impact of SSAT overexpression on acetyl-CoA pools was investigated, because, in addition to serving as a cofactor to SSAT, the molecule is critically involved in fatty acid synthesis, histone acetylation, and other metabolic processes that could affect cell growth. As shown by electropherogram (Fig. 9*A*), acetyl-CoA was detectable by HPCE as a distinct and highly reproducible peak. Peak changes under −Tet *versus* +Tet conditions were quantitated relative to the internal standard

TABLE I
Polyamine pools under conditions of SSAT overexpression and enzyme inhibition in LNCaP cells

SSAT/LNGK9 clone 53	48-h treatment[a]	Polyamine pools (cells)[b]					
		Put	AcSpd	Spd	AcSpm	DiAcSpm	Spm
		pmol / 10^6 cells					
+Tet	Untreated	<10	<10	685 ± 10	<10	<10	4,180 ± 102
−Tet	Untreated	960 ± 25	16,910 ± 623	885 ± 70	525 ± 20	5,300 ± 320	3,050 ± 147
+Tet	1 mM DFMO	<10	<10	40 ± 2	<10	<10	3,850 ± 88
−Tet	1 mM DFMO	<10	320 ± 80	90 ± 15	40 ± 3	<10	3,455 ± 373
+Tet	10 μM MDL-72527	215 ± 15	<10	1,135 ± 68	<10	<10	4,390 ± 328
−Tet	10 μM MDL-72527	985 ± 160	21,795 ± 852	1,110 ± 57	1,030 ± 55	8,765 ± 345	2,625 ± 179

[a] Treatment began at Tet removal.
[b] Data are expressed as means ± S.E., where *n* is 3.

isobutyryl-CoA. Following analysis, intracellular acetyl-CoA pools were found to decrease by ~25% at 48 h and by ~45% at 96 h (Fig. 9*B*) suggesting a cause-and-effect linkage. The inability of acetyl-CoA to penetrate cells precluded more defining prevention studies such as those involving amino acids (Fig. 8). Attempts to prevent growth inhibition with exogenous 1 mM pyruvate as an acetyl-CoA precursor, proved unsuccessful (data not shown). It is puzzling, however, that these pools were not protected during DFMO prevention of growth inhibition (Fig. 10*A*). Because inhibition of ODC by DFMO results in a marked increase in SAMDC activity and dcSAM pools (Fig. 6), it is possible that acetylated polyamines may be back-converted to Put and Spd and then forward-converted to Spd and Spm due to excess dcSAM. These would then become available for re-acetylation by overexpressed SSAT. If sufficiently rapid, this cycling could account for the depleted acetyl-CoA pools during DFMO treatment.

As noted above, SAM pools were significantly reduced 12 h following Tet removal (Fig. 6). Repletion experiments were not feasible because, like acetyl-CoA, SAM does not penetrate cells effectively. Although SAM pools fell ~50% at 96 h (Figs. 6 and 10*B*), Spd and Spm pools did not similarly decline indicating that there was at least sufficient levels to sustain polyamine biosynthesis. A further disconnect between SAM levels and growth inhibition was noted in the finding that SAM pools remained reduced during treatment with DFMO (Fig. 10*B*), even though growth inhibition was prevented. Finally, we note that, as SAM pools declined, dcSAM pools increased in a correlative manner. Because the accumulation of dcSAM may cause growth inhibition (46), we considered that the significant rise in dcSAM seen following SSAT induction might be toxic (Fig. 6). This possibility, however, was also excluded by the finding that DFMO markedly increased dcSAM pools while preventing growth inhibition (Fig. 10*C*). Accumulation of the dcSAM metabolite, MTA, is also capable of exerting an antiproliferative effect (47, 48), but this seems unlikely in the present system, because there was no indication of Spd and Spm pool depletion, which is usually regarded as a major indication of MTA toxicity via feedback inhibition of the Spd and Spm synthases (49).

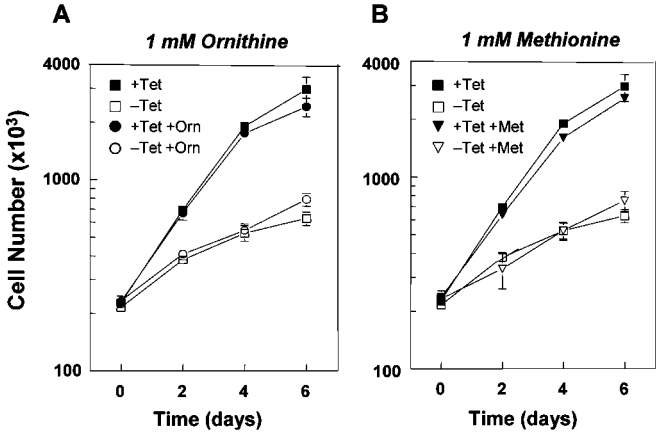

FIG. 8. **Effects of polyamine precursors on SSAT-induced cell growth inhibition.** SSAT/LNGK9-clone 53 cells grown in the presence and absence of Tet were simultaneous treated with 1 mM of the polyamine precursors, ornithine (*A*) or methionine (*B*), for the indicated time and analyzed for prevention of growth inhibition. Note that both amino acids failed to prevent SSAT-induced growth inhibition when included during Tet removal. Data represent means ± S.E., where *n* is 3.

DISCUSSION

We have previously shown that activation of polyamine catabolism by conditional overexpression of SSAT led to growth inhibition in MCF-7 breast cancer cells (31). We undertook the present study to examine whether LNCaP prostate tumor cells might respond differently to such perturbations in polyamine homeostasis. The data presented here are consistent with this possibility. Although both cell lines expressed a similar ~20-fold increase in SSAT activity, growth inhibition in MCF-7 breast carcinoma cells correlated closely with a depletion in intracellular polyamine pools (31). By contrast, growth inhibi-

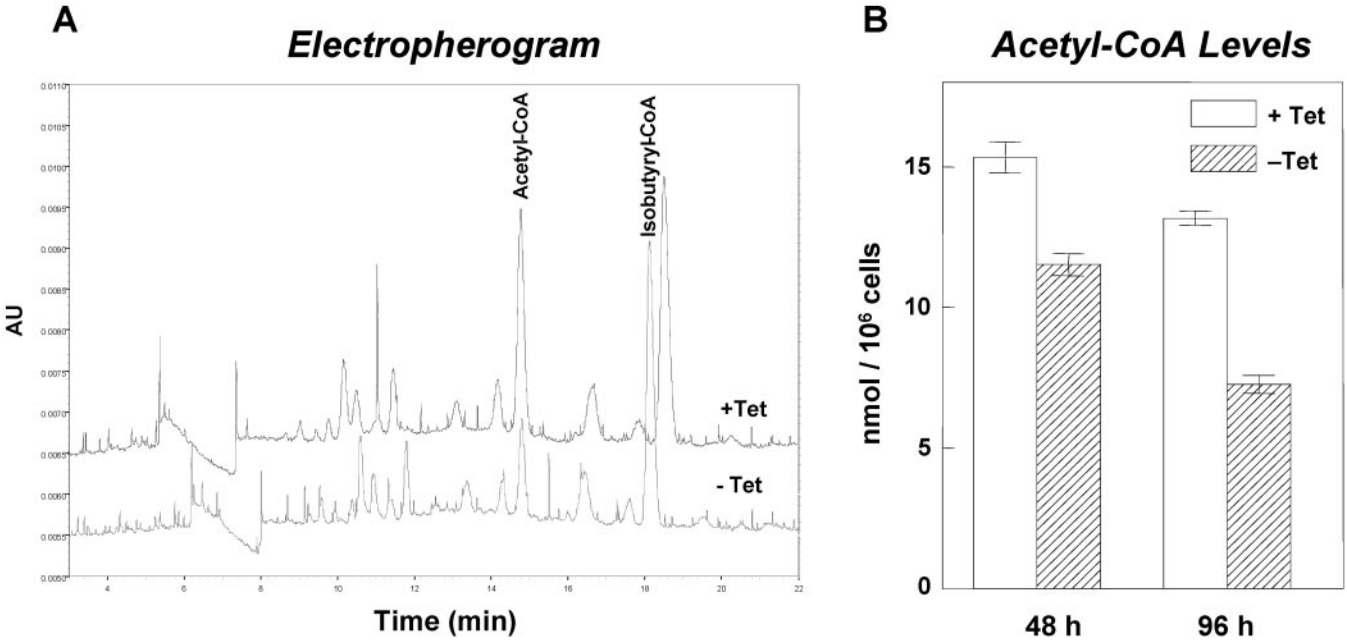

FIG. 9. **Effects of SSAT overexpression on acetyl-CoA levels.** SSAT/LNGK9-clone 53 cells were grown in the presence (+*Tet*, *open bar*) and absence of Tet (−*Tet*, *hatched bar*) for 48 and 96 h and analyzed by HPCE for acetyl-CoA. *A*, an electropherogram from HPCE showing levels of acetyl-CoA in clone 53 cells and an exogenous internal standard, isobutyryl-CoA in the presence (+*Tet*) and absence (−*Tet*) of Tet at 96 h. The internal standard isobutyryl-CoA was added to each sample to allow for calculation of loss during extraction. Note that the acetyl-CoA peak is much lower in −Tet cells compared with +Tet cells. Quantitation of the peaks (*B*) reveals a 25% decline in acetyl-CoA by 48 h and a 45% decline by 96 h in −Tet cells (*hatched bars*) when compared with their levels in +Tet cells (*open bars*). Data represent means ± S.E., where *n* is 3.

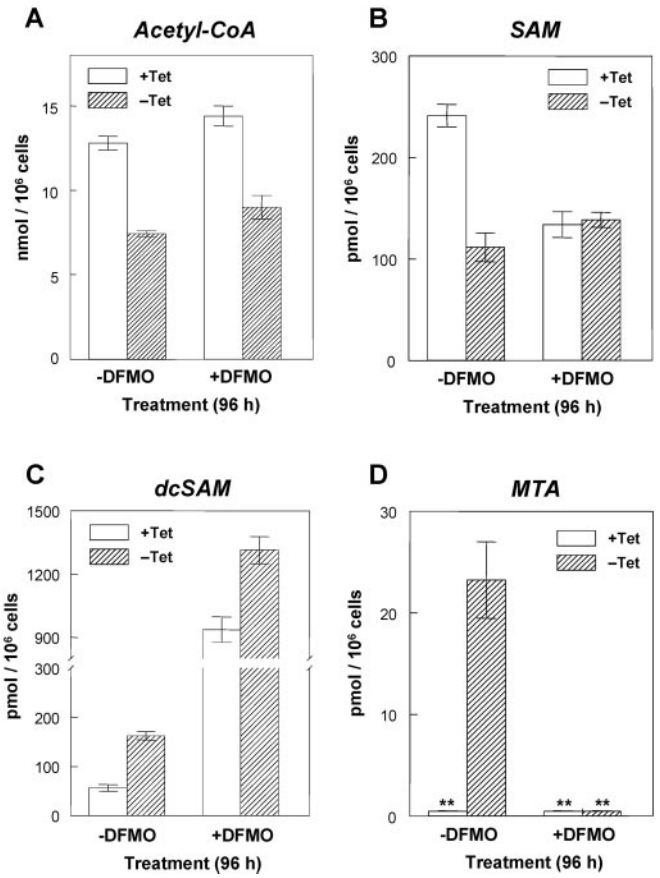

FIG. 10. **Effects of DFMO treatment on the levels of acetyl-CoA (*A*), SAM (*B*), dcSAM (*C*), and MTA (*D*) during SSAT overexpression.** SSAT/LNGK9-clone 53 cells were grown in the presence (+*Tet*, *open bar*) and absence of Tet (−*Tet*, *hatched bar*) with or without 1 mM DFMO for 96 h and analyzed by HPCE for acetyl-CoA and by HPLC for SAM, dcSAM, and MTA. Data represent means ± S.E., where *n* is 3.

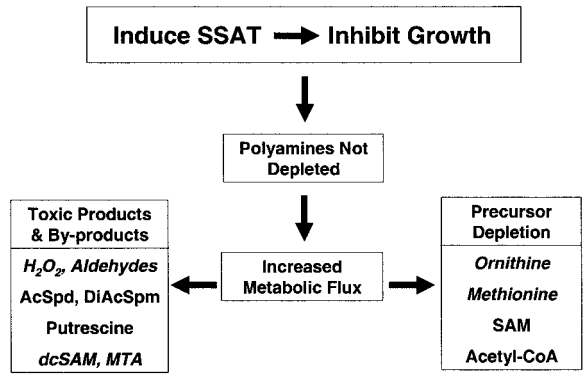

FIG. 11. **Diagrammatic representation of the possible causes of growth inhibition in SSAT overexpressing LNCaP cells.** Activation of polyamine catabolism by overexpressing SSAT causes growth inhibition in LNCaP cells, which is not accompanied by polyamine pool depletion. It is, however, associated with compensatory increase in polyamine biosynthetic activity that leads to heightened flux thru polyamine metabolism. When biosynthesis is interrupted by the ODC inhibitor, DFMO, growth inhibition is prevented (not shown), thus linking flux to the antiproliferative effect. The possible causes of growth inhibition emanating from heightened flux are presented as accumulation of product or by-product excess (*left panel*) or as depletion of critical precursors and cofactors (*right panel*). Of the product/by-product possibilities, overproduction of hydrogen peroxide (H_2O_2) and reactive aldehydes (such as acetamidopropanal), dcSAM, and MTA have been experimentally eliminated (*italic type*). Of the possible precursor possibilities, depletion of ornithine and methionine has been experimentally excluded (*italic type*). Thus, the possibilities that were not excluded and that may contribute to growth inhibition include accumulation of acetylated polyamine products, decreased levels of the polyamine aminopropyl donor, SAM, and/or a reduction in stores of the SSAT co-factor, acetyl-CoA.

tion in LNCaP prostate carcinoma cells took place in the absence of polyamine pool depletion. As will be discussed below, the difference appears to be due to the ability of LNCaP cells to metabolically compensate for activated catabolism or conversely, to the inability of MCF-7 cells to mount such a response.

The idea of activating polyamine catabolism derived from observations made with polyamine analogues (23–27). We note that conditional overexpression of SSAT produces a 10- to 20-fold increase in SSAT activity, whereas induction by polyamine analogues such as DENSPM reaches ~1000-fold in certain cell lines. A significant portion of DENSPM-induced enzyme protein, however, is inhibited by analogue binding and is unable to acetylate polyamines (50). Accumulation of acetylated products represents a better indication of SSAT functional overexpression in cells. Thus, the seemingly modest 20-fold increase in SSAT activity seen here in LNCaP cells resulted in exceedingly high levels of intracellular and extracellular acetylated polyamines, which undoubtedly had a profound impact on the metabolic equilibrium of polyamines. We also note that enzyme induction is also associated with polyamine species such as DiAcSpm that are rarely seen in cells unless SSAT is overexpressed (31) or analogue-induced (29).

It was expected that the massive acetylation of Spd and Spm and their export into the media would deplete intracellular pools as was previously seen in MCF-7 cells (31). In LNCaP cells, however, depletion of Spd and Spm was averted by a compensatory increase in polyamine biosynthesis: ODC activity rose by ~16-fold at 48 h following Tet removal and SAMDC, by ~8-fold. Thus, instead of decreasing, intracellular polyamine pools actually increased rapidly despite the diversion of huge amounts of Spd and Spm to intracellular and extracellular acetylated polyamines. Although a similar up-regulation of polyamine biosynthesis has been reported in SSAT stably transfected cell lines and most tissues of transgenic mice (51–53), it is likely to have evolve over time via a process of selection. By contrast, the increase in ODC and SAMDC activities in LNCaP cells began almost simultaneously with SSAT activation. The net effect of this response was heightened flux through the biosynthetic pathway as indicated by the decline in SAM pools and by the related rise in MTA, a by-product of the Spd and Spm synthase reactions. The relationship between this flux and cell growth was clearly established by the observation that DFMO, an inhibitor of ODC, effectively prevented SSAT-induced growth inhibition. The finding is particularly significant, because DFMO typically inhibits, rather than prevents, cell growth (16). Whether this linkage is common to prostate-derived tumor cells or whether it is MCF-7 cells that are unusual remains to be determined. If the former is confirmed, the finding is consistent with other known biochemical idiosyncrasies regarding polyamine metabolism in prostate carcinoma cell lines (11, 15).

SSAT-induced growth inhibition in the absence of polyamine pool depletion raises obvious questions regarding the basis for the antiproliferative effect. As diagrammed in Fig. 11, the high rate of metabolic flux through both the biosynthetic and catabolic arms of the pathway suggests that accumulation of pathway products or by-products may reach toxic levels (*left panel*) or that certain metabolites may become growth-limiting (*right panel*). The various possibilities that were experimentally eliminated as causes of flux-induced growth inhibition include: elaboration of PAO toxic by-products, accumulation of dcSAM, and depletion of the amino acids ornithine and methionine (Fig. 11, *italic type*). Possibilities that were not clearly elimi-

nated include high levels of acetylated polyamines and Put, depletion of SAM pools, and decreases in acetyl-CoA pools (Fig. 11).

Our HPCE analysis of acetyl-CoA pools revealed that these pools decreased by 45% during SSAT induction in LNCaP cells. To our knowledge, this is the first time that such a linkage has been demonstrated between polyamine metabolism and depletion of acetyl-CoA stores. We examined this possibility with the view that the massive amounts of acetylated polyamines being generated may render the SSAT cofactor acetyl-CoA limiting for critical cellular functions such as fatty acid synthesis, cholesterol synthesis, and histone regulation. Indeed, fatty acid synthase expression and lipidogenesis are known to be increased by androgens and highly relevant to the normal prostate biology and prostate cancer (54–56). In addition, Ettinger *et al.* (57) recently showed that androgen independence in LNCaP xenograft models is closely associated with dysregulation of enzymes that coordinately control lipogenesis and cholesterol synthesis. These various findings imply a high dependence of prostate cancer on acetyl-CoA stores.

Taken together, findings indicate that activation of polyamine catabolism at the level of SSAT leads to: (*a*) altered polyamine pool homeostasis, (*b*) a compensatory increase in polyamine biosynthesis, (*c*) heightened metabolic flux through both the biosynthetic and catabolic pathways, (*d*) synthesis of enormous quantities of acetylated polyamines, (*e*) significant depletion of critical metabolite pools such as the polyamine precursor *S*-adenosylmethionine (SAM) and the SSAT cofactor, acetyl-CoA, and (*f*) inhibition of cell growth. We emphasize that this analysis applies strictly to selective SSAT overexpression and not to enzyme induction by polyamine analogues such as DENSPM, which in addition to potently inducing SSAT also down-regulate polyamine biosynthesis and, thereby, preclude the heightened metabolic flux seen in LNCaP cells. Importantly, studies from our laboratory (58) have shown that cross-breeding SSAT transgenic mice that are genetically predisposed to develop prostate cancer (*i.e.* TRAMP mice (59) results in metabolic responses similar to those seen in LNCaP cells and leads to a marked suppression of prostate tumor outgrowth.

Although the present findings are based on an artificial system (*i.e.* conditional overexpression of SSAT), there are many pharmacological examples of SSAT induction by classes of drugs other than polyamine analogues to levels comparable to those obtained here (43). For example, we and others have shown that anticancer drugs unrelated to polyamines can also elicit very significant increases in SSAT gene expression. Maxwell *et al.* (60) found that SSAT was the most potently induced gene by the antimetabolite 5-fluorouracil from among >3000 represented in a gene profiling study of MCF-7 cells. Similarly, we have shown that SSAT mRNA is among the top 10 genes induced by the DNA-alkylating platinum compounds, oxaliplatin and cisplatin (61). Finally, studies from our laboratory (58) have shown that cross-breeding SSAT transgenic mice that are genetically predisposed to develop prostate cancer (*i.e.* TRAMP mice (59)) markedly suppressed genitourinary tumors. These findings support the possibility that selective small molecule inducers of SSAT may have therapeutic and/or preventive potential against prostate cancer.

Acknowledgments—We gratefully acknowledge the helpful discussions with Drs. Janice Sufrin and Ying Chen, and Jason A. Jell for technical assistance. We also acknowledge Mehboob Shivji for assistance in isolating acetyl-CoA.

REFERENCES

1. Porter, C. W., Regenass, U., and Bergeron, R. J. (1992) in *Falk Symposium on Polyamines in the Gastrointestinal Tract* (Dowling, R. H., Folsch, U. R., and Loser, C., eds) pp. 301–322, Kluwer Academic Publishers Group, Dordrecht, Netherlands
2. Porter, C. W., Herrera-Ornelas, L., Pera, P., Petrelli, N. F., and Mittelman, A. (1987) *Cancer* **60,** 1275–1281
3. Kramer, D. L. (1996) in *Critical Roles of Polyamines in Cancer: Basic Mechanisms and Clinical Approaches* (Nishioka, K., ed) pp. 151–189, R. G. Landes Co., New York
4. Thomas, T., and Thomas, T. J. (2003) *J. Cell Mol. Med.* **7,** 113–126
5. Thomas, T., and Thomas, T. J. (2001) *Cell Mol. Life Sci.* **58,** 244–258
6. Seiler, N. (2003) *Curr. Drug Targets* **4,** 537–564
7. Harrison, G. A. (1931) *Biochem. J.* **25,** 1885–1892
8. Mann, T. (1964) *The Biochemistry of Semen and of the Male Reproductive Tract*, John Wiley, New York, pp. 193–200
9. Pegg, A. E., and Williams-Ashman, H. G. (1968) *Biochem. J.* **108,** 533–539
10. Williams-Ashman, H. G., and Canellakis, Z. N. (1979) *Perspect. Biol. Med.* **22,** 421–453
11. Mi, Z., Kramer, D. L., Miller, J. T., Bergeron, R. J., Bernacki, R., and Porter, C. W. (1998) *Prostate* **34,** 51–60
12. Rhodes, D. R., Barrette, T. R., Rubin, M. A., Ghosh, D., and Chinnaiyan, A. M. (2002) *Cancer Res.* **62,** 4427–4433
13. Bettuzzi, S., Davalli, P., Astancolle, S., Carani, C., Madeo, B., Tampieri, A., Corti, A., Saverio, B., Pierpaola, D., Serenella, A., Cesare, C., Bruno, M., Auro, T., and Arnaldo, C. (2000) *Cancer Res.* **60,** 28–34
14. Heston, W. D., Watanabe, K. A., Pankiewicz, K. W., and Covey, D. F. (1987) *Biochem. Pharmacol.* **36,** 1849–1852
15. Heston, W. D. (1991) *Cancer Surv.* **11,** 217–238
16. Mamont, P. S., Duchesne, M. C., Grove, J., and Bey, P. (1978) *Biochem. Biophys. Res. Commun.* **81,** 58–66
17. Regenass, U., Mett, H., Stanek, J., Mueller, M., Kramer, D., and Porter, C. W. (1994) *Cancer Res.* **54,** 3210–3217
18. Kramer, D. L., Khomutov, R. M., Bukin, Y. V., Khomutov, A. R., and Porter, C. W. (1989) *Biochem. J.* **259,** 325–331
19. Danzin, C., Marchal, P., and Casara, P. (1990) *Biochem. Pharmacol.* **40,** 1499–1503
20. Gupta, S., Ahmad, N., Marengo, S. R., MacLennan, G. T., Greenberg, N. M., and Mukhtar, H. (2000) *Cancer Res.* **60,** 5125–5133
21. Bergeron, R. J., Feng, Y., Weimar, W. R., McManis, J. S., Dimova, H., Porter, C., Raisler, B., and Phanstiel, O. (1997) *J. Med. Chem.* **40,** 1475–1494
22. Casero, R. A., Jr., Celano, P., Ervin, S. J., Porter, C. W., Bergeron, R. J., and Libby, P. R. (1989) *Cancer Res.* **49,** 3829–3833
23. Libby, P. R., Bergeron, R. J., and Porter, C. W. (1989) *Biochem. Pharmacol.* **38,** 1435–1442
24. Casero, R. A., Jr., Ervin, S. J., Celano, P., Baylin, S. B., and Bergeron, R. J. (1989) *Cancer Res.* **49,** 639–643
25. Shappell, N. W., Miller, J. T., Bergeron, R. J., and Porter, C. W. (1992) *Anticancer Res.* **12,** 1083–1089
26. Pegg, A. E., Wechter, R., Pakala, R., and Bergeron, R. J. (1989) *J. Biol. Chem.* **264,** 11744–11749
27. Porter, C. W., Ganis, B., Libby, P. R., and Bergeron, R. J. (1991) *Cancer Res.* **51,** 3715–3720
28. McCloskey, D. E., and Pegg, A. E. (2000) *J. Biol. Chem.* **275,** 28708–28714
29. Chen, Y., Kramer, D. L., Li, F., and Porter, C. W. (2003) *Oncogene* **22,** 4964–4972
30. Chen, Y., Kramer, D. L., Jell, J., Vujcic, S., and Porter, C. W. (2003) *Mol. Pharmacol.* **64,** 1153–1159
31. Vujcic, S., Halmekyto, M., Diegelman, P., Gan, G., Kramer, D. L., Janne, J., and Porter, C. W. (2000) *J. Biol. Chem.* **275,** 38319–38328
32. Liu, G., Chen, J., Che, P., and Ma, Y. (2003) *Anal. Chem.* **75,** 78–82
33. Gossen, M., and Bujard, H. (1992) *Proc. Natl. Acad. Sci. U. S. A.* **89,** 5547–5551
34. Gschwend, J. E., Fair, W. R., and Powell, C. T. (1997) *Prostate* **33,** 166–176
35. Fogel-Petrovic, M., Shappell, N. W., Bergeron, R. J., and Porter, C. W. (1993) *J. Biol. Chem.* **268,** 19118–19125
36. Xiao, L., Celano, P., Mank, A. R., Pegg, A. E., and Casero, R. A., Jr. (1991) *Biochem. Biophys. Res. Commun.* **179,** 407–415
37. Porter, C. W., Cavanaugh, P. F., Jr., Stolowich, N., Ganis, B., Kelly, E., and Bergeron, R. J. (1985) *Cancer Res.* **45,** 2050–2057
38. Kramer, D., Mett, H., Evans, A., Regenass, U., Diegelman, P., and Porter, C. W. (1995) *J. Biol. Chem.* **270,** 2124–2132
39. Kramer, D., Stanek, J., Diegelman, P., Regenass, U., Schneider, P., and Porter, C. W. (1995) *Biochem. Pharmacol.* **50,** 1433–1443
40. Yarlett, N., and Bacchi, C. J. (1988) *Mol. Biochem. Parasitol.* **27,** 1–10
41. Seiler, N., Bolkenius, F. N., and Knodgen, B. (1980) *Biochim. Biophys. Acta* **633,** 181–190
42. Seiler, N., Bolkenius, F. N., and Rennert, O. M. (1981) *Med. Biol.* **59,** 334–346
43. Seiler, N. (1987) *Can. J. Physiol. Pharmacol.* **65,** 2024–2035
44. Ha, H. C., Woster, P. M., Yager, J. D., and Casero, R. A., Jr. (1997) *Proc. Natl. Acad. Sci. U. S. A.* **94,** 11557–11562
45. Devens, B. H., Weeks, R. S., Burns, M. R., Carlson, C. L., and Brawer, M. K. (2000) *Prostate Cancer Prostatic Dis.* **3,** 275–279
46. Pegg, A. E. (1984) *Biochem. J.* **224,** 29–38
47. Yamanaka, H., Kubota, M., and Carson, D. A. (1987) *Cancer Res.* **47,** 1771–1774
48. Williams-Ashman, H. G., Seidenfeld, J., and Galletti, P. (1982) *Biochem. Pharmacol.* **31,** 277–288
49. Pajula, R. L., and Raina, A. (1979) *FEBS Lett.* **99,** 343–345
50. Libby, P. R., Ganis, B., Bergeron, R. J., and Porter, C. W. (1991) *Arch. Biochem. Biophys.* **284,** 238–244
51. Pietila, M., Alhonen, L., Halmekyto, M., Kanter, P., Janne, J., and Porter, C. W. (1997) *J. Biol. Chem.* **272,** 18746–18751
52. Alhonen, L., Karppinen, A., Uusi-Oukari, M., Vujcic, S., Korhonen, V. P., Halmekyto, M., Kramer, D. L., Hines, R., Janne, J., and Porter, C. W. (1998) *J. Biol. Chem.* **273,** 1964–1969
53. McCloskey, D. E., Coleman, C. S., and Pegg, A. E. (1999) *J. Biol. Chem.* **274,**

6175–6182
54. Swinnen, J. V., Esquenet, M., Goossens, K., Heyns, W., and Verhoeven, G. (1997) *Cancer Res.* **57,** 1086–1090
55. Swinnen, J. V., Ulrix, W., Heyns, W., and Verhoeven, G. (1997) *Proc. Natl. Acad. Sci. U. S. A.* **94,** 12975–12980
56. Swinnen, J. V., Vanderhoydonc, F., Elgamal, A. A., Eelen, M., Vercaeren, I., Joniau, S., Van Poppel, H., Baert, L., Goossens, K., Heyns, W., and Verhoeven, G. (2000) *Int. J. Cancer* **88,** 176–179
57. Ettinger, S. L., Sobel, R., Whitmore, T. G., Akbari, M., Bradley, D. R., Gleave, M. E., and Nelson, C. C. (2004) *Cancer Res.* **64,** 2212–2221
58. Kee, K., Vujcic, S., Kisiel, N., Diegelman, P., Kramer, D. L., and Porter, C. W. (2003) *Proc. Am. Assoc. Cancer Res.* **44,** 1277
59. Greenberg, N. M., DeMayo, F., Finegold, M. J., Medina, D., Tilley, W. D., Aspinall, J. O., Cunha, G. R., Donjacour, A. A., Matusik, R. J., and Rosen, J. M. (1995) *Proc. Natl. Acad. Sci. U. S. A.* **92,** 3439–3443
60. Maxwell, P. J., Longley, D. B., Latif, T., Boyer, J., Allen, W., Lynch, M., McDermott, U., Harkin, D. P., Allegra, C. J., and Johnston, P. G. (2003) *Cancer Res.* **63,** 4602–4606
61. Hector, S., Porter, C. W., Kramer, D. L., Clark, K., Chen, Y., and Pendyala, L. (2004) *Mol. Cancer Ther.*, in press

THE JOURNAL OF BIOLOGICAL CHEMISTRY
Vol. 279, No. 38, Issue of September 17, pp. 40076–40083, 2004

Printed in U.S.A.

Activated Polyamine Catabolism Depletes Acetyl-CoA Pools and Suppresses Prostate Tumor Growth in TRAMP Mice*

Received for publication, May 28, 2004
Published, JBC Papers in Press, July 13, 2004, DOI 10.1074/jbc.M406002200

Kristin Kee‡, Barbara A. Foster‡, Salim Merali§, Debora L. Kramer‡, Mary L. Hensen‡, Paula Diegelman‡, Nicholas Kisiel‡, Slavoljub Vujcic‡, Richard V. Mazurchuk¶, and Carl W. Porter‡‖

From the Departments of ‡Pharmacology and Therapeutics and ¶Cancer Biology, Roswell Park Cancer Institute, Buffalo, New York 14263 and the §Department of Medical and Molecular Parasitology, New York University School of Medicine, New York, New York 10010

The enzyme spermidine/spermine N^1-acetyltransferase (SSAT) regulates the catabolism and export of intracellular polyamines. We have previously shown that activation of polyamine catabolism by conditional overexpression of SSAT has antiproliferative consequences in LNCaP prostate carcinoma cells. Growth inhibition was causally linked to high metabolic flux arising from a compensatory increase in polyamine biosynthesis. Here we examined the *in vivo* consequences of SSAT overexpression in a mouse model genetically predisposed to develop prostate cancer. TRAMP (transgenic adenocarcinoma of mouse prostate) female C57BL/6 mice carrying the SV40 early genes (T/t antigens) under an androgen-driven probasin promoter were cross-bred with male C57BL/6 transgenic mice that systemically overexpress SSAT. At 30 weeks of age, the average genitourinary tract weights of TRAMP mice were ~4 times greater than those of TRAMP/SSAT bigenic mice, and by 36 weeks, they were ~12 times greater indicating sustained suppression of tumor outgrowth. Tumor progression was also affected as indicated by a reduction in the prostate histopathological scores. By immunohistochemistry, SV40 large T antigen expression in the prostate epithelium was the same in TRAMP and TRAMP/SSAT mice. Consistent with the 18-fold increase in SSAT activity in the TRAMP/SSAT bigenic mice, prostatic N^1-acetylspermidine and putrescine pools were remarkably increased relative to TRAMP mice, while spermidine and spermine pools were minimally decreased due to a compensatory 5–7-fold increase in biosynthetic enzymes activities. The latter led to heightened metabolic flux through the polyamine pathway and an associated ~70% reduction in the SSAT cofactor acetyl-CoA and a ~40% reduction in the polyamine aminopropyl donor *S*-adenosylmethionine in TRAMP/SSAT compared with TRAMP prostatic tissue. In addition to elucidating the antiproliferative and metabolic consequences of SSAT overexpression in a prostate cancer model, these findings provide genetic support for the discovery and development of specific small molecule inducers of SSAT as a novel therapeutic strategy targeting prostate cancer.

Although prostate cancer can be clinically managed in its early phases, the inability to control the more aggressive late stage disease has prompted the search for novel therapies. We became interested in the possibility that strategies targeting polyamine homeostasis may be effective against prostate cancer. The prostate has the highest level of polyamine biosynthesis of any tissue, and it is the only tissue in which polyamines are purposely synthesized for export. More particularly, massive amounts of polyamines are excreted by the prostate into semen. Thus, we reasoned that polyamine homeostasis may be altered in the prostate relative to other tissues and that tumors derived from this gland may exhibit atypical regulatory responses to polyamine analogues and inhibitors (1). An additional rationale for targeting polyamines in prostate cancer derives from a recent meta-analysis of four independent microarray data sets comparing gene expression profiles of benign and malignant patient prostate samples showing that polyamine metabolism was the most systematically affected of all biochemical and signaling pathways (2). Genes that supported polyamine biosynthesis were up-regulated, while those that detracted from biosynthesis were down-regulated. The findings agree with earlier clinical studies showing a significant increase in ornithine decarboxylase (ODC)[1] and *S*-adenosylmethionine (AdoMet) decarboxylase transcripts in human prostatic cancer relative to benign hyperplasia (3).

Polyamines have been targeted in anticancer strategies for some time (4). Various antagonists such as the ODC inhibitor α-difluoromethylornithine (DFMO), AdoMet decarboxylase inhibitor (SAM486), and the polyamine analogue N^1,N^{11}-diethylnorspermine have undergone clinical testing as therapeutic and/or preventive agents (5, 6). Recognizing the unique physiology of the prostate gland, Heston and collaborators (7, 8) have proposed that polyamine inhibitors may be particularly effective against prostate cancer. In support of this concept, Gupta *et al.* (9) have shown that DFMO is effective in depleting polyamine pools and in preventing development of prostate cancer in the transgenic adenocarcinoma of mouse prostate (TRAMP) model (10).

Targeting polyamines has traditionally involved interference with or down-regulation of polyamine biosynthesis with small molecule inhibitors or analogues, respectively. As an alterna-

* This work was supported in part by National Institutes of Health Grant CA-76428 and by Department of Defense Grant DAMD17-03-1-0024, Core Grant CA16056, and Predoctoral Training Grant CA10972. The costs of publication of this article were defrayed in part by the payment of page charges. This article must therefore be hereby marked "*advertisement*" in accordance with 18 U.S.C. Section 1734 solely to indicate this fact.

‖ To whom correspondence and requests for reprints should be addressed: Dept. of Pharmacology and Therapeutics, Roswell Park Cancer Inst., Elm and Carlton Sts., Buffalo, NY 14263. Tel.: 716-845-3002; Fax: 716-845-2353; E-mail: carl.porter@roswellpark.org.

[1] The abbreviations used are: ODC, ornithine decarboxylase; AcSpd, N^1-acetylspermidine; DFMO, α-difluoromethylornithine; GU, genitourinary; HPCE, high performance capillary electrophoresis; MR, magnetic resonance; Put, putrescine; AdoMet, *S*-adenosylmethionine; Spd, spermidine; Spm, spermine; SSAT, spermidine/spermine N^1-acetyltransferase; Tag, SV40 large T antigen; TRAMP, transgenic adenocarcinoma of mouse prostate; H&E, hematoxylin and eosin; PBS, phosphate-buffered saline; AcSpm, acetylspermine.

tive to blocking biosynthesis, we propose that activation of polyamine catabolism by inducing the rate-limiting enzyme spermidine/spermine N^1-acetylspermine transferase (SSAT) may offer distinct advantages. The approach derives from our studies of the polyamine analogue N^1,N^{11}-diethylnorspermine that, in addition to down-regulating ODC and AdoMet decarboxylase, very potently up-regulates SSAT in tumor cells and tissues (11–14). The latter was shown to occur to a greater degree in human tumor xenografts than in normal host tissues (15). Correlations between SSAT induction and growth inhibition have been repeatedly suggested by early work in a variety of tumor types (14, 16, 17). Recently that relationship was more precisely defined by the finding that SSAT-targeted small interfering RNA minimizes analogue-mediated enzyme induction and at the same time prevents polyamine pool depletion and apoptosis (18, 19).

We have previously reported that conditional overexpression of SSAT in MCF-7 breast carcinoma cells leads to polyamine pool depletion and growth inhibition (20). As a prelude to the present study, we showed that conditional enzyme overexpression in LNCaP prostate carcinoma cells causes growth inhibition that differed from that seen in MCF-7 cells in that it was not accompanied by polyamine pool depletion (21). Instead cells averted the latter by increasing polyamine biosynthesis at the levels of ODC and AdoMet decarboxylase activities causing heightened metabolic flux through the biosynthetic and catabolic pathways. In a critical experiment, it was shown that interruption of flux by blocking ODC activity prevented growth inhibition (21). Additional studies concluded that growth inhibition deriving from overexpression of SSAT was probably attributable to overproduction of pathway products such as acetylated polyamines or to depletion of polyamine precursor metabolites such as AdoMet and/or the SSAT cofactor acetyl-CoA (21). Whatever the downstream mechanism, these *in vitro* data suggest that activation of polyamine catabolism by selective induction of SSAT may constitute an effective antitumor strategy against prostate cancer.

The goal of the present study was to further validate the above concept by providing critical *in vivo* evidence based on a genetic approach. For this purpose, we utilized the TRAMP model that is genetically engineered to develop prostate cancer (10, 22, 23). Cross-breeding these mice with SSAT transgenic mice that systemically overexpress the enzyme (24) resulted in a profound suppression of prostate tumor outgrowth that may be related to consequences emanating from depletion of acetyl-CoA pools.

EXPERIMENTAL PROCEDURES

Materials—The polyamines putrescine (Put), spermidine (Spd), spermine (Spm), and acetylated polyamine N^1-acetylspermidine (Ac-Spd) were purchased from Sigma. Acetyl-CoA was also purchased from Sigma and solubilized as described by Liu *et al.* (25).

Breeding and Screening of Transgenic Animals—TRAMP mice (10), heterozygous for the transgene rat probasin-SV40 large T antigen (PB-Tag) (lineage of founder 8247; Jackson Laboratory, Bar Harbor, ME) were maintained in a pure C57BL/6 background. Mouse tail DNA was isolated using the DNeasy® tissue kit (Qiagen Inc., Valencia, CA). Genotyping of TRAMP animals was performed by PCR according to the Jackson Laboratory protocol.

We previously generated mice that systemically overexpressed SSAT under its endogenous murine gene promoter (24). These SSAT transgenic mice, in the CD2F1 genetic background (24), were backcrossed for >8 generations into C57BL/6, the same genetic background as the TRAMP mouse. The SSAT transgenic mice are characterized by pronounced hair loss by 3–4 weeks of age (24), making genotyping unnecessary. Since female SSAT transgenic mice are infertile and male mice have normal reproductive capabilities, the latter were cross-bred with female TRAMP mice to generate the bigenic mice used in this study.

Magnetic Resonance (MR) Imaging—Longitudinal analysis of prostate cancer progression in TRAMP mice using MR imaging has been reported by Hsu *et al.* (26). More specifically, it was used to assess tumor volume and to track tumor development in TRAMP and TRAMP/SSAT mice. High resolution MR imaging scans were performed using a General Electric CSI 4.7T/33-cm horizontal bore magnet (GE NMR Instruments, Fremont, CA) with upgraded radio frequency and computer systems. MR imaging data were acquired using a custom designed 35-mm radio frequency transceiver coil and a G060 removable gradient coil insert generating a maximum field strength of 950 milliteslas/m. Transaxial, T1-weighted images were acquired through the lower abdomen with a standard spin echo MR imaging sequence. Images were comprised of 20 × 1-mm thick slices with a 3.2× 3.2-cm field of view acquired with a 192 × 192 matrix to provide contiguous image data of the prostate tumor. Acquisition parameters consisted of an echo time/repetition time = 10/724 ms and 4 number of excitations.

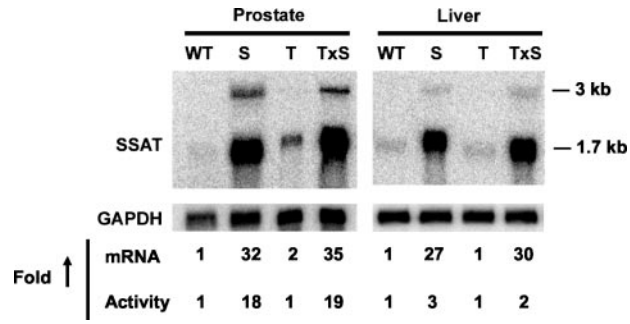

FIG. 1. **SSAT expression in the prostates and livers from SSAT transgenic mice.** Total RNA was isolated from the prostates and livers of littermates obtained from the TRAMP × SSAT cross and subjected to Northern blot analysis and enzyme activity assay (33, 39). Note the presence of a 3-kb heteronuclear SSAT RNA and a 1.7-kb mature SSAT mRNA. For quantitation, the 1.7-kb SSAT mRNA bands were scanned densitometrically and normalized to the glyceraldehyde-3-phosphate dehydrogenase (*GAPDH*) signal. Both SSAT mRNA and activity were expressed as -fold increase (*Fold* ↑) of wild-type tissue. SSAT mRNA was highly expressed in both prostate and liver of the SSAT (*S*) and the bigenic TRAMP/SSAT (*TxS*) mice but poorly expressed in the wild-type (*WT*) and TRAMP (*T*) animals. Northern blots are representative of those obtained during two experiments using 30 μg of total RNA/lane.

Pathology—Mouse genitourinary (GU) tracts consisting of bladder, urethra, seminal vesicles, ampullary gland, and the prostate were excised and weighed. The correlation of GU weight as a function of cancer progression in the TRAMP mouse is well documented by Kaplan-Lefko *et al.* (27). Once GU tracts were grossly examined and documented by fixed angle photography, the dorsal, lateral, ventral, and anterior lobes of the prostate as well as the seminal vesicles were microdissected and placed into multichamber cassettes for fixation in 4% paraformaldehyde for 4 h at 4 °C after which they were paraffin-embedded, sectioned at 5 μm, and stained with hematoxylin and eosin (H&E). H&E slides were reviewed by two experienced morphologists without knowledge of the genotype or age of the mice. Each prostatic lobe (dorsal, lateral, ventral, and anterior) was scored according to the grading system established by Gingrich *et al.* (28). The histological scores were then averaged and expressed as mean ± S.E.

Immunohistochemistry—Slides containing 5-μm sections were quenched with aqueous 3% hydrogen peroxide for 30 min and rinsed with PBS/T (500 μl/liter Tween 20) to remove endogenous peroxidases. Antigen retrieval involved continuous microwaving of the slides in 10 mM citrate buffer (pH 6.0) for 20 min. Cooled slides were washed for 5 min in PBS/T at room temperature and blocked with 0.03% casein in PBS/T for 30 min prior to the addition of primary antibodies. For anti-SV40 large T antigen staining, monoclonal anti-SV40 large T antigen antibody (catalog number 554149, BD Pharmingen) was used at a 1:400 dilution in a humidity chamber. Following overnight incubation at 4 °C, slides were washed with PBS/T and incubated for 30 min with secondary biotinylated anti-rabbit and anti-mouse immunoglobulins from the LSAB+ kit (DAKO, Carpinteria, CA) diluted according to the manufacturer's protocol. The slides were then washed with PBS/T and complexed with streptavidin (LSAB+ kit, DAKO, prediluted) for 30 min. Immunoreactive anti-SV40 large T antigen was detected by the application of the substrate 3,3′-diaminobenzidine tetrahydrochloride (DAKO) for 5 min. All sections were counterstained with hematoxylin.

Analytical Methods—Tissues were snap-frozen in liquid nitrogen, crushed into a fine powder in a mortar or a Bio-Pulverizer (BioSpec Products, Inc., Bartlesville, OK), and then sonicated on ice in Tris/

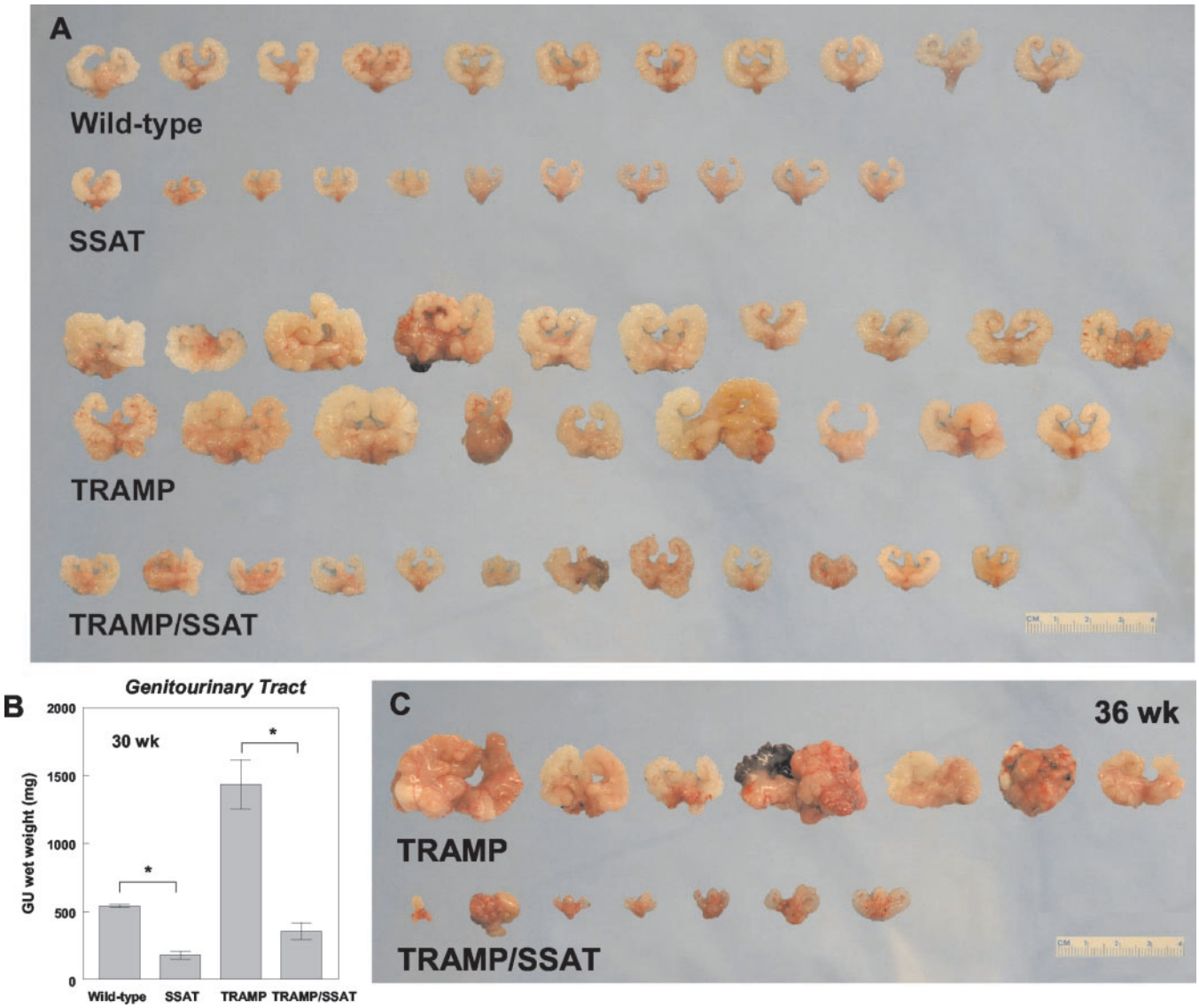

FIG. 2. **Comparison of GU tracts.** *A*, GU tracts of the four genetic cohorts deriving from the TRAMP × SSAT cross at 30 weeks. Note that the GU tracts of SSAT mice were smaller than those of wild-type mice and that the GU tracts of TRAMP/SSAT mice were much smaller and less variable in size and shape than those of TRAMP mice. *B*, GU tract weights at 30 weeks of four genetic cohorts deriving from the TRAMP × SSAT cross. The GU tracts of TRAMP/SSAT animals weighed less than TRAMP mice (*, $p < 0.0001$), and GU tracts of SSAT mice were also different from wild type (*, $p < 0.0001$) as determined by Student's unpaired *t* test. *C*, comparison of GU tracts for TRAMP and TRAMP/SSAT mice at 36 weeks of age. During the period of 30–36 weeks, the average TRAMP GU tract increased by 200%, while the average TRAMP/SSAT GU tract remained statistically the same (see Table I for detailed analysis).

EDTA buffer for polyamine enzyme activities and pool analysis. SSAT activity was assayed as described previously (29) and expressed as pmol of N^1-[^{14}C]acetylspermidine generated/min/mg of protein. Decarboxylase activities were determined by a CO_2 trap assay and expressed as pmol of CO_2 released/h/mg of protein (30). Polyamines and the acetylated derivatives of Spd and Spm were measured by high pressure liquid chromatography following methods reported by Kramer *et al.* (30). For Northern blot analysis, frozen tissues were crushed into a fine powder using a mortar and pestle after which total RNA was extracted with guanidine isothiocyanate (31) and purified by CsCl gradient centrifugation (32). RNA was loaded onto a gel at 30 μg/lane and subjected to Northern blot analysis following procedures described by Fogel-Petrovic *et al.* (33).

Acetyl-CoA Determinations—High performance capillary electrophoresis (HPCE) separation and quantitation of acetyl-CoA in tissue samples as recently described (21) was carried out following the method of Liu *et al.* (25). Tissues extracts were then analyzed on a Beckman P/ACE MDQ capillary electrophoresis system (Fullerton, CA) equipped with a photodiode array detector and an uncoated fused silica capillary electrophoresis column of 75-μm inner diameter and 60 cm in length with 50 cm from inlet to the detection window (Polymicro Technologies, Phoenix, AZ). Electrophoretic conditions were according to Liu *et al.* (25) with minor modifications as described previously (21). Data were collected and processed by Beckman P/ACE 32 Karat software version 4.0. Acetyl-CoA levels were expressed as nmol/g of tissue.

Statistics—Statistical significance (*p* value) was determined by Student's *t* test or analysis of variance with Fisher's protected least significant difference test at a 95% confidence level using a StatView computer program (SAS Institute Inc., Cary, NC).

RESULTS AND DISCUSSION

The goal of this study was to provide *in vivo* genetic validation for the concept that activating polyamine catabolism at the level of SSAT will give rise to an antitumor response due to homeostatic perturbations in polyamine metabolism. The effort was catalyzed by our recent reports showing that conditional overexpression of SSAT inhibits *in vitro* growth of both MCF-7 breast carcinoma cells (20) and LNCaP prostate carcinoma cells (21). Consistent with these findings, we now demonstrate that overexpression of SSAT markedly suppresses tumor outgrowth of early and advanced prostatic cancer in TRAMP mice. As will be discussed, this may be due to unusual sensitivity of

prostate-derived tumors to polyamine perturbations and/or to novel metabolic disturbances emanating from compensatory responses to activated polyamine catabolism.

SSAT-overexpressing transgenic male mice were cross-bred with female TRAMP mice to yield four cohorts of offspring: wild type, SSAT transgenic mice, and TRAMP and TRAMP/SSAT bigenics 15 weeks of age. Prostate and liver tissues were excised from wild-type, SSAT, TRAMP, and TRAMP/SSAT mice to confirm SSAT mRNA expression and enzyme activity. As shown in Fig. 1, prostate gland SSAT mRNA levels were elevated 32- and 35-fold in both SSAT and TRAMP/SSAT cohorts, respectively, relative to wild-type mice. Consistent with SSAT gene overexpression prostatic enzyme activity in both SSAT and TRAMP/SSAT mice was elevated by ~18-fold. SSAT mRNA in liver of SSAT and TRAMP/SSAT mice was increased 20- and 30-fold over wild-type mice, but unlike the prostate, enzyme activities were only increased 3- and 2-fold, presumably due to tissue-specific differences in translational control (24). The data confirm that overexpression of SSAT occurs in the prostate of transgene-bearing mice.

Longitudinal assessment of the prostate by MR imaging was used to monitor tumor appearance and development in representative TRAMP animals. GU tumors were first apparent at ~20 weeks of age in TRAMP animals. By 30 weeks, all TRAMP mice had visible prostate tumors that, with time, infiltrated the seminal vesicles as is typical in the pure C57BL/6 genetic background (10, 22, 27, 34). As observed using MR imaging and confirmed at necropsy, some TRAMP mice exhibited predominantly prostatic tumors, while the majority showed significant prostate tumors with seminal vesicle involvement. Both pathologies were reduced in the TRAMP/SSAT mice. On the basis of tumor size in TRAMP mice, the experimental end point was set at week 30.

The suppressive effect of SSAT overexpression on tumor outgrowth is apparent in comparisons of dissected GU tracts shown in Fig. 2*A*. Gross examination of both wild-type and SSAT animals revealed GU tracts that were generally uniform in size and shape. As graphed in Fig. 2*B*, GU tracts of the SSAT mice were significantly smaller (178 ± 30 mg) than those of the wild-type mice (504 ± 11 mg) despite close similarities in body weight (~29.7 ± 0.6 *versus* 28.5 ± 0.5 g, respectively). All of the TRAMP mice displayed visible evidence of prostatic tumors with variable involvement of the seminal vesicles. On the basis of weight, TRAMP GU tracts (1,435 ± 181 mg) were, on average, 4 times larger than those of TRAMP/SSAT mice (356 ± 62 mg). Taken together, the data indicate that SSAT overexpression effectively suppresses tumor outgrowth in the TRAMP model. Since by itself, the 30-week data may reflect a delay in tumor development as opposed to a sustained antitumor effect, we examined tumor size at a later time point. For this, 36 weeks was the longest time possible without encountering tumor excess. Relative to the 30-week data, the average GU tract weight in the TRAMP mice became 200% larger, while that in the TRAMP/SSAT mice at 36 weeks remained statistically unchanged. Thus, suppression of tumor outgrowth became even more exaggerated during the 30–36-week period. Although these findings suggest that the survival time of the TRAMP/SSAT mice would be significantly extended beyond that of the TRAMP mice, such studies were precluded by the strong tendency of the older bigenics to develop skin pathologies.

Histopathological analysis from littermates of the TRAMP and SSAT transgenic crosses at 30 weeks demonstrated that the prostate tumors of TRAMP mice were heterogeneous, ranging from high grade prostatic intraepithelial neoplasia (grade 3) to poorly differentiated adenocarcinoma (grade 6), while

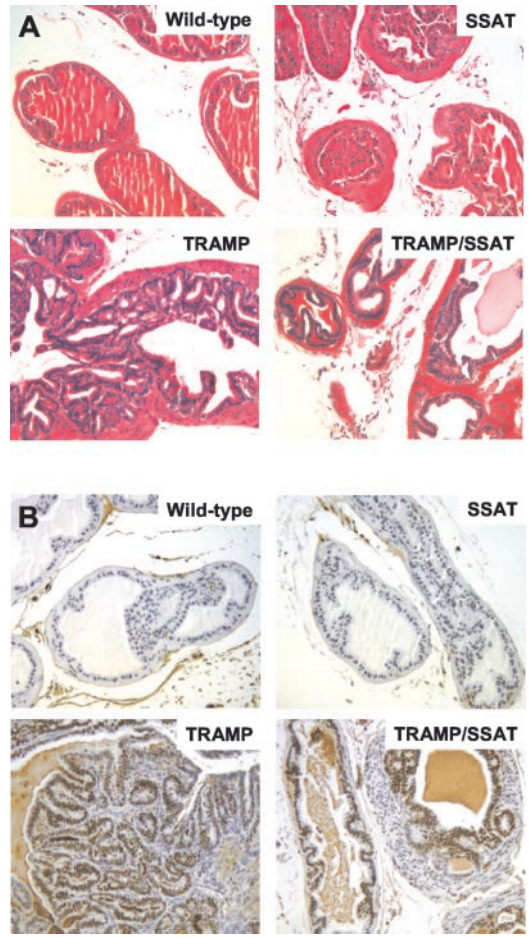

FIG. 3. **Sections of microdissected dorsal prostate.** *A*, representative H&E histological sections of the epithelium of the dorsal lobe of the mouse prostate. The four lobes of the prostate were graded and reported in Table I. TRAMP/SSAT prostates consistently displayed lower tumor grades than TRAMP prostates, which exhibited high grade prostatic intraepithelial neoplasia and well differentiated prostate carcinoma. The SSAT prostates showed normal epithelium. *B*, immunohistochemical detection of SV40 large T antigen. Expression of SV40 large T antigen was detected by immunohistochemistry in the epithelium of the dorsal lobe of 30-week-old TRAMP and TRAMP/SSAT mice but not in wild-type and SSAT mice. Large T antigen was also expressed in the glandular epithelial cells lateral, ventral, and anterior lobes (data not shown). Prostate tissues were analyzed from three mice per group. (H&E staining; microscopic magnification, 200×.)

tumors from TRAMP/SSAT mice were more homogeneous with a moderate range of prostatic intraepithelial neoplasia lesions (grades 2 and 3) and only rare evidence of well differentiated adenocarcinoma (grade 4) (Fig. 3*A*). Consistent with previous reports (28), disease in the TRAMP mouse was apparent in the dorsal, lateral, and ventral lobes with substantial seminal vesicle involvement, and it tended to be heterogeneous among mice. When all prostate lobes were averaged (Table I), the mean TRAMP/SSAT mouse grade (4.2) was significantly lower than that of the TRAMP mice (5.0) suggesting interference with disease progression. A similar trend was also seen at 36 weeks. Thus, while the major effect of SSAT overexpression is most obviously manifested as suppression of tumor outgrowth, there is also a delay in tumor progression. Because prostatic disease in the C57BL/6 background infiltrated the seminal vesicles, we derived an index to quantify overall GU disease. Thus, the average histological grades of the four lobes were averaged and then multiplied by the mean GU tract weight to derive a GU disease index for each cohort of animals (Table I). Based on this determination, the disease index at 30 weeks in

TABLE I
Genitourinary disease index of TRAMP/SSAT mice at 30 weeks

Mouse genotype	Age	No. of animals	Average prostate grade[a]			Average GU weight	GU disease index[c]	*p* value[d]
			Overall	Highest	Total[b]			
	wk				*g*			
TRAMP	30	15	2.1 ± 0.1	2.9 ± 0.1	5.0 ± 0.2	1.44 ± 0.18	7.44 ± 1.12	<0.0001
TRAMP/SSAT	30	10	2.0 ± 0.2	2.2 ± 0.2	4.2 ± 1.0	0.36 ± 0.06	1.51 ± 0.27	
TRAMP	36	8	2.8 ± 0.4	3.5 ± 0.4	6.3 ± 0.7	2.92 ± 0.81	22.57 ± 9.75	0.06
TRAMP/SSAT	36	6	2.5 ± 0.5	3.2 ± 0.5	5.6 ± 1.0	0.24 ± 0.12	2.08 ± 1.33	

[a] See Fig. 3*A* for representative histology of the prostate epithelium.
[b] The average prostate total grade for wild-type or SSAT mice was 2.0.
[c] GU disease index = (average overall grade + average highest grade) × average GU weight as determined per animal.
[d] Statistical significance (*p* value) was determined by analysis of variance with Fisher's protected least significant difference test.

TABLE II
Tissue polyamine metabolism in TRAMP × SSAT littermates
Data represent mean values ± S.E. where $n = 3$.

Mouse genotype	Tissue	Polyamine enzyme activities			Polyamine pools			
		SSAT	ODC	AdoMet DC	AcSpd[a]	Put	Spd	Spm
		pmol/min/mg protein	*pmol/h/mg protein*		*pmol/mg protein*			
Wild type	Prostate	5 ± 1	<20	60 ± 33	<40	140 ± 12	3,710 ± 402	7,990 ± 739
SSAT	Prostate	90 ± 20	190 ± 23	560 ± 81	2,440 ± 613	3,730 ± 805	7,350 ± 423	7,030 ± 458
TRAMP	Prostate	5 ± 1	<20	50 ± 19	<40	214 ± 34	4,830 ± 443	7,960 ± 881
TRAMP/SSAT	Prostate	90 ± 28	100 ± 21	370 ± 88	1,390 ± 187	3,520 ± 529	4,780 ± 858	5,280 ± 662
Wild type	Liver	15 ± 4	<20	120 ± 45	<40	<40	7,900 ± 368	8,510 ± 225
SSAT	Liver	50 ± 12	180 ± 32	940 ± 134	790 ± 210	4,260 ± 805	13,990 ± 794	5,060 ± 146
TRAMP	Liver	15 ± 2	<20	110 ± 75	<40	<40	9,510 ± 1389	10,840 ± 1,507
TRAMP/SSAT	Liver	30 ± 4	210 ± 15	550 ± 45	710 ± 241	4,520 ± 1,235	15,010 ± 2,376	5,770 ± 935

[a] AcSpm not detected in any samples.

the TRAMP/SSAT mice (1.51 ± 0.27) was found to be ~5-fold lower than that of the TRAMP mice (7.44 ± 1.12).

The suppression of tumor outgrowth seen here is consistent with a previous report showing that SSAT transgenic animals are more resistant to the development of skin papillomas under the two-stage skin carcinogenesis protocol (35). However, both studies differ from a report indicating that transgenic overexpression of SSAT in the mouse skin causes an increase in chemically induced tumor incidence (36). This is unexpected since our observations over the last 7 years find that spontaneous tumor formation was not increased in SSAT transgenic mice.[2] While the basis for this discrepancy is not immediately apparent, it is reasonable to consider that it may be due to promoter-dictated gene expression and/or to tissue-specific responses. For example, various tissues of the SSAT transgenic mouse adapt differently at the level of polyamine pool profiles (24) with some tissues, such as small intestine, displaying a greater effect on Spd than Spm pools and others, such as liver, showing a greater effect on Spm than Spd pools. Similarly different responses may be expected at the level of compensatory ODC induction, which as discussed below seems integral to the antitumor effect.

While several studies have undertaken genetic crosses with TRAMP mice, only one reports a negative effect on tumor outgrowth but not as great as that seen here. Abdulkadir *et al.* (37) showed that prostate tumorigenesis was impaired when Egr1-deficient mice were crossed with TRAMP mice. More particularly, the appearance of grossly evident tumors was delayed from 20 weeks in the TRAMP mouse to 35 weeks in the TRAMP × Egr1$^{-/-}$ mice. Of the reports in which TRAMP mice have been treated with various therapeutic and prevention agents, the most relevant involves chemoprevention of prostate carcinogenesis with the ODC inhibitor DFMO. Gupta *et al.* (9) found that DFMO in the drinking water of TRAMP mice from 8 to 28 weeks of age reduced the weight of the prostate and GU tracts by ~60% at 28 weeks while at the same time eliminating distant metastases. This is less than the 75% difference in GU weights seen here at 30 weeks. It is interesting to consider, however, that the Gupta study achieved the antitumor effect by pharmacologically *decreasing* polyamine biosynthesis, while the present study appears to have achieved a comparable effect by *increasing* polyamine biosynthesis secondary to SSAT overexpression as will be discussed below.

Before investigating the mechanistic basis for the tumor suppressive effect, we first determined that the SSAT overexpression did not interfere with expression of the driving oncogene in the TRAMP model Tag. Reduced expression of this transgene could originate systemically at the level of reduced androgen production, for example, or locally at the level of oncogene regulation. Both possibilities were eliminated by immunostaining for Tag protein levels in histological sections of 30-week TRAMP and TRAMP/SSAT prostates and tumors (Fig. 3*B*). Comparable levels of Tag were detected in the prostate epithelium of TRAMP and TRAMP/SSAT mice. Only minimal background staining was seen in the wild-type or SSAT transgenic mouse prostates or in appropriate controls lacking primary antibody. The findings confirm that Tag expression was not diminished in the TRAMP/SSAT mice and therefore was not responsible for the observed antitumor effects of SSAT.

To determine how polyamine-related events contribute to suppression of tumor outgrowth, we measured the activities of SSAT and the biosynthetic enzymes ODC and AdoMet decarboxylase as well as tissue polyamine and acetylated polyamine pools in both tumors and liver at 30 weeks. As shown in Table II, SSAT activity in the prostate tissue was elevated ~20-fold in both the SSAT and TRAMP/SSAT mice compared with wild-type and TRAMP mice. The more modest 2–3-fold enhancement of SSAT activity in the liver despite a 20-fold increase SSAT mRNA (38, 39) would seem to reflect tissue-specific translational control of this gene (38, 39). Increases in SSAT activity were accompanied by a profound (*i.e.* >10-fold) rise in biosynthesis at the level of ODC and AdoMet decarboxylase activities in both the prostate and the liver. As previously described in LNCaP cells (21), this represents a compensatory

[2] K. Kee, D. L. Kramer, and C. W. Porter, unpublished observations.

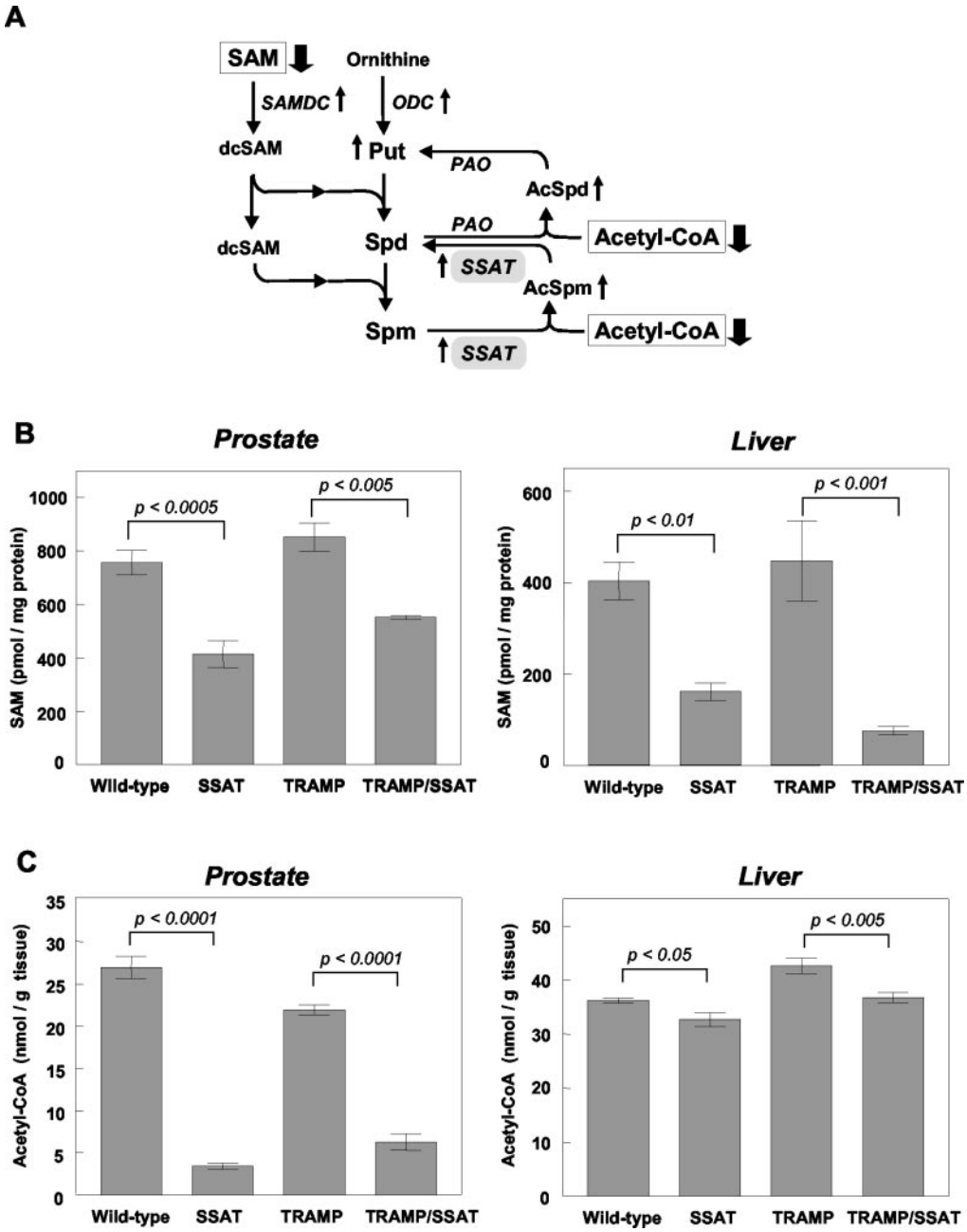

FIG. 4. **Downstream effects of SSAT overexpression.** *A*, metabolic consequences to SSAT overexpression. Activation of polyamine catabolism at the level of SSAT results in a compensatory increase in the activities of the polyamine biosynthetic enzymes ODC and AdoMet decarboxylase (*SAMDC*). This activated polyamine synthesis minimizes polyamine pool depletion despite massive production of AcSpd. At the same time, it gives rise to heightened metabolic flux through the biosynthetic and catabolic pathways (not shown). The possible downstream consequences connecting heightened metabolic flux to growth inhibition include overproduction of pathway products such as Put and AcSpd and/or depletion of critical metabolic precursors such as the aminopropyl donor AdoMet (*SAM*) and the SSAT cofactor acetyl-CoA, both of which are markedly decreased in SSAT transgenic and TRAMP/SSAT bigenic animals. *B*, AdoMet (*SAM*) levels in prostate and liver tissues of TRAMP/SSAT littermates as determined on tissue extracts by high performance liquid chromatography. Note that AdoMet pools were much lower (>40%) in the prostate and liver of SSAT and TRAMP/SSAT mice. *C*, acetyl-CoA levels in prostate and liver tissues of TRAMP × SSAT littermates as detected by HPCE. Note that during SSAT overexpression, there was significant reduction (~70%) of acetyl-CoA in the prostates of SSAT and TRAMP/SSAT mice but not in the livers. Data represents means ± S.E. where $n = 3$ animals per group. Statistical significance (p value) was determined by analysis of variance with Fisher's protected least significant difference test for pairwise comparisons. *PAO*, polyamine oxidase; *dcSAM*, decarboxylated AdoMet.

homeostatic response to activated polyamine catabolism. These changes in enzyme activities produced significant disturbances in tissue polyamine profiles particularly involving the acetylated polyamines. Although AcSpm remained undetectable, AcSpd increased from undetectable levels in the prostate and liver of wild-type and TRAMP mice to extraordinarily high levels in SSAT and TRAMP/SSAT mouse tissues. Another major finding was the accumulation of huge amounts of Put in both prostate and liver of SSAT-bearing mice, presumably due to the back conversion of Spd due to SSAT overexpression and to the forward conversion of ornithine due to high levels of ODC activity.

Despite the generation of large amounts of AcSpd, Spd pools remained relatively unaffected in the TRAMP/SSAT prostate tumors relative to TRAMP mice, while Spm decreased by ~33%, presumably due to back catabolism. This modest reduc-

tion in prostatic Spm pools hardly seems sufficient to account for the observed tumor growth suppression. As in LNCaP cells (21), the data suggest that the compensatory increase in polyamine biosynthesis and related metabolic flux may be playing a critical role in growth inhibition. More particularly, SSAT overexpression leads to massive acetylation and potential loss of cellular polyamines. To maintain a normal polyamine profile, the system responds by up-regulating ODC and AdoMet decarboxylase activities leading to a heightened metabolic flux through both arms of the pathway. Thus, ornithine is more rapidly converted to Spd and Spm, which in turn are more rapidly acted upon by SSAT to yield acetylated products. These findings are nearly identical to those elucidated in SSAT-overexpressing LNCaP prostate carcinoma cells (21) where activation of polyamine catabolism was also accompanied by increased polyamine biosynthesis. As a result, the Spd and Spm pools were unaffected despite massive production of acetylated polyamines. In a defining experiment, the relationship between this compensatory increase in ODC and growth inhibition in LNCaP cells was confirmed by the finding that growth inhibition is prevented by treatment with the ODC inhibitor DFMO. The compensatory increase in ODC and AdoMet decarboxylase activities in response to activated polyamine catabolism has been previously noted in various other tissues of the SSAT mouse (24) and, thus, is not unique to the prostate. The consequence of this effect, however, seems to be selective for both the male and female reproductive tracts since, as noted above, these are the only two organs that are underdeveloped in SSAT transgenic mice.

Guided by earlier findings in the LNCaP system (21), we examined the downstream consequences connecting heightened metabolic flux to growth inhibition or, in this case, suppression of tumor outgrowth (Fig. 1). Hence we focused on two classes of contributing events: toxic accumulation of metabolic products such as acetylated polyamines or depletion of critical metabolic precursors such as the aminopropyl donor AdoMet and/or the SSAT cofactor acetyl-CoA. Among the accumulated products, Put and AcSpd represent possible sources of tumor growth inhibition in bigenic mice and were not investigated further. On the precursor depletion side, the polyamine aminopropyl donor AdoMet and the SSAT cofactor acetyl-CoA were found to be significantly decreased in both SSAT and TRAMP/SSAT prostates. AdoMet pools were 40% lower in bigenic than in TRAMP mice (Fig. 4*B*). Even greater decreases were observed in the livers of SSAT transgenic mice. Although AdoMet is known to be critically involved in methylation reactions, it seems doubtful that the 40% pool reduction seen in the prostate tumors was growth-limiting since the liver showed a much greater decrease (85%) without obvious pathology and since the polyamines synthesized using AdoMet, Spd and Spm, were not decreased in the prostate tumors of bigenics. This does not, however, exclude the possibility that AdoMet is being preferentially diverted to polyamine biosynthesis at the expense of methylation reactions.

Attention was then focused on acetyl-CoA, which in addition to serving as a cofactor to SSAT is critically involved in fatty acid metabolism, cholesterol synthesis, and chromatin structure involving histone acetylation. Acetyl-CoA was impressively ~90% lower in prostates of SSAT mice than in wild-type mice and ~70% lower in TRAMP/SSAT mice than in TRAMP mice (Fig. 4*C*). By contrast, the acetyl-CoA pools in the livers of SSAT-bearing mice relative to non-SSAT-bearing mice were not similarly affected, consistent with the primary role of this organ in fat metabolism. Given the metabolic significance of acetyl-CoA, it is conceivable that the 70% reduction in pools seen in TRAMP/SSAT mice could impact negatively on tumor growth. An indication that such perturbations may, in fact, interfere with fatty acid metabolism is strongly suggested by the observation that SSAT mice have markedly depleted abdominal and subdermal fat stores relative to wild-type mice (Fig. 5), an effect not previously reported in the original characterization of these mice (24).

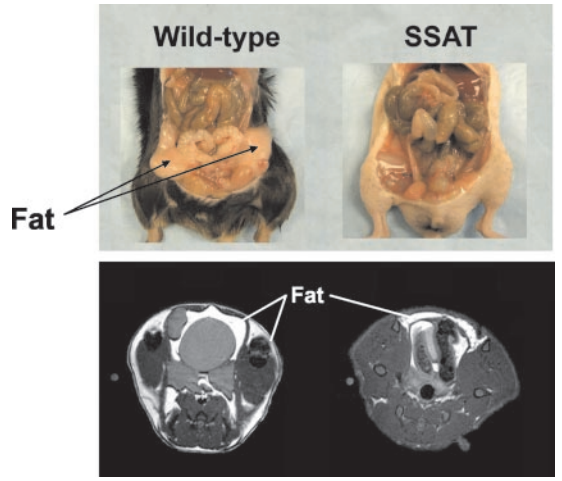

FIG. 5. **Abdominal fat stores in wild-type and SSAT transgenic mice at 30 weeks.** A comparison of dissected mice (*upper panel*) shows the presence of large abdominal/mesenteric fat deposits in wild-type animals (*left*) and the absence of similar deposits in the SSAT transgenic animals (*right*). Representative high resolution transaxial MR images (*lower panels*) of wild-type (*left*) and SSAT (*right*) mice are shown. Note the presence of abdominal and subdermal fat (seen as *bright areas*) in wild-type mice and the absence of similar deposits in SSAT transgenic mice.

As previously reported (21), acetyl-CoA was also found to be decreased during conditional overexpression of SSAT in LNCaP cells although not to the same extent as seen here. In cells, the effect correlated closely with growth inhibition, but it could not be causally linked to it. There are many previous reports suggesting a critical role for fatty acid metabolism in the prostate and prostate cancer. Intracellular lipidogenesis and *de novo* fatty acid metabolism at the level of fatty-acid synthase expression are known to be increased by androgens and have been implicated in aberrant growth of prostate tumor cells (40–42). The concept that tumors are more dependent than normal tissues on *de novo* fatty acid synthesis has led to the development of fatty-acid synthase inhibitors as anticancer agents for specific tumor types including prostate cancer (43–45). Recently Pflug *et al.* (45) demonstrated that the up-regulation of fatty-acid synthase expression plays a role in tumorigenesis in the TRAMP model and that prostate tumor cells are particularly sensitive to fatty-acid synthase inhibition. Since acetyl-CoA and malonyl-CoA are condensed by fatty-acid synthase to ultimately generate the 16-carbon polyunsaturated fatty acid palmitate, these findings imply a high dependence of prostate cancer on acetyl-CoA stores. In addition to playing a critical role in fatty acid metabolism, acetyl-CoA is also involved in controlling chromatin structure via histone acetylation. The latter opens chromatin structure and transcriptionally activates certain genes including some that mediate cell growth (46). Under conditions of limiting acetyl-CoA, such as those achieved in the prostate, it is possible that transcription of these growth-related genes may be repressed.

CONCLUSIONS

The present data provide unique insights into the *in vivo* biological potential of SSAT as a modulator of polyamine homeostasis, cellular metabolism, and tumor cell growth. These findings are reinforced by similar *in vitro* observations in

SSAT-overexpressing LNCaP cells (21). Both findings indicate that SSAT overexpression leads to up-regulation of ODC activity and to heightened metabolic flux through the polyamine pathway, which, in turn, has a significant impact on AdoMet and acetyl-CoA metabolism in both prostate cancer cells and tumors. To our knowledge, this has not been previously reported. The further possibility that these various metabolic perturbations may be responsible for the observed antitumor effect lends a novel dimension to SSAT induction that was not previously appreciated. More importantly, this study provides *in vivo* validation for the idea that pharmacological induction of SSAT may represent an effective therapeutic or preventive strategy. The finding that the normal prostate was underdeveloped in the SSAT transgenic mice would seem to indicate that such an approach may be best suited for prostate cancer in part because the organ itself appears to be uniquely dependent on acetyl-CoA as discussed above. The findings further suggest that a specific small molecule inducer of SSAT may find usefulness in targeting prostate cancer. There are a number of compounds that induce SSAT (5) with the best known being polyamine analogues such as N^1,N^{11}-diethylnorspermine (13, 47, 48). Although such analogues are potent inducers of SSAT, they also down-regulate polyamine biosynthesis, a response that would preclude heightened metabolic flux, which appears to be critical to the antiproliferative effect seen here (21). In addition, down-regulation of polyamine biosynthetic enzymes may account for the toxicity of polyamine analogues (12, 15, 16) since it is known that, unlike SSAT overexpression, which permits normal development except for hair loss and hypodeveloped reproductive tracts, ODC knock-out is embryonically lethal in mice (49). When taken together with the current data, these rationales present a compelling case for the discovery and development of a specific small molecule inducer of SSAT as a potential anticancer agent. In addition to having single agent potential, such a molecule may find application in augmenting the activity of certain clinically useful anticancer agents. For example, we have recently shown (50) that oxaliplatin and cisplatin potently up-regulate SSAT gene expression and that co-treatment with N^1,N^{11}-diethylnorspermine potentiates induction of SSAT enzyme activity as well as inhibition of cell growth. Presumably a specific SSAT inducer would behave similarly but with less host toxicity.

Acknowledgments—We gratefully acknowledge the suggestion of Dr. Paul Soloway to undertake this study and helpful discussions with Michael Moser. We also acknowledge Mehboob Shivji for assistance in the acetyl-CoA isolation protocol and greatly appreciate Mary Vaughan of the Roswell Park Institute histology core for help with histologic staining and immunohistochemistry.

REFERENCES

1. Mi, Z., Kramer, D. L., Miller, J. T., Bergeron, R. J., Bernacki, R., and Porter, C. W. (1998) *Prostate* **34,** 51–60
2. Rhodes, D. R., Barrette, T. R., Rubin, M. A., Ghosh, D., and Chinnaiyan, A. M. (2002) *Cancer Res.* **62,** 4427–4433
3. Bettuzzi, S., Davalli, P., Astancolle, S., Carani, C., Madeo, B., Tampieri, A., Corti, A., Saverio, B., Pierpaola, D., Serenella, A., Cesare, C., Bruno, M., Auro, T., and Arnaldo, C. (2000) *Cancer Res.* **60,** 28–34
4. Thomas, T., and Thomas, T. J. (2003) *J. Cell. Mol. Med.* **7,** 113–126
5. Seiler, N. (2003) *Curr. Drug Targets* **4,** 565–585
6. Seiler, N. (2003) *Curr. Drug Targets* **4,** 537–564
7. Heston, W. D., Watanabe, K. A., Pankiewicz, K. W., and Covey, D. F. (1987) *Biochem. Pharmacol.* **36,** 1849–1852
8. Heston, W. D. (1991) *Cancer Surv.* **11,** 217–238
9. Gupta, S., Ahmad, N., Marengo, S. R., MacLennan, G. T., Greenberg, N. M., and Mukhtar, H. (2000) *Cancer Res.* **60,** 5125–5133
10. Greenberg, N. M., DeMayo, F., Finegold, M. J., Medina, D., Tilley, W. D., Aspinall, J. O., Cunha, G. R., Donjacour, A. A., Matusik, R. J., and Rosen, J. M. (1995) *Proc. Natl. Acad. Sci. U. S. A.* **92,** 3439–3443
11. Libby, P. R., Bergeron, R. J., and Porter, C. W. (1989) *Biochem. Pharmacol.* **38,** 1435–1442
12. Casero, R. A., Jr., Ervin, S. J., Celano, P., Baylin, S. B., and Bergeron, R. J. (1989) *Cancer Res.* **49,** 639–643
13. Porter, C. W., Ganis, B., Libby, P. R., and Bergeron, R. J. (1991) *Cancer Res.* **51,** 3715–3720
14. Shappell, N. W., Miller, J. T., Bergeron, R. J., and Porter, C. W. (1992) *Anticancer Res.* **12,** 1083–1089
15. Porter, C. W., Bernacki, R. J., Miller, J., and Bergeron, R. J. (1993) *Cancer Res.* **53,** 581–586
16. Casero, R. A., Jr., Celano, P., Ervin, S. J., Porter, C. W., Bergeron, R. J., and Libby, P. R. (1989) *Cancer Res.* **49,** 3829–3833
17. McCloskey, D. E., and Pegg, A. E. (2000) *J. Biol. Chem.* **275,** 28708–28714
18. Chen, Y., Kramer, D. L., Li, F., and Porter, C. W. (2003) *Oncogene* **22,** 4964–4972
19. Chen, Y., Kramer, D. L., Jell, J., Vujcic, S., and Porter, C. W. (2003) *Mol. Pharmacol.* **64,** 1153–1159
20. Vujcic, S., Halmekyto, M., Diegelman, P., Gan, G., Kramer, D. L., Janne, J., and Porter, C. W. (2000) *J. Biol. Chem.* **275,** 38319–38328
21. Kee, K., Vujcic, S., Merali, S., Diegelman, P., Kisiel, N., Powell, C. T., Kramer, D. L., and Porter, C. W. (2004) *J. Biol. Chem.* **279,** 27050–27058
22. Gingrich, J. R., and Greenberg, N. M. (1996) *Toxicol. Pathol.* **24,** 502–504
23. Gingrich, J. R., Barrios, R. J., Kattan, M. W., Nahm, H. S., Finegold, M. J., and Greenberg, N. M. (1997) *Cancer Res.* **57,** 4687–4691
24. Pietila, M., Alhonen, L., Halmekyto, M., Kanter, P., Janne, J., and Porter, C. W. (1997) *J. Biol. Chem.* **272,** 18746–18751
25. Liu, G., Chen, J., Che, P., and Ma, Y. (2003) *Anal. Chem.* **75,** 78–82
26. Hsu, C. X., Ross, B. D., Chrisp, C. E., Derrow, S. Z., Charles, L. G., Pienta, K. J., Greenberg, N. M., Zeng, Z., and Sanda, M. G. (1998) *J. Urol.* **160,** 1500–1505
27. Kaplan-Lefko, P. J., Chen, T. M., Ittmann, M. M., Barrios, R. J., Ayala, G. E., Huss, W. J., Maddison, L. A., Foster, B. A., and Greenberg, N. M. (2003) *Prostate* **55,** 219–237
28. Gingrich, J. R., Barrios, R. J., Foster, B. A., and Greenberg, N. M. (1999) *Prostate Cancer Prostatic Dis.* **2,** 70–75
29. Bernacki, R. J., Oberman, E. J., Seweryniak, K. E., Atwood, A., Bergeron, R. J., and Porter, C. W. (1995) *Clin. Cancer Res.* **1,** 847–857
30. Kramer, D., Mett, H., Evans, A., Regenass, U., Diegelman, P., and Porter, C. W. (1995) *J. Biol. Chem.* **270,** 2124–2132
31. Chomczynski, P., and Sacchi, N. (1987) *Anal. Biochem.* **162,** 156–159
32. Ross, J. (1976) *J. Mol. Biol.* **106,** 403–420
33. Fogel-Petrovic, M., Shappell, N. W., Bergeron, R. J., and Porter, C. W. (1993) *J. Biol. Chem.* **268,** 19118–19125
34. Gingrich, J. R., Barrios, R. J., Morton, R. A., Boyce, B. F., DeMayo, F. J., Finegold, M. J., Angelopoulou, R., Rosen, J. M., and Greenberg, N. M. (1996) *Cancer Res.* **56,** 4096–4102
35. Pietila, M., Parkkinen, J. J., Alhonen, L., and Janne, J. (2001) *J. Investig. Dermatol.* **116,** 801–805
36. Coleman, C. S., Pegg, A. E., Megosh, L. C., Guo, Y., Sawicki, J. A., and O'Brien, T. G. (2002) *Carcinogenesis* **23,** 359–364
37. Abdulkadir, S. A., Qu, Z., Garabedian, E., Song, S. K., Peters, T. J., Svaren, J., Carbone, J. M., Naughton, C. K., Catalona, W. J., Ackerman, J. J., Gordon, J. I., Humphrey, P. A., and Milbrandt, J. (2001) *Nat. Med.* **7,** 101–107
38. Fogel-Petrovic, M., Vujcic, S., Brown, P. J., Haddox, M. K., and Porter, C. W. (1996) *Biochemistry* **35,** 14436–14444
39. Fogel-Petrovic, M., Vujcic, S., Miller, J., and Porter, C. W. (1996) *FEBS Lett.* **391,** 89–94
40. Swinnen, J. V., Esquenet, M., Goossens, K., Heyns, W., and Verhoeven, G. (1997) *Cancer Res.* **57,** 1086–1090
41. Swinnen, J. V., Ulrix, W., Heyns, W., and Verhoeven, G. (1997) *Proc. Natl. Acad. Sci. U. S. A.* **94,** 12975–12980
42. Swinnen, J. V., Vanderhoydonc, F., Elgamal, A. A., Eelen, M., Vercaeren, I., Joniau, S., Van Poppel, H., Baert, L., Goossens, K., Heyns, W., and Verhoeven, G. (2000) *Int. J. Cancer* **88,** 176–179
43. Kuhajda, F. P., Pizer, E. S., Li, J. N., Mani, N. S., Frehywot, G. L., and Townsend, C. A. (2000) *Proc. Natl. Acad. Sci. U. S. A.* **97,** 3450–3454
44. Pizer, E. S., Pflug, B. R., Bova, G. S., Han, W. F., Udan, M. S., and Nelson, J. B. (2001) *Prostate* **47,** 102–110
45. Pflug, B. R., Pecher, S. M., Brink, A. W., Nelson, J. B., and Foster, B. A. (2003) *Prostate* **57,** 245–254
46. Marks, P., Rifkind, R. A., Richon, V. M., Breslow, R., Miller, T., and Kelly, W. K. (2001) *Nat. Rev. Cancer* **1,** 194–202
47. Casero, R. A., Jr., Celano, P., Ervin, S. J., Wiest, L., and Pegg, A. E. (1990) *Biochem. J.* **270,** 615–620
48. Pegg, A. E., Pakala, R., and Bergeron, R. J. (1990) *Biochem. J.* **267,** 331–338
49. Pendeville, H., Carpino, N., Marine, J. C., Takahashi, Y., Muller, M., Martial, J. A., and Cleveland, J. L. (2001) *Mol. Cell. Biol.* **21,** 6549–6558
50. Hector, S., Porter, C. W., Kramer, D. L., Clark, K., Chen, Y., and Pendyala, L. (2004) *Mol. Cancer Ther.* **3,** 813–822

Polyamine catabolism in platinum drug action: Interactions between oxaliplatin and the polyamine analogue N^1,N^{11}-diethylnorspermine at the level of spermidine/spermine N^1-acetyltransferase

Suzanne Hector,[1] Carl W. Porter,[2] Debora L. Kramer,[2] Kimberly Clark,[1] Joshua Prey,[1] Nicholas Kisiel,[2] Paula Diegelman,[2] Ying Chen,[2] and Lakshmi Pendyala[1]

Departments of [1]Medicine and [2]Pharmacology and Therapeutics, Roswell Park Cancer Institute, Buffalo, New York

Abstract

A great deal of experimental evidence connects induction of polyamine catabolism via spermidine/spermine N^1-acetyltransferase (SSAT) to antiproliferative activity and apoptosis. Following our initial observation from gene expression profiling that platinum drugs induce SSAT, we undertook this present study to characterize platinum drug induction of SSAT and other polyamine catabolic enzymes and to examine how these responses might be enhanced with the well-known inducer of SSAT and clinically relevant polyamine analogue, N^1,N^{11}-diethylnorspermine (DENSPM). The results obtained in A2780 ovarian cancer cells by real-time quantitative RT-PCR and Northern blot analysis show that a 2-hour exposure of A2780 cells to platinum drugs induces expression of SSAT, a second SSAT (SSAT-2), spermine oxidase, and polyamine oxidase in a dose-dependent manner. At equitoxic doses, oxaliplatin is more effective than cisplatin in SSAT induction. The most affected enzyme, SSAT, increased 15-fold in mRNA expression and 2-fold in enzyme activity. When combined with DENSPM to further induce SSAT and to enhance conversion of mRNA to activity, oxaliplatin increased SSAT mRNA 50-fold and activity, 210-fold. Polyamine pools declined in rough proportion to levels of SSAT induction. At pharmacologically relevant oxaliplatin exposure times (20 hours) and drug concentrations (5 to 15 μmol/L), these responses were increased even further. Combining low-dose DENSPM with oxaliplatin produced a greater than additive inhibition of cell growth based on the sulforhodamine-B assay. Taken together, the findings confirm potent induction of polyamine catabolic enzymes, such as SSAT by platinum drugs, and demonstrate that these biochemical responses as well as growth inhibition can be potentiated by co-treatment with the polyamine analogue DENSPM. With appropriate *in vitro* and *in vivo* optimization, these findings could lead to clinically relevant therapeutic strategies. [Mol Cancer Ther 2004; 3(7):813–22]

Received 12/24/03; revised 3/23/04; accepted 5/4/04.

Grant support: CA-22153, CA-76428, and CA-16056.

The costs of publication of this article were defrayed in part by the payment of page charges. This article must therefore be hereby marked advertisement in accordance with 18 U.S.C. Section 1734 solely to indicate this fact.

Requests for reprints: Lakshmi Pendyala, Department of Medicine, Roswell Park Cancer Institute, Buffalo, NY 14263. Phone: 716-845-3287; Fax: 716-845-1659. E-mail: lakshmi.pendyala@roswellpark.org

Introduction

Platinum drugs are an important component of modern chemotherapy regimens. Cisplatin (*cis*-diamminedichloro platinum II) is the prototype platinum drug showing activity in many cancers, including testicular, ovarian, head and neck, and bladder. Oxaliplatin (*trans-l*-1,2-diaminocyclohexane oxalato platinum II) is a third-generation platinum drug which in addition to exhibiting activity in tumors that are traditionally sensitive to cisplatin (1, 2) has shown activity in colon cancer, a disease in which cisplatin is inactive (3). Oxaliplatin is approved for the treatment of colorectal cancer in the United States.

Many *in vitro* studies and some *in vivo* studies indicate that oxaliplatin is non-cross-resistant to cisplatin (4-7). Comparative cytotoxicity studies of cisplatin and oxaliplatin conducted in the NCI human tumor cell line panel indicate that the two drugs may have different mechanisms of action (8). Both drugs produce intra- and inter-strand DNA-platinum adducts (7, 9, 10) that are believed to account for cytotoxicity. To gain insight into other potential mechanisms of platinum drug action, we did gene expression profiling of A2780 ovarian carcinoma cells exposed to cisplatin or oxaliplatin (11). Affymetrix oligonucleotide arrays revealed a large number of genes that were up- or down-regulated by both platinum drugs. Self-Organizing Map cluster analysis indicated that the expression changes for many genes were progressive with time and that the greatest increases or decreases occurred 16 to 24 hours following a 2-hour, IC_{90} drug exposure. Of particular interest, the polyamine catabolic enzyme spermidine/spermine N^1-acetyltransferase (SSAT) was among the top 10 genes up-regulated by oxaliplatin and among the top 20 genes up-regulated by cisplatin. This unexpected and provocative finding warranted further investigation.

The requirement of polyamines in cell growth is typically met by a biosynthetic pathway regulated by ornithine decarboxylase and *S*-adenosylmethionine decarboxylase and balanced by a polyamine catabolic or back-conversion pathway regulated by SSAT. Because tumor cells typically contain higher polyamine levels and greater rates of

polyamine biosynthetic activity than their normal tissue counterparts (12), antitumor strategies have been developed to deplete polyamine pools. Traditionally, this has been achieved with specific inhibitors of the biosynthetic enzymes ornithine decarboxylase or *S*-adenosylmethionine decarboxylase. More recently, this has been accomplished with regulators of polyamine metabolism, such as the polyamine analogue N^1,N^{11}-diethylnorspermine (DENSPM), which down-regulates both ornithine decarboxylase and *S*-adenosylmethionine decarboxylase while potently up-regulating SSAT and polyamine catabolism (13). Several lines of evidence strongly suggest that SSAT is a key determinant of DENSPM action (14-16) and directly responsible for the differential sensitivity of various cell types to the analogue (17). DENSPM has been evaluated in phase I clinical trials (18, 19).

Polyamine catabolism or back-conversion is mediated by the sequential action of SSAT and polyamine oxidase (PAO). Thus, spermine and spermidine are acetylated by SSAT and then oxidized to spermidine and putrescine, respectively, by PAO (20). In addition, acetylated spermidine is efficiently exported out of the cells, thus, contributing to polyamine pool depletion (21). Two additional genes involved in polyamine catabolism have recently been identified: spermine oxidase (SMO) and a second SSAT (SSAT-2). SMO differs from PAO in its preference for the direct oxidation of unacetylated spermine to spermidine (22), a reaction that effectively bypasses the SSAT/PAO-mediated back-conversion pathway (23). Human SSAT-2 is located on chromosome 17 (24) and shares 46% amino acid sequence identity with SSAT that is located on the human chromosome X (25). The substrate specificity of the new enzyme is distinctly different from that of SSAT and it seems from transfection studies, that the enzyme may be isolated from intracellular polyamines by organelle compartmentalization (24). Under conditions of induction, both enzymes have the potential to impact on polyamine homeostasis and, thus, affect cell growth.

We have undertaken the current study because our earlier Affymetrix data identified SSAT induction as a prominent gene response to platinum drugs and because SSAT induction has been causally linked to growth inhibition and apoptosis (26, 27). The goals of this investigation are to further characterize the effect of platinum drugs on SSAT and other components of polyamine catabolism and to examine how these responses might be exaggerated by drug combinations involving the well-known SSAT inducer DENSPM.

Materials and Methods

Drugs

Oxaliplatin was a gift from Dr. Paul Juniewicz of Sanofi-Synthelabo (Malvern, PA). Cisplatin was purchased from Sigma Chemical Co. (St. Louis, MO). DENSPM was generously provided by Dr. Ronald Merriman from Pfizer Pharmaceuticals (Ann Arbor, MI).

Cell Culture

A2780 human ovarian carcinoma cell line was a gift from Dr. Ozols (Fox Chase Cancer Center, Philadelphia, PA). The *Mycoplasma*-free cells are maintained in RPMI 1640 supplemented with 10% fetal bovine serum and 1% L-glutamine and maintained at 37°C in humidified 5% CO_2 atmosphere. This cell line shows similar sensitivity to both oxaliplatin and cisplatin. The human melanoma cell lines MALME-3M and SK-MEL-28 were obtained from American Type Culture Collection (Manassas, VA) and cultured as previously described (27). The transformed human kidney HEK-293 cells were obtained from Life Technologies (Gaithersburg, MD) and cultured as previously described (22).

Drug Treatment Conditions

All drug treatments were conducted on logarithmically growing cells that were plated the previous day. Initial experiments were carried out to validate the previous Affymetrix data (11). For these, cells (1×10^6/25 cm^2 culture flask) were exposed to IC_{10} to IC_{90} concentrations of either oxaliplatin or cisplatin for 2 hours, and incubated for 24 hours in drug-free medium. Control cultures were identically manipulated but, in the absence of drug. To study the effects on gene expression, activity, and polyamine pools, 5×10^6 cells/175 cm^2 culture flask were exposed to the drug(s). For sequential drug treatments, cells were exposed for 2 hours to oxaliplatin (32 μmol/L), washed thoroughly with PBS, and incubated in drug-free or in 10 μmol/L DENSPM-containing medium for 24 hours. DENSPM treatment alone consisted of incubating cells in drug-free medium for 2 hours, followed by incubation in 10 μmol/L DENSPM for 24 hours. For concurrent drug treatments, cells were exposed to 32 μmol/L oxaliplatin and 10 μmol/L DENSPM for 2 hours, washed free of the drugs, and re-incubated for a further 24 hours in DENSPM. Cells were harvested at the end of each of the two treatments and assayed for gene expression, enzyme activity, and polyamine pools as described below. SSAT induction and polyamine pool depletion were also examined during treatment with pharmacologically relevant exposure time and concentrations of oxaliplatin. Thus, cells were treated with 5, 10, and 15 μmol/L oxaliplatin for 20 hours, cells washed free of the drug, and incubated for another 24 hours before harvesting the cells. For evaluating the combined effect with DENSPM, cells were treated concurrently with 10 μmol/L oxaliplatin and 10 μmol/L DENSPM for 20 hours, followed by a further 24 hours in drug-free medium; single agent treatments were carried out under identical exposure and further incubation conditions.

Cell Growth

Growth inhibition experiments were carried out using sulforhodamine-B micro-culture colorimetric assay as previously described (5). Sulforhodamine-B assay is a colorimetric assay in which the protein biomass is determined by dye binding to basic amino acids (28). In sequential drug treatment, cells were first treated for 2 hours with oxaliplatin, washed free of drug, and then incubated in DENSPM-containing medium (at the concentrations

indicated) for an additional 24 hours. In concurrent drug treatment, cells were exposed to varying concentrations of oxaliplatin and 0.5 μmol/L DENSPM for 2 hours, washed free of the drugs, and then incubated in 0.5 μmol/L DENSPM-containing medium for an additional 24 hours. Following either sequential or concurrent drug treatments, cells were incubated in drug-free medium for a further 48 hours, before fixation and staining with sulforhodamine-B.

Northern Blot Analysis

Northern blot analysis was used in initial experiments to evaluate the effect of oxaliplatin on the expression of both the heteronuclear mRNA (3.5 kb) and the processed mature mRNA (1.3 kb), as described previously (29). Briefly, total RNA was extracted with RNeasy Mini Kit (Qiagen Inc., Valencia, CA). RNA samples (10 μg/lane) were separated on 1.5% agarose/formaldehyde gels and transferred to nylon membrane. The membrane was hybridized to ^{32}P-labeled cDNA probes for detection of SSAT mRNA and exposed for autoradiography. The glyceraldehyde-3-phosphate dehydrogenase signal was used as a loading control.

Real-time Quantitative RT-PCR

Real-time quantitative RT-PCR (QRT-PCR; Taqman assay) with PE-ABI Prism 7700 Sequence Detection System was used to measure the expression of SSAT, SSAT-2, SMO, and PAO. The mRNA levels of the gene of interest and that of the internal standard (β-actin) were measured concurrently from the same cDNA preparations. Total RNA was extracted using Qiagen RNeasy spin columns (Qiagen, Valencia, CA). cDNA was synthesized using Superscript II reverse transcriptase followed by PCR with PE-ABI 7700 (Foster City, CA). The detection and quantitation of PCR product with PE-ABI 7700 is by fluorescence with the use of gene specific primers and a fluorogenic probe. The comparative C_T method of quantitation was used as described previously (5). All mRNA expression values are ratios to β-actin and all values are $\times 10^{-3}$. Data shown are fold increase for treated relative to untreated controls.

The primers and probes for SSAT, SSAT-2, and β-actin were purchased from Applied Biosystems Inc. (Foster City, CA), as ready-to-use kits (SSAT, Assay on Demand, Assay no. Hs00161511_m1; SSAT-2, Assay-on-Demand, Assay no. Hs00374138_g1; β-actin, pre-developed assay reagent, part no. 4310881E). The SSAT probe lies on the exon 3/exon 4 junction (accession no. NM_002970). The SSAT-2 probe lies on the exon 2/exon 3 junction (accession no. AF348524). Primers and probes for SMO and PAO were designed through Applied Biosystems Inc., under ''Assay-by-Design'' option and are as follows:

SMO (accession no. AK000753)
Forward primer: 5′-GGCAGTGGCCGAGATCTG-3′
Reverse primer: 5′-CGCCGAGGTTTTGGAATGTT-3′
Probe: 5′-FAM-TTCACAGGGAACCCC-NFQ-3′
PAO (accession no. XM_113593)
Forward primer: 5′-GGTTCCGGAAGCTCATTGG-3′
Reverse primer: 5′-GGCAATGAACCCACAGAGAAC-3′
Probe: 5′-FAM-TGGACAGACGCAAAGG-NFQ-3′
(Reverse)

Both Assay on Demand and Assay by Design probes are MGB (Minor Groove Binding) with a 5′ FAM (6-carboxy-fluorescein) reporter dye and 3′ NFQ (non-fluorescent quencher).

SSAT Activity

SSAT activity assay was done as described previously (17). In brief, the reaction mixture consists of [^{14}C]acetyl-CoA, spermidine, and cell extract in Tris-HCl buffer and the [^{14}C]acetylated spermidine product generated by the enzyme reaction is captured on discs and subjected to radioactivity counting. The activity is expressed as pmol/min/mg protein.

Polyamine Pools

Intracellular polyamine pools and acetylated polyamine pools were extracted with 0.6 N perchloric acid, dansylated and analyzed using reverse phase high-performance liquid chromatography with fluorescence detection as previously described (16).

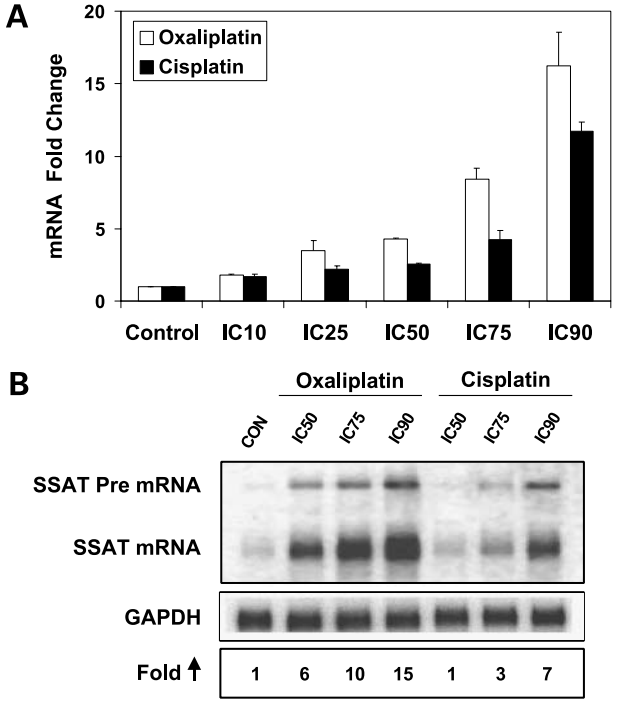

Figure 1. Effect of platinum drugs on SSAT mRNA. **A,** changes in SSAT mRNA in A2780 cells following exposure to increasing concentrations of either oxaliplatin or cisplatin, measured by real-time QRT-PCR. Cells were treated for 2 hours with IC_{10}, IC_{25}, IC_{50}, IC_{75}, and IC_{90} concentrations of oxaliplatin at 2.8, 4.8, 8.5, 17, and 32 μmol/L, respectively, or cisplatin at 2.6, 4.0, 6.4, 12, and 25 μmol/L, respectively, followed by 24 hours incubation in drug-free medium before RNA extraction. SSAT/β-actin mRNA in control cells was 2.7 ± 0.1. *Columns*, mean fold change (relative to untreated controls) from two separate experiments, each consisting of three separate PCRs; *bars*, SE. **B,** Northern blot analysis of A2780 cells exposed to oxaliplatin versus cisplatin. Cells were treated for 2 hours with oxaliplatin or cisplatin at IC_{50}, IC_{75}, and IC_{90} concentrations followed by 24 hours incubation in drug-free medium before RNA extraction and hybridization. SSAT mRNA bands were scanned densitometrically, normalized to glyceraldehyde-3-phosphate dehydrogenase, and expressed as fold increase for treated relative to control (*CON*). The data show that the heteronuclear (*Pre mRNA*, ~3.5 kb) as well as the mature message (~1.3 kb) increased with treatment.

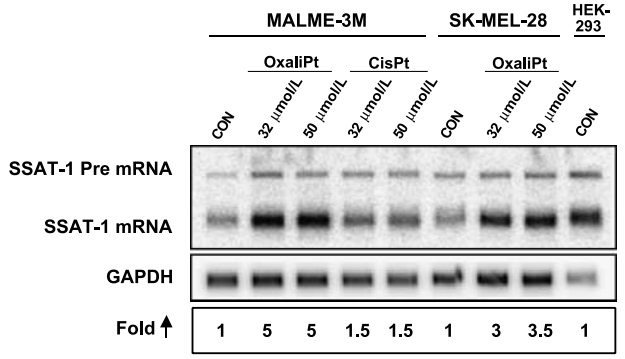

Figure 2. Effect of oxaliplatin or cisplatin on SSAT-1 mRNA expression in MALME-3M and SK-MEL-28 cells as evaluated by Northern blot analysis. Cells were treated for 2 hours with oxaliplatin (*OxaliPt*) or cisplatin (*CisPt*) at 32 or 50 μmol/L and then incubated in drug-free medium for an additional 24 hours before RNA isolation (10 μg total RNA loaded per lane). Data are representative of findings from two experiments.

Results

The changes in SSAT gene expression previously noted by Affymetrix analysis were evaluated by real-time QRT-PCR after a 2-hour exposure of cells to IC_{10} to IC_{90} concentration of oxaliplatin or cisplatin followed by a 24-hour incubation in drug-free medium. As shown in Fig. 1A, there was a dose-dependent increase in the SSAT expression following treatment with either platinum drug. At equitoxic concentrations, oxaliplatin was more effective at increasing SSAT mRNA than cisplatin. Oxaliplatin increased expression 2-fold at an IC_{10} concentration and ~16-fold at an IC_{90} dose.

Northern blot analysis was carried out on oxaliplatin- and cisplatin-treated A2780 cells (Fig. 1B). A major increase in mature SSAT mRNA (~1.3 kb) was accompanied by a concomitant increases in heteronuclear pre-processed SSAT mRNA (~3.5 kb), suggesting an increase in SSAT gene transcription (30). The increases in both the heteronuclear and mature SSAT mRNA were concentration dependent and confirm the QRT-PCR observation, that at equitoxic concentrations, oxaliplatin is a more potent inducer of SSAT than cisplatin. To determine whether SSAT induction by platinum drugs was unique to A2780 cells, induction of SSAT was examined in MALME-3M and SK-MEL-28 human melanoma cell lines. Northern blot analysis (Fig. 2) revealed that in similarity to A2780 cells, oxaliplatin induced SSAT expression by 3- to 5-fold in these cell lines.

Although the IC_{90} of oxaliplatin produced a 15-fold increase in SSAT mRNA, SSAT activity rose by only ~2-fold (Fig. 3A). This is consistent with a known translational control of SSAT message that limits induction of SSAT activity (30). As shown in Fig. 3B, this modest increase in activity was associated with a ~30% reduction in the cellular spermine, 40% decrease in spermidine, and 60% decrease in putrescine. Despite these polyamine changes, the actual SSAT products, acetylspermine or acetylspermidine, were not detected in polyamine pool analysis.

We have previously shown that SSAT activity is under posttranscriptional regulation and that significant mRNA induction is not always followed by comparable increases in enzyme activity (30, 31). This translational block can be overcome by posttreatment with a natural polyamine, such as spermine, or even more effectively, with a polyamine analogue, such as DENSPM (30). Thus, nonspecific induction of SSAT mRNA by inhibitors of proteins synthesis, for example, could be converted to huge increases in enzyme activity by posttreatment with DENSPM (30). Following this paradigm, we first treated cells for 2 hours with 32 μmol/L oxaliplatin to transcriptionally induce SSAT mRNA and then exposed them to 10 μmol/L DENSPM for 24 hours to facilitate translation of message and stabilization of enzyme protein. The effects of this drug combination on SSAT gene expression and SSAT activity and the resulting impact on intracellular polyamine pools are shown in Fig. 4A and B. Oxaliplatin alone increased SSAT mRNA 15-fold, DENSPM increased it 5-fold, and the drug

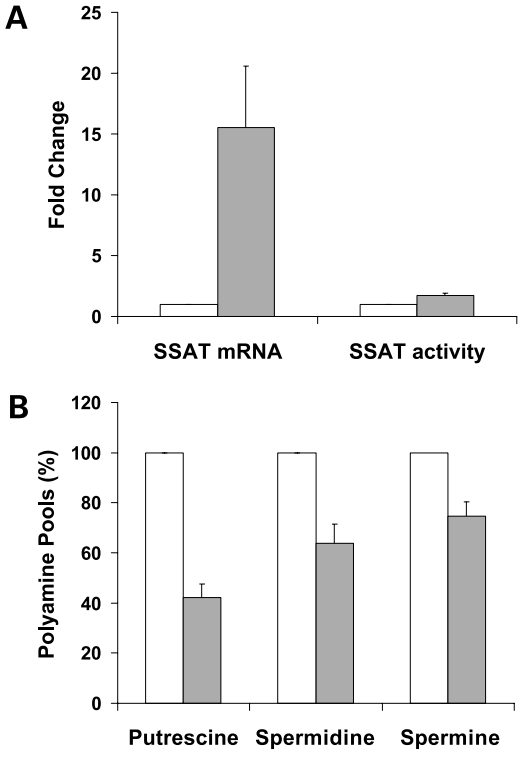

Figure 3. Effect of oxaliplatin on SSAT mRNA, activity, and polyamine pools in A2780 cells. **A,** changes in SSAT mRNA and enzyme activity in A2780 cells following exposure to 32 μmol/L oxaliplatin for 2 hours and incubation in drug-free medium for 24 hours. *Open bars*, control cells that did not receive the drug; *filled bars*, oxaliplatin-treated cells. SSAT/β-actin mRNA in control cells was 3.1 ± 0.24; SSAT enzyme activity in control cells was 29.1 ± 0.3 pmol/min/mg protein. Gene expression data: *Columns*, mean fold change (relative to untreated controls) from two separate experiments, each consisting of three separate PCRs; *bars*, SE. Enzyme activity data: *Columns*, mean fold change (relative to untreated controls), where $n = 3$; *bars*, SE. **B,** changes in putrescine, spermidine, and spermine pools in A2780 cells following exposure to 32 μmol/L oxaliplatin for 2 hours and incubation in drug-free medium for 24 hours. *Open bars*, control cells that did not receive the drug; *filled bars*, oxaliplatin-treated cells. *Columns*, means ($n = 3$); *bars*, SE. Putrescine in control cells was 604 ± 130 pmol/10^6 cells; spermidine, 3,704 ± 496 pmol/10^6 cells; spermine, 2,387 ± 332 pmol/10^6 cells.

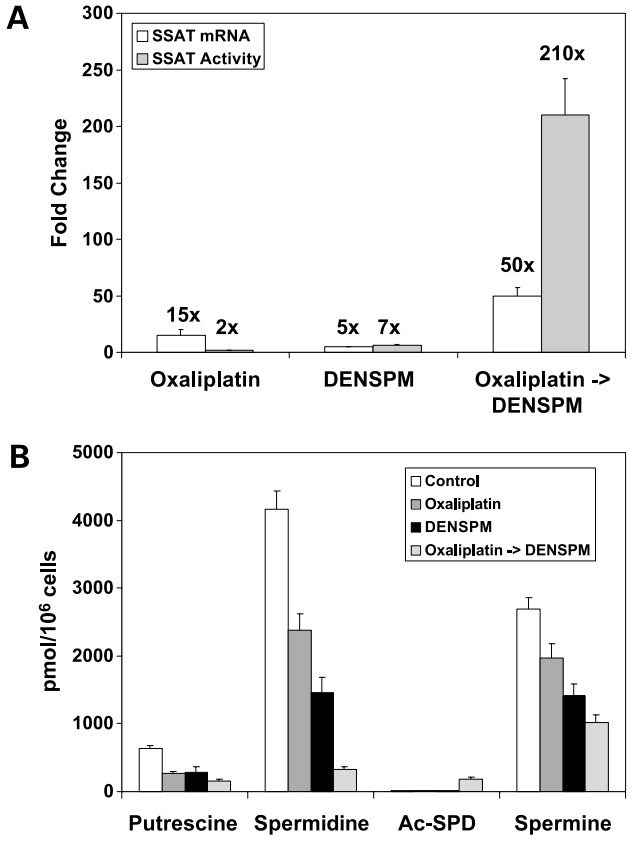

Figure 4. Effect of oxaliplatin alone (32 μmol/L oxaliplatin for 2 hours followed by 24 hours in drug-free medium), DENSPM alone (2 hours drug-free medium followed by 10 μmol/L DENSPM for 24 hours), or oxaliplatin plus DENSPM (32 μmol/L oxaliplatin for 2 hours followed by 10 μmol/L DENSPM for 24 hours) on (**A**) SSAT mRNA, SSAT activity, and (**B**) polyamine pools. In **A,** SSAT/β-actin mRNA in control cells was 3.1 ± 0.24; SSAT enzyme activity in control cells was 29.1 ± 0.3 pmol/min/mg protein. Gene expression data: *Columns*, mean fold change (relative to untreated controls) from two separate experiments, each consisting of three separate PCRs; *bars*, SE. Enzyme activity data: *Columns*, mean fold change (relative to untreated controls), where $n = 3$; *bars*, SE. In **B,** polyamine pools are expressed as pmol/10^6 cells ± SE, where $n = 3$. *Ac-SPD*, N^1-acetylspermidine.

combination brought a 50-fold increase. An even greater interaction between the two drugs was seen at the level of SSAT activity. Relative to the untreated control, oxaliplatin increased enzyme activity ~2-fold, DENSPM, 7-fold and the drug combination, 210-fold. We note that these fold increases in activity almost certainly underestimate the actual increase in activity because nonspecific cellular acetyltransferases detected by the assay contribute significantly to the basal enzyme levels but to a much lesser extent to the drug-induced levels (17). Consistent with the increase in SSAT activity, all the polyamine pools were markedly lowered after each of the three drug treatments (Fig. 4B). They were most affected, however, by the sequential combination, which produced a 76% depletion in putrescine, a 92% depletion of spermidine, and a 62% depletion of spermine pools. A very significant increase in N^1-acetylspermidine (i.e., from not detectable levels to 182 pmol/10^6 cells) was observed in cells treated with the drug combination, with the presumption that even more product was probably exported into the media.

We next determined whether the potent increase in SSAT mRNA and activity was affected by how the two drugs were combined. Thus, the effects of a 2-hour concurrent exposure to oxaliplatin (32 μmol/L) and DENSPM (10 μmol/L) followed by 24 hours DENSPM was compared with the sequential exposure described above. As shown in Fig. 5, the increase in SSAT mRNA and activity was significantly greater when oxaliplatin and DENSPM were administered concurrently and then followed by additional DENSPM treatment. SSAT activity rose 423-fold during concurrent treatment as compared with 210-fold during sequential treatment. Under these same conditions, near total depletion of all three polyamines was achieved (i.e., putrescine was depleted by 97%; spermidine, by 97%; and spermine, by 76%).

We next examined the effects of platinum drugs on the expression of the three recently identified polyamine catabolic enzymes: SMO (22), PAO (20), and SSAT-2 (24). As shown in Fig. 6, both platinum drugs induced all three genes in a dose-dependent manner with SMO expression being the most affected followed by PAO and SSAT-2. The effect of the drug combination on these genes was then examined (Fig. 7). In similarity to observations in other cell lines (24), DENSPM did not increase SSAT-2 mRNA levels in A2780 cells. It did, however, increase PAO and SMO, but not as effectively as oxaliplatin. Following 24 hours treatment with 10 μmol/L DENSPM, the fold change for SMO, PAO, and SSAT-2, mRNA was 2.5-, 1.4-, and 0.7-fold, respectively, compared with 7-, 3-, and 3.2-fold, respectively,

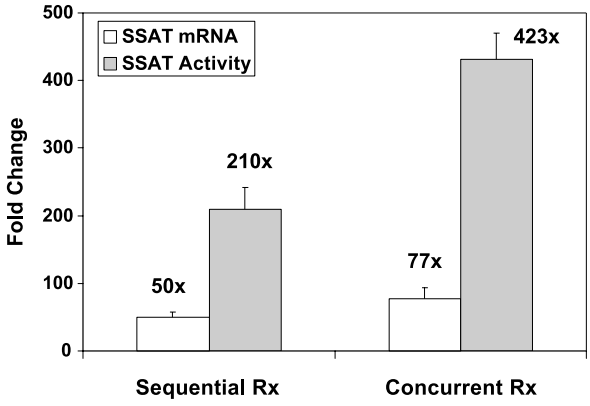

Figure 5. Effect of drug (oxaliplatin and DENSPM) exposure schedule on SSAT mRNA and activity. For sequential exposures, cells were treated with 32 μmol/L oxaliplatin for 2 hours, followed by 10 μmol/L DENSPM for 24 hours; the mRNA and activity levels in control cells are as shown in Fig. 4. For concurrent exposure, cells were treated with 32 μmol/L oxaliplatin and 10 μmol/L DENSPM for 2 hours, followed by 10 μmol/L DENSPM for 24 hours. SSAT/β-actin mRNA in control cells was 4.7 ± 0.4; SSAT enzyme activity in control cells was 24 ± 1.0 pmol/min/mg protein. Gene expression data: *Columns*, mean fold change (relative to untreated controls) from two separate experiments, each consisting of three separate PCRs; *bars*, SE. Enzyme activity data: *Columns*, mean fold change (relative to untreated controls), where $n = 3$; *bars*, SE.

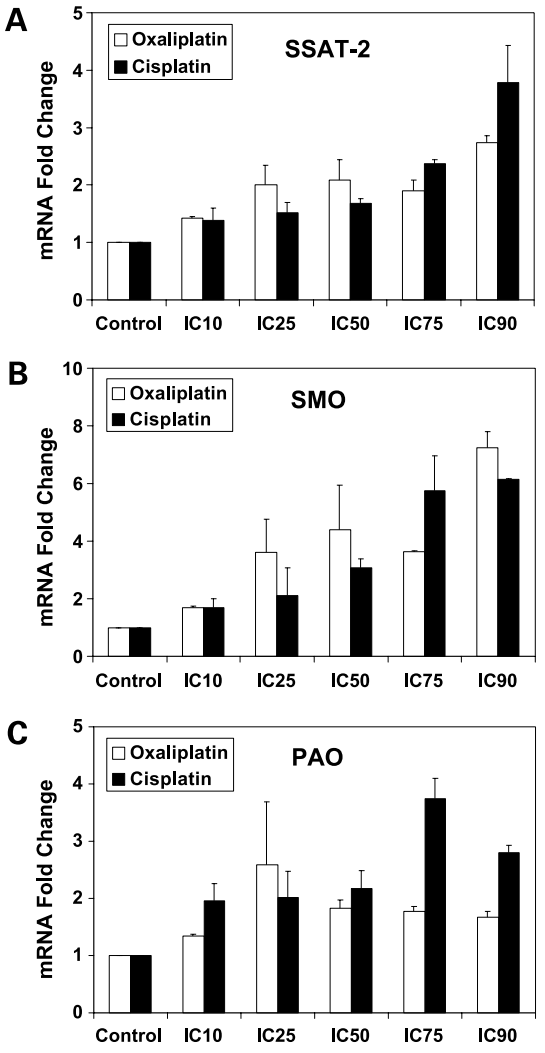

Figure 6. Changes in mRNA expression for SSAT-2, SMO, and PAO in A2780 cells following exposure to increasing concentrations of either oxaliplatin or cisplatin, measured by real-time QRT-PCR. The experimental details are the same as those described for Fig. 1. Aliquots of the same cDNA generated for SSAT mRNA expression experiments described in Fig.1A are used here for the measurement of SSAT-2 (**A**), SMO (**B**), and PAO (**C**) expression. The levels of SSAT-2, SMO, and PAO mRNA in control (no drug) were 27.5 ± 0.7, 0.9 ± 0.2, and 1.9 ± 1.0, respectively. *Columns*, mean fold change (relative to untreated controls) from two separate experiments, each consisting of three separate PCRs; *bars*, SE.

with 32 μmol/L oxaliplatin for 2 hours. The sequential drug combination induced significantly more SMO mRNA than either drug alone, whereas induction of PAO and SSAT-2 was similar to that of oxaliplatin alone (Fig. 7). Thus, the fold increase in expression of SMO was 2.5-fold by DENSPM alone, 7-fold by oxaliplatin alone, and 16-fold, by the drug combination. Concurrent treatment conditions yielded nearly identical effects on the three genes as sequential treatment (data not shown).

Considering that clinical pharmacokinetic studies of oxaliplatin indicate a 20-hour half-life for the free platinum and that the plasma concentrations of free and total platinum are in the order of 5 to 15 μmol/L (32, 33), we evaluated the effect of a 20-hour exposure of 5, 10, and 15 μmol/L oxaliplatin followed by a 24 incubation in drug-free medium on SSAT mRNA, activity, and polyamine pools. As shown in Fig. 8A, these pharmacologically relevant treatment conditions induced higher levels of SSAT mRNA and activity than those seen under the more intensive treatment conditions depicted in Fig. 4. Similarly, cellular spermine and spermidine pools were depleted by

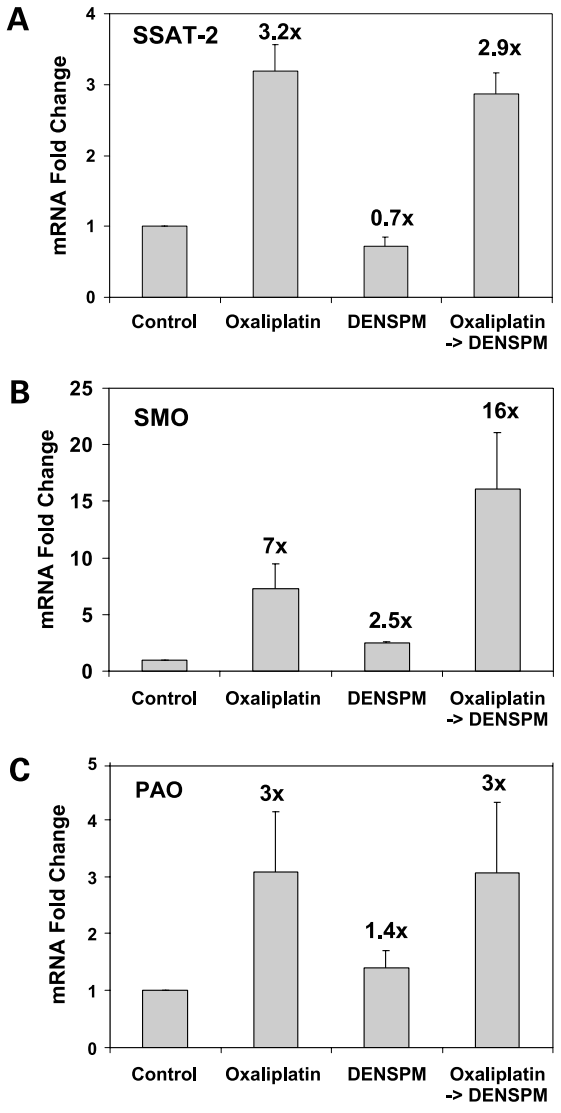

Figure 7. Effect of combining oxaliplatin with DENSPM on the expression of SSAT-2, SMO, and PAO mRNA. A2780 cells treated with oxaliplatin alone, DENSPM alone, or oxaliplatin followed by DENSPM were analyzed for levels of SSAT-2, SMO, and PAO mRNA using real-time QRT-PCR as described in Fig. 4. Aliquots of the same cDNA generated for SSAT mRNA expression experiments described in Fig. 4 are used here for the measurement of SSAT-2 (**A**), SMO (**B**), and PAO (**C**) expression. The levels for SSAT-2, SMO, and PAO mRNA in control (no drug) were 35.6 ± 7.8, 1.1 ± 0.1, and 0.9 ± 0.02, respectively. *Columns*, mean fold change (relative to untreated controls) from two separate experiments, each consisting of three separate PCRs; *bars*, SE.

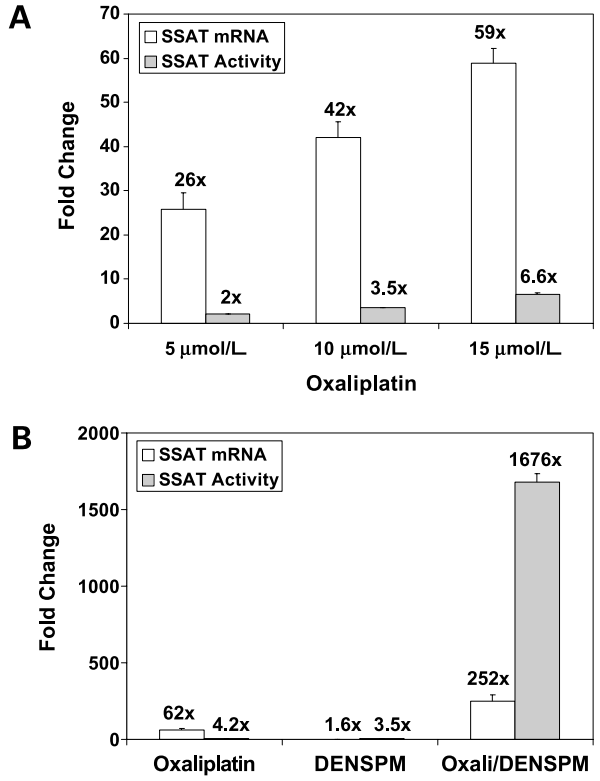

Figure 8. **A,** effects of pharmacologically relevant exposure time (20 hours) and concentrations (5, 10, or 15 μmol/L) of oxaliplatin on SSAT mRNA and enzyme activity. Cells were treated with oxaliplatin at the defined dose for 20 hours followed by a 24-hour incubation in drug-free medium, before extraction. SSAT/β-actin mRNA in control cells was 12.4 ± 0.82; SSAT enzyme activity in control cells was 23.0 ± 2.1 pmol/min/mg protein. **B,** effect of a concurrent 20 hours treatment of cells with 10 μmol/L oxaliplatin and 10 μmol/L DENSPM on SSAT mRNA and enzyme activity. Cells were treated with either drug alone or oxaliplatin and DENSPM combination followed by a 24-hour incubation in drug-free medium before extraction. SSAT/β-actin mRNA in control cells was 17.0 ± 0.68; SSAT enzyme activity in control cells was 16.9 ± 0.72 pmol/min/mg protein. **A** and **B,** gene expression data: *Columns*, mean fold change (relative to untreated controls) from three separate experiments, each consisting of six separate PCRs; *bars*, SE. Enzyme activity data: *Columns*, mean fold change (relative to untreated controls), where $n = 3$; *bars*, SE.

~80% at the highest oxaliplatin dose and there was a significant accumulation of the SSAT product, N^1-acetylspermidine. Under these same oxaliplatin treatment conditions, concurrent treatment with 10 mol/L DENSPM followed by a 24-hour incubation in drug-free medium resulted in massive 250-fold increase in SSAT mRNA and nearly 1,700-fold increase in enzyme activity (Fig. 8B). This led to a near-total depletion in cellular spermine and spermidine.

Because induction of SSAT has been convincingly linked to the antiproliferative effects of DENSPM (14-16), we sought to determine whether the substantial increases in SSAT activity seen with the drug combinations would translate into similarly enhanced effects on cell growth. A dose response of DENSPM alone for 24 hours revealed an IC_{50} of ~1 μmol/L (Fig. 9A). Because the concentration of DENSPM used in enzyme induction studies (10 μmol/L) was cytotoxic in the growth inhibition assay, we used analogue concentrations that minimally affected cell growth on their own. Thus, 0.1, 0.25, and 0.5 μmol/L DENSPM reduced growth by 0%, 10% and 20%, respectively. Figure 9B depicts the dose-response curves following 2 hours exposure of cells to oxaliplatin at concentrations ranging from 0.1 to 100 μmol/L followed by a 24-hour exposure to each of the above DENSPM concentrations and a further 48 hours in drug-free medium. When combined sequentially with 0.5 μmol/L DENSPM, the oxaliplatin-dose-response curve shifted ~1 log to the left, indicating DENSPM sensitization of the cells to oxaliplatin.

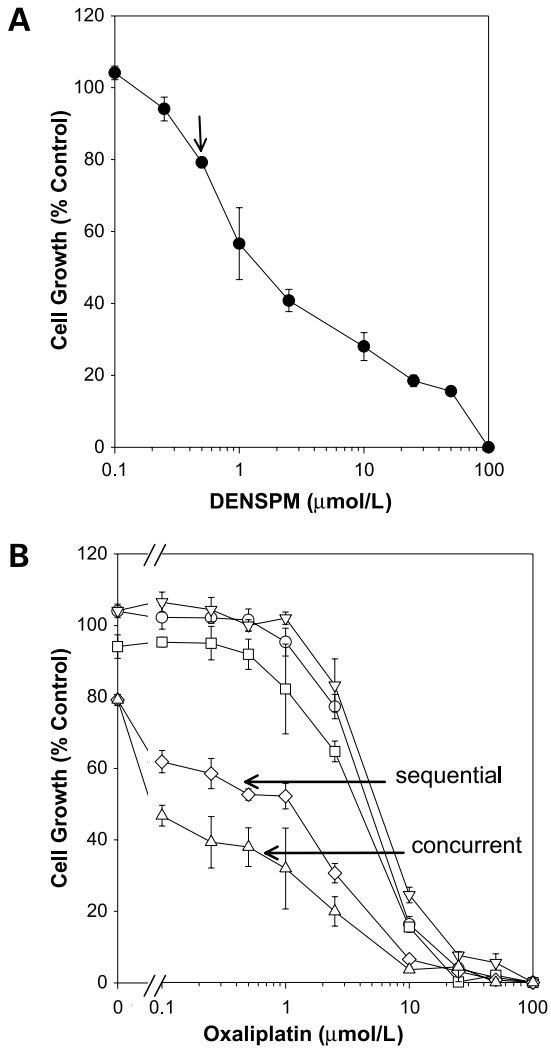

Figure 9. Growth inhibition dose-response curves to DENSPM alone (**A**) or oxaliplatin combined with low-dose DENSPM (**B**). **B,** ○, oxaliplatin; ▽, oxaliplatin (2 hours) followed by 0.1 μmol/L DENSPM for 24 hours; □, oxaliplatin (2 hours) followed by 0.25 μmol/L DENSPM for 24 hours; ◇, oxaliplatin (2 hours) followed by 0.5 μmol/L DENSPM for 24 hours; △, is concurrent 2 hours exposure to oxaliplatin and DENSPM (0.5 μmol/L) followed by 24 hours DENSPM (0.5 μmol/L). Data are percentage growth as determined by ($A_{570\ nm}$ of treated cells/$A_{570\ nm}$ of untreated cells) × 100. *Columns*, means, where $n = 3$ to 9; *bars*, SE. In **A,** the *arrow arrow* indicates the 0.5 μmol/L DENSPM with zero oxaliplatin.

Concurrent exposure to oxaliplatin and 0.5 μmol/L DENSPM followed by 24 hours DENSPM at 0.5 μmol/L shifted the curve even further to the left and, thus, produced even greater sensitization to oxaliplatin. As shown in Fig. 8B, concentrations of oxaliplatin which themselves were not growth inhibitory became growth inhibitory in combination with 0.5 μmol/L DENSPM to an extent that was greater than that produced by DENSPM alone.

Discussion

The work presented here indicates that the platinum drugs oxaliplatin and cisplatin have a profound effect on the expression of SSAT, the polyamine catabolic enzyme that acetylates spermidine and spermine and thereby promotes their degradation and/or export out of the cell. Under the conditions of these experiments, both oxaliplatin and cisplatin increased SSAT mRNA in A2780 cells more effectively than the best known inducer of SSAT gene expression, DENSPM (34). Thus, our earlier observation made with Affymetrix analysis that platinum drugs potently induce SSAT was confirmed here by real-time QRT-PCR and by Northern blot analysis. SSAT gene expression increased in a dose-dependent manner with both drugs from ~2-fold at IC_{10} up to >10-fold at IC_{90} concentrations and oxaliplatin tended to have a greater effect on SSAT gene expression than cisplatin at the equitoxic concentrations. The observation by Northern blotting that SSAT heteronuclear RNA also increased would seem to indicate that in similarity to DENSPM (29), platinum drugs induced SSAT expression by activating gene transcription, an observation that warrants further investigation.

In addition to polyamine analogues (34), a relatively large number of agents have been shown to induce SSAT activity, such as hormones, growth factors, toxic compounds, drugs, and pathophysiologic insults (35). Recently, it was shown that SSAT is the most potently induced gene from among 2,400 candidate genes in MCF-7 breast cancer cells treated with 5-flurouracil (36). Given the wide range of agents that induce SSAT, it is tempting to consider that polyamine acetylation may represent a generalized stress response. This interpretation, however, is offset by the fact that expression of other polyamine catabolic enzymes, such as SMO, PAO, and SSAT-2, is also increased, suggesting a more concerted metabolic response to the drug. It is also relevant that our earlier Affymetrix studies of platinum drug-treated cells indicated a 2-fold decline in expression of the polyamine biosynthetic enzyme, *S*-adenosylmethionine decarboxylase expression (11), although this finding has not yet been validated and explored in a manner similar to these studies with SSAT. The finding that under pharmacologically relevant treatment conditions, oxaliplatin induces both SSAT mRNA and enzyme activity and that the levels of enzyme induction are similar to those attained with DENSPM suggests that SSAT induction could represent a previously unrecognized contributor to oxaliplatin mechanism of action.

A major finding of this present study is that the platinum drug-induced SSAT mRNA can be converted to a massive increase in enzyme activity by co- or posttreatment with the polyamine analogue DENSPM. More specifically, oxaliplatin increased SSAT activity by ~2-fold, DENSPM by ~7-fold, and the combination of oxaliplatin and DENSPM by >200 or 400-fold, depending on drug combination schedule. As indication of enzyme functionality, polyamine pools were almost totally depleted due presumably to acetylation followed by either export or oxidation by PAO. The DENSPM/SSAT interaction was further enhanced when cells were concurrently exposed to oxaliplatin and DENSPM for 20 hours, treatment conditions reflecting exposures obtained during clinical studies (32, 33). The combination increased the SSAT enzyme activity by 1,676-fold, whereas as single agents, oxaliplatin and DENSPM induced a 4.2- and 3.5-fold increases in enzyme activity, respectively. Although induction of SSAT is a notoriously heterogeneous response among cell lines (37), we note that the basal SSAT enzyme activity and the polyamine pool levels in these cells are similar to those reported for other cell lines, such as MCF-7 breast cancer cells and various human melanoma cell lines (37). The finding that DENSPM enhances the oxaliplatin effect significantly is consistent with previous reports from our laboratory showing that ''super-induction'' of SSAT mRNA by inhibitors of protein synthesis resulted in minor increases in enzyme activity unless followed by treatment with polyamines or a polyamine analogue which facilitate translation and stabilization of the enzyme protein and greatly amplified the initial mRNA response at the level of SSAT activity (30, 31). Such an amplification of SSAT has not, however, been previously shown with a clinically relevant anticancer agent, such as the platinum drugs. The implications of this effect are raised by the fact that SSAT induction is causally linked to either the apoptotic or antiproliferative effects of DENSPM (14-16). Some of the more defining evidence for this relationship is as follows: (1) cells made resistant to DENSPM are unable to induce SSAT (38); (2) conditional overexpression of SSAT leads to growth inhibition in both MCF-7 breast cancer cells (26) and in LNCaP prostate carcinoma cells (39); and (3) transient transfection of cells with SSAT-directed siRNA prevents the induction of SSAT and apoptotic response (27). An obvious possibility that flows from this evidence is that this drug combination may have similarly enhanced effects on cell growth and/or cytotoxicity and, thus, therapeutic potential. Thus, using a SSAT-based rationale for combining oxaliplatin and DENSPM, we examined the effects of analogue concentrations which themselves, were minimally cytotoxic. As shown in Fig. 9, at least one such dose (0.5 μmol/L) which is known to be clinically achievable (18, 19), potentiated oxaliplatin cytotoxicity. Despite the promising nature of these findings, more detailed studies in which the drug combination is pharmacologically and mechanistically optimized are likely to produce cytotoxicity responses approaching true drug synergy. It is also relevant that induction of SSAT gene expression by platinum drugs was

not unique to A2780 cells but also occurs in additional cell types, as shown here for melanoma cells MALME-3M and SK-MEL-28. How it compares to normal cells and, thus, to drug selectivity has not yet been determined.

Synergy between DENSPM and cisplatin has been reported against murine cell lines L1210 leukemia and B16F1 melanoma both *in vitro* and *in vivo* systems (40). Synergy between N^1,N^{12}-diethylspermine (DESPM) and cisplatin was reported in cisplatin-sensitive and -resistant 2,008 ovarian carcinoma cells (41). Another study reported that pretreatment of human brain tumor cell lines with polyamine analogues, such as DENSPM, increased the incorporation of platinum into the linker regions of DNA and also the cytotoxicity of cisplatin (42). To our knowledge, only one other laboratory has reported a relationship between cisplatin and polyamine analogues that converges at SSAT. Marverti et al. (41) found that cisplatin-resistant cell lines were cross-resistant to the polyamine analogue DESPM and that there is a reduced ability by the polyamine analogue to induce SSAT in the resistant cells. Their studies further showed a reduced SSAT protein turnover following treatment with DESPM in cisplatin-sensitive cells relative to the resistant cells, indicating that cisplatin resistance modulates the SSAT response to DESPM at the transcriptional and posttranscriptional levels (43). In distinction to the present study, these investigators did not determine that cisplatin induces SSAT expression or that a polyamine analogue can potently augment this response.

In conclusion, our study showed that platinum drugs and especially oxaliplatin potently induce SSAT gene expression and that, this induction can be amplified by DENSPM by mechanisms that would seem to involve analogue-facilitated translation of the platinum-drug induced mRNA into enzyme protein. It is also clear that the platinum drug effects on polyamine catabolism are not limited to SSAT but include the enzymes SMO, PAO, and SSAT-2. We propose that with further refinement, these observations can be translated to clinical benefit. This belief is consistent with the facts that polyamine metabolism represents a validated target for therapeutic intervention, SSAT induction is known to inhibit cell growth, the potent SSAT inducer DENSPM has undergone clinical evaluation, and oxaliplatin is an important chemotherapeutic agent for treating various human cancers.

References

1. Mathe G, Kidani Y, Segiguchi M, et al. Oxalato-platinum or 1-OHP, a third-generation platinum complex: an experimental and clinical appraisal and preliminary comparison with *cis*-platinum and carboplatinum. Biomed Pharmacother 1989;43:237-50.

2. Misset JL, Kidani Y, Gastiaburu J, et al. Oxalatoplatinum (1-OHP): experimental and clinical studies. In: Howell SB, editor. Platinum and other metal coordination compounds in cancer chemotherapy. New York: Plenum Press; 1991. p. 369-75.

3. Wiseman LR, Adkins JC, Plosker GL, Goa K. Oxaliplatin. A review of its use in the management of metastatic colorectal cancer. Drugs Aging 1999;14:459-75.

4. Pendyala L, Creaven PJ. *In vitro* cytotoxicity, protein binding, red blood cell partitioning and biotransformation of oxaliplatin. Cancer Res 1993;53:5970-6.

5. Hector S, Bolanowska-Higdon W, Zdanowicz J, Hitt S, Pendyala L. *In vitro* studies on the mechanisms of oxaliplatin resistance. Cancer Chemother Pharmacol 2001;48:398-406.

6. Raymond E, Faivre S, Chaney S, Woynarowski J, Cvitkovic E. Cellular and molecular pharmacology of oxaliplatin [Review] [100 refs]. Mol Cancer Ther 2002;1:227-35.

7. Di Francesco AM, Riccardi R. Cellular and molecular aspects of the drugs of the future. Cell Mol Life Sci 2002;59:1914-27.

8. Rixie O, Ortuzar W, Alvarez M, et al. Oxaliplatin, tetraplatin, cisplatin and carboplatin: spectrum of activity in drug-resistant cell lines and in the cell lines of the National Cancer Institute's anticancer drug screen panel. Biochem Pharmacol 1996;52:1855-65.

9. Woynarowski JM, Chapman WG, Napier C, Herzig MS, Juniewicz P. Sequence- and region-specificity of oxaliplatin adducts in naked and cellular DNA. Mol Pharmacol 1998;54:770-7.

10. Woynarowski JM, Faivre S, Herzig MS, et al. Oxaliplatin-induced damage of cellular DNA. Mol Pharmacol 2000;58:920-7.

11. Hector S, Hawthorn L, Greco W, Pendyala L. Gene expression profiles after oxaliplatin treatment in A2780 ovarian carcinoma cells. Proc AACR 2002;43:62.

12. Porter C, Herrera-Omelas L, Pera P, Petrelli NF, Mittleman A. Polyamine biosynthetic activity in normal and neoplastic human colorectal tissues. Cancer 1987;60:1275-81.

13. Thomas T, Thomas TJ. Polyamines in cell growth and cell death: molecular mechanisms and therapeutic applications. Cell Mol Life Sci 2001;58:244-58.

14. Casero RAJ, Celano P, Ervin SJ, Porter CW, Bergeron RJ, Libby PR. Differential induction of spermidine/spermine N^1-acetyltransferase in human lung cancer cells by the bis(ethyl)polyamine analogues. Cancer Res 1989;49:3829-33.

15. McCloskey DE, Coleman CS, Pegg AE. Properties and regulation of human spermidine/spermine N^1-acetyltransferase stably expressed in Chinese hamster ovary cells. J Biol Chem 1999;274:6175-82.

16. Chen Y, Kramer DL, Diegelman P, Vujcic S, Porter CW. Apoptotic signaling in polyamine analogue-treated SK-MEL-28 human melanoma cells. Cancer Res 2001;61:6437-44.

17. Porter CW, Ganis B, Libby PR, Bergeron RJ. Correlations between polyamine analogue-induced increases in spermidine/spermine N^1-acetyltransferase activity, polyamine pool depletion, and growth inhibition in human melanoma cell lines. Cancer Res 1991;51:3715-20.

18. Hahm HA, Ettinger DS, Bowling K, et al. Phase I study of N^1,N^{11}-diethylnorspermine in patients with non-small cell lung cancer. Clin Cancer Res 2002;8:684-90.

19. Creaven PJ, Perez R, Pendyala L, et al. Unusual central nervous system toxicity in a Phase I study of N^1,N^{11} diethylnorspermine in patients with advanced malignancy. Invest New Drugs 1997;15:227-34.

20. Vujcic S, Liang P, Diegelman P, Kramer DL, Porter CW. Genomic identification and biochemical characterization of the mammalian polyamine oxidase involved in polyamine back-conversion. Biochem J 2003;370:19-28.

21. Urdiales JL, Medina MA, Sanchez-Jimenez F. Polyamine metabolism revisited. Eur J Gastroenterol 2001;13:1015-9.

22. Vujcic S, Diegelman P, Bacchi CJ, Kramer DL, Porter CW. Identification and characterization of a novel flavin-containing spermine oxidase of mammalian cell origin. Biochem J 2002;367:665-75.

23. Wu T, Yankovskaya V, McIntire WS. Cloning, sequencing, and heterologous expression of the murine peroxisomal flavoprotein, N^1-acetylated polyamine oxidase. J Biol Chem 2003;278:20514-25.

24. Chen Y, Vujcic S, Liang P, Diegelman P, Kramer DL, Porter C. Genomic Identification and biochemical characterization of a second spermidine/spermine N^1-acetyltransferase. Biochem J 2003;373:661-7.

25. Xiao L, Celano P, Mank AR, et al. Structure of the human spermidine/spermine N^1-acetyltransferase gene (exon/intron gene organization and localization to Xp22.1). Biochem Biophys Res Commun 1992;187:1493-502.

26. Vujcic S, Halmekyto M, Diegelman P, et al. Effects of conditional overexpression of spermidine/spermine N^1-acetyltransferase on polyamine pool dynamics, cell growth, and sensitivity to polyamine analogs. J Biol Chem 2000;275:38319-28.

27. Chen Y, Kramer D, Jell J, Vujcic S, Porer CW. siRNA suppression of polyamine analogue-induced spermidine/spermine N^1-acetyltransferase. Mol Pharmacol 2003;64:1153-9.

28. Rubinstein LV, Shoemaker RH, Paull KD, et al. Comparison of *in vitro* anticancer drug screening data generated with a tetrazolium assay versus a protein assay against a diverse panel of human tumor cell lines. J Natl Cancer Inst 1990;82:1113-8.

29. Fogel-Petrovic M, Shappell NW, Bergeron RJ, Porter CW. Polyamine and polyamine analog regulation of spermidine/spermine N^1-acetyltransferase in MALME-3M human melanoma cells. J Biol Chem 1993;268:19118-25.

30. Fogel-Petrovic M, Vujcic S, Miller J, Porter CW. Differential post-transcriptional control of ornithine decarboxylase and spermidine-spermine N^1-acetyltransferase by polyamines. FEBS Lett 1996;391:89-94.

31. Fogel-Petrovic M, Vujcic S, Brown PJ, Haddox MK, Porter CW. Effects of polyamines, polyamine analogs, and inhibitors of protein synthesis on spermidine-spermine N^1-acetyltransferase gene expression. Biochemistry 1996;35:14436-44.

32. Smith PF, Booker B, Pendyala L, et al. Pharmacokinetic modeling of oxaliplatin with and without 5-FU and radiation. Proc AACR 2001;42:542.

33. Graham MA, Lockwood GF, Greenslade D, Brienza S, Bayssas M, Gamelin E. Clinical pharmacokinetics of oxaliplatin: a critical review [Review] [49 refs]. Clin Cancer Res 2000;6:1205-18.

34. Fogel-Petrovic M, Kramer DL, Vujcic S, et al. Structural basis for differential induction of spermidine/spermine N^1-acetyltransferase activity by novel spermine analogs. Mol Pharmacol 1997;52:69-74.

35. Seiler N. Functions of polyamine acetylation [Review] [114 refs]. Can J Physiol Pharmacol 1987;65:2024-35.

36. Maxwell P, Longley DB, Latif T, et al. Identification of 5-fluorouracil-inducible target genes using cDNA microarray profiling. Cancer Res 2003; 63:4602-6.

37. Shappell NW, Miller JT, Bergeron RJ, Porter CW. Differential effects of the spermine analog, N^1,N^{12}-bis(ethyl)-spermine, on polyamine metabolism and cell growth in human melanoma cell lines and melanocytes. Anticancer Res 1992;12:1083-9.

38. McCloskey DE, Pegg AE. Altered spermidine/spermine N^1-acetyltransferase activity as a mechanism of cellular resistance to bis(ethyl)polyamine analogues. J Biol Chem 2000;275:28708-14.

39. Kee K, Vujcic S, Kisiel N, Diegelman P, Kramer D, Porter CW. Activation of polyamine catabolism as a novel strategy for treating and/or preventing prostate cancer. Proc AACR 2003;44:1277.

40. Hawthorne TR, Kramer Austin J Jr. Synergism of the polyamine analog, N^1,N^{11}-bisethylnorspermine with *cis*-diaminedichloroplatinum (II) against murine neoplastic cell lines *in vitro* and *in vivo*. Cancer Lett 1996; 99:99-107.

41. Marverti G, Piccinnini G, Ghaironi S, Barbieri D, Quaglino D, Moruzzi MS. N^1,N^{12}-bis(ethyl)spermine effect on growth of *cis*-diamminedichloroplatinum(II)-sensitive and -resistant human ovarian-carcinoma cell lines. Int J Cancer 1998;78:33-40.

42. Paliwal J, Janumpalli G, Basu HS. The mechanism of polyamine analog-induced enhancement of cisplatin cytotoxicity in the U-251 MG human malignant glioma cell line. Cancer Chemother Pharmacol 1998;41:398-402.

43. Marverti G, Bettuzzi S, Astancolle S, Pinna C, Monti MG, Moruzzi MS. Differential induction of spermidine/spermine N^1-acetyltransferase activity in cisplatin-sensitive and -resistant ovarian cancer cells in response to N^1,N^{12}-bis(ethyl)spermine involves transcriptional and post-transcriptional regulation. Eur J Cancer 2001;37:281-9.

Potent Modulation of Intestinal Tumorigenesis in *Apc*$^{min/+}$ Mice by the Polyamine Catabolic Enzyme Spermidine/Spermine N^1-acetyltransferase

Jody M. Tucker,[1] John T. Murphy,[1] Nicholas Kisiel,[2] Paula Diegelman,[2] Karen W. Barbour,[1] Celestia Davis,[1] Moussumi Medda,[1] Leena Alhonen,[3] Juhani Jänne,[3] Debora L. Kramer,[2] Carl W. Porter,[2] and Franklin G. Berger[1]

[1]Department of Biological Sciences, University of South Carolina, Columbia, South Carolina; [2]Grace Cancer Drug Center, Roswell Park Cancer Institute, Buffalo, New York; and [3]A.I. Virtanen Institute for Molecular Sciences, University of Kuopio, Kuopio, Finland

Abstract

Intracellular polyamine pools are homeostatically maintained by processes involving biosynthesis, catabolism, and transport. Although most polyamine-based anticancer strategies target biosynthesis, we recently showed that activation of polyamine catabolism at the level of spermidine/spermine N^1-acetyltransferase-1 (SSAT) suppresses tumor outgrowth in a mouse prostate cancer model. Herein, we examined the effects of differential SSAT expression on intestinal tumorigenesis in the *Apc*$^{Min/+}$ (MIN) mouse. When MIN mice were crossed with SSAT-overproducing transgenic mice, they developed 3- and 6-fold more adenomas in the small intestine and colon, respectively, than normal MIN mice. Despite accumulation of the SSAT product, N^1-acetylspermidine, spermidine and spermine pools were only slightly decreased due to a huge compensatory increase in polyamine biosynthetic enzyme activities that gave rise to enhanced metabolic flux. When MIN mice were crossed with SSAT knock-out mice, they developed 75% fewer adenomas in the small intestine, suggesting that under basal conditions, SSAT contributes significantly to the MIN phenotype. Despite the loss in catabolic capability, tumor spermidine and spermine pools failed to increase significantly due to a compensatory decrease in biosynthetic enzyme activity giving rise to a reduced metabolic flux. Loss of heterozygosity at the *Apc* locus was observed in tumors from both SSAT-transgenic and -deficient MIN mice, indicating that loss of heterozygosity remained the predominant oncogenic mechanism. Based on these data, we propose a model in which SSAT expression alters flux through the polyamine pathway giving rise to metabolic events that promote tumorigenesis. The finding that deletion of SSAT reduces tumorigenesis suggests that small-molecule inhibition of the enzyme may represent a nontoxic prevention and/or treatment strategy for gastrointestinal cancers. (Cancer Res 2005; 65(12): 5390-8)

Introduction

Cell proliferation, differentiation and cell death depend on or are affected by a sustained supply of intracellular polyamine pools. Enzymes such as ornithine decarboxylase (ODC) and *S*-adenosylmethionine decarboxylase (SAMDC) contribute to the *de novo* biosynthesis of polyamines, whereas catabolic enzymes such as spermidine/spermine N^1-acetyltransferase-1 (SSAT) and polyamine-directed oxidases play important roles in lowering polyamine pools by export and in catalyzing their interconversion (1–4). Alterations in polyamine homeostasis, whether pharmacologically- or genetically induced, lead to changes in intracellular polyamine pools that have important ramifications in cell physiology and cell growth. For example, increased ODC and SAMDC activity, and the associated elevations in intracellular polyamines, have been implicated in certain cancers, including those of the gastrointestinal tract (3, 5–10). As such, polyamines and their key biosynthetic enzymes have been viewed as attractive targets for the treatment and prevention of cancer. Findings to be presented here suggest that catabolic enzymes such as SSAT may represent even more compelling targets in gastrointestinal cancers.

SSAT, which is encoded by the X-linked *Sat1* gene, is the rate-limiting enzyme of polyamine catabolism. It catalyzes the acetylation of spermine and spermidine in response to cell stress (4) and to excess polyamines (11). Acetylated polyamines are either oxidized by polyamine oxidase, which leads to the back-conversion of higher polyamines (i.e., spermine) to lower polyamines (i.e., spermidine and putrescine or more typically, they are efficiently excreted out of the cell as a means of lowering intracellular polyamine pools (1, 2). Whether achieved genetically (12, 13) or pharmacologically with polyamine analogues (14, 15), induction of SSAT typically gives rise to growth inhibition or apoptosis, depending upon the cell type and the extent of enzyme overexpression. In such experiments, growth inhibition has been closely linked to depletion of intracellular polyamine pools (12) and disturbances in polyamine metabolism (13), whereas apoptosis has been associated with downstream events emanating from polyamine oxidase–mediated oxidation of acetylated polyamines and the associated release of oxidatively reactive by-products such as hydrogen peroxide and the aldehyde, 3-acetamidopropanal (4, 16, 17).

The relationship between SSAT and cancer is only now being defined. Because maintenance of cell proliferation requires a constant supply of polyamines (1–3), it might be expected that tumor cells would keep polyamine biosynthetic activity high and catabolic activity low, so as to create a selection pressure favoring polyamine availability. Several studies showing induced apoptosis in tumor cells overexpressing SSAT are consistent with this paradigm (1, 13, 16, 17). Conditional overexpression of SSAT in LNCaP prostate carcinoma cells has been shown to bring about near total growth inhibition (13). Extending this finding to an *in vivo* system, we recently reported that cross-breeding SSAT-overexpressing transgenic mice with prostate cancer–predisposed TRAMP [transgenic adenocarcinoma of mouse prostate; ref. (18)]

Requests for reprints: Carl W. Porter, Grace Cancer Drug Center, Roswell Park Cancer Institute, Elm and Carlton Streets, Buffalo, NY 14263. Phone: 716-845-3002; Fax: 716-845-2353; E-mail: Carl.Porter@roswellpark.org.

mice inhibits tumor outgrowth (19). This provocative finding suggests quite clearly that high levels of SSAT expression can exert tumor-suppressive effects. However, in contrast to expectations, polyamine pools were not significantly depleted by SSAT in either LNCaP cells or in prostate tumors of TRAMP mice (13, 19). Rather, the antitumor effect seems to be directly related to a compensatory up-regulation of polyamine biosynthesis in response to SSAT overproduction. This, in turn, leads to heightened metabolic flux through the biosynthetic and catabolic arms of the pathway and an associated depletion of metabolic precursors such as the SSAT cosubstrate acetyl-CoA. On the assumption that this somewhat unexpected metabolic response may be unique to prostate-derived tumors, we sought to determine the consequences of SSAT overexpression in a murine model of intestinal cancer.

Apc$^{Min/+}$ mice (MIN) carry a truncation mutation (the *Min* allele) within the adenomatous polyposis coli (*Apc*) tumor suppressor gene (20, 21). The same gene defect is frequently seen in both inherited and spontaneous colon cancer in humans (22). Heterozygous *Apc*$^{Min/+}$ animals are predisposed to the development of multiple adenomas in the small intestine and, to a much lesser extent, in the colon (20, 21). The formation of these polyps is initiated by loss of heterozygosity (LOH) at the *Apc* locus (23), which leads to stabilization of the transcription factor β-catenin, constitutive activation of the WNT signaling pathway, and induced expression of target genes, such as those encoding cyclin D1, c-MYC, and others (24). Of relevance to the current study, polyamine metabolism is known to be directly related to β-catenin expression via c-MYC-mediated transactivation of ODC (25). Indeed, ODC mRNA levels and polyamine pools have been shown to be increased in the small intestine and colon of MIN mice (26). Furthermore, treatment of MIN mice with the specific ODC inhibitor α-difluoromethylornithine causes a reduction in intestinal polyamines and a significant decrease in tumor number (26, 27). Thus, there is a strong rationale for examining the consequences of altered SSAT expression in this particular model system. Herein, we report that transgenic overexpression of SSAT markedly increases tumor development in the MIN mouse, whereas genetic depletion of the enzyme has the opposite effect.

Materials and Methods

Animals. *Apc*$^{Min/+}$ mice (MIN) in the C57BL/6J background (21) were obtained from the Jackson Laboratories (Bar Harbor, ME), and maintained by breeding MIN males to C57BL/6J females. Heterozygous progeny were identified by PCR analysis of tail DNA using allele-specific primers (20).

SSAT transgenic mice (SSAT-tg, genotype *Sat1*$^{tg/0}$), which carry multiple copies of a full-length murine *Sat1* gene, have been previously described (28). These animals express elevated levels of SSAT enzyme activity in most tissues (28). Carriers of the transgene were identified by the occurrence of hair loss, which begins at about 3 to 4 weeks of age in these animals (28). Prior to onset in the present mice, the transgene was introduced into the C57BL/6J background by 10 generations of back-crossing. Mice containing the SSAT transgene and the *Apc*$^{Min/+}$ mutation were generated by mating female MIN mice to male SSAT-tg mice.

Generation of embryonic stem cells carrying a targeted inactivating mutation within the X-linked *Sat1* gene was described earlier (29). These cells were injected into C57BL6/6J blastocysts to produce chimeric mice that were bred to yield SSAT knock-out mice (SSAT-ko, genotypes *Sat1*$^{-/-}$ and *Sat1*$^{-/Y}$). Male MIN/SSAT-ko mice (genotype *Apc*$^{Min/+}$/*Sat1*$^{-/Y}$) contain the inactive SSAT-ko allele within the *Apc*$^{Min/+}$ background, and were produced by mating female SSAT-ko mice to male MIN mice. The presence of the SSAT-ko allele was determined by PCR using three primers: 20 pmol each of two allele-specific forward primers (wild-type primer, 5′-CTCCTCCTGCTGTTCAAGTA-3′; null primer, 5′-TACCTGCCCATTCGACC-3′) and 40 pmol of a reverse primer that recognizes both the wild-type and null alleles (5′-CAGTTCCTGGGGACGAC-3′). Reaction mixtures containing all three primers were subjected to 34 cycles of standard PCR conditions with a 56°C annealing temperature. Products were resolved using 5% acrylamide gel electrophoresis and stained with ethidium bromide for the presence of wild-type *SSAT* allele (408 bp) or the null allele (615 bp).

Tumor scoring. Tumor burdens were determined as described previously (30). Following cervical dislocation, the small and large intestines were removed, flushed free of debris, sliced longitudinally, and fixed flat between sheets of filter paper for 3 hours in 10% buffered formalin. Fixed tissues were stained with 0.002% methylene blue. Adenomatous polyps were counted under a dissecting microscope by a single observer who was blinded to the genotypes of the animals. Upon counting, each tumor was classified as being >1 or <1 mm in diameter using an ocular micrometer. All data are reported as mean ± SE, except where noted. Student's *t* test was used to compare the means of each group; differences were considered to be significant if *P* values were <0.05.

Enzyme and polyamine analyses. Biochemical analyses were done on mice that were different from those used for intestinal tumor counts but which were derived from the same litter. Tissues were excised from 9-week-old mice under a dissecting microscope, and tumor tissue was snap-frozen and stored at −70°C. Following removal of tumors, the normal small intestinal and colonic mucosa was scraped from the muscularis externa layer with a glass slide and snap-frozen. Frozen mucosa and tumor tissues were crushed into a fine powder using a Bio-Pulverizer (BioSpec Products, Inc., Bartlesville, OK). Tris/EDTA (pH 7) breaking buffer was added to ~50 to 100 mg of sample for sonication and centrifugation to obtain the soluble supernatant extracts for enzyme and polyamine analyses.

SSAT activity was assayed radiochemically as described previously (31) and expressed as picomoles of N^1-[^{14}C]acetylspermidine generated per minute per milligram of protein. Both ODC and SAMDC activities were determined by a CO_2 trap assay as previously described (32), and reported as nanomoles of radiolabeled CO_2 per hour milligram of protein.

For intracellular polyamine pool analysis, buffered extracts were further extracted with 1.2 N perchloric acid, and dansylated prior to assessment by high-performance liquid chromatography using methods described elsewhere (12).

Histologic analysis of tumors. Tumor tissues for histologic analysis were removed and fixed for a minimum of 3 hours in 10% formalin, after which they were rolled, embedded in paraffin, sectioned, and stained with H&E. Stained sections were observed at 100× magnification under a light microscope.

Assessment of loss of heterozygosity. Intestinal epithelial cells from tumors or from adjacent histologically normal regions were collected using a PixCell IIe Laser Capture Microdissection System (Arcturus, Mountain View, CA). The cells were incubated for 12 hours at 50°C in 0.5 mg/mL proteinase K, 10 mmol/L Tris-HCl (pH 8.0), 50 mmol/L KCl, 0.45% NP40, and 0.45% Tween 20 (33) and genomic DNA was extracted by standard methods. LOH at the *Apc* locus was determined using PCR-based methods (23, 34). A 155-bp fragment of the *Apc* gene was amplified in the presence of [^{32}P]dCTP; the forward primer was 5′-TCTCGTTCTGAGAAAGACAGAAGCT-3′, and the reverse primer was 5′-TGATACTTCTTCCAAAGCTTTGGCTAT-3′. The resulting product was digested with *Hin*dIII, resolved by gel electrophoresis in 8% acrylamide, and visualized by autoradiography. The wild-type *Apc* allele yields a 123 bp product, whereas the *Min* allele yields a 144 bp product. Quantitation of relative band intensities was carried out by densitometry (Storm 860 Imager and Image Quant 5.2 software; Molecular Dynamics, Sunnyvale, CA).

Results

SSAT overproduction enhances tumor development in MIN mice. To test the effects of elevated SSAT expression on intestinal tumorigenesis in the MIN mouse model, we intercrossed MIN (genotype *Apc*$^{Min/+}$) and SSAT-tg (genotype *Sat1*$^{tg/0}$) mice. The latter were produced and characterized in an earlier study (28), and were

shown to express increased levels of SSAT mRNA and enzyme activity in most tissues, including the small intestine and colon. The genotypes of the progeny of the cross of MIN females and SSAT-tg males were determined at weaning, and were found to segregate in a non-Mendelian fashion. The number of MIN/SSAT-tg progeny ($Apc^{Min/+}/Sat1^{tg/0}$) was only about 1/3 of that expected (Table 1; $P = 4.6 \times 10^{-9}$). Furthermore, SSAT-tg segregants ($Apc^{+/+}/Sat1^{tg/0}$) were also reduced in number relative to mice with wild-type ($Apc^{+/+}$) or MIN ($Apc^{Min/+}$) genotypes (Table 1; $P = 0.013$), although the deficiency of this genotype was not as dramatic as that for MIN/SSAT-tg progeny. Thus, overproduction of SSAT seems to be deleterious to survival, particularly in combination with APC haploinsufficiency. Although the basis for this phenomenon is unknown, it is likely manifested during gestation because there were no noticeable increases in postnatal mortality. Normal Mendelian segregation of genotypes was observed previously in a cross of SSAT transgenic and TRAMP mice (13, 19). The deficiency of MIN/SSAT-tg progeny in the current cross may be related to the report of Jacoby et al. (26, 27), who observed that treatment with the ODC inhibitor α-difluoromethylornithine during embryonic development is selectively lethal to fetuses bearing a heterozygous mutation in the *Apc* gene.

Previous work showed that SSAT mRNA and enzyme concentrations in the small intestine and the colon are ~10-fold higher in SSAT transgenic as compared with nontransgenic mice (28). We carried out similar activity measurements on MIN and MIN/SSAT-tg tissues (Fig. 1*A*). We consistently observed higher SSAT levels in normal small intestinal mucosa ($P = 0.03$) and in colonic tumors ($P = 0.01$) of the MIN/SSAT-tg progeny. There was a tendency toward higher SSAT activities in MIN/SSAT-tg intestinal tumors and in normal colon tissue, but the differences did not reach statistical significance. SSAT enzyme activities were significantly higher in colonic tumors relative to normal mucosa in MIN/SSAT-tg mice ($P = 0.01$), but not in MIN mice. Small intestinal tumors exhibited slightly higher activities relative to normal tissues in both MIN and MIN/SSAT-tg progeny, but the increases were not statistically significant. One difficulty with these assays is that SSAT-specific activities are masked by the high levels of nonspecific acetyltransferases in tissue extracts (35), leading to an underestimation of the magnitude of change in SSAT expression. Thus, we consider the accumulation of the SSAT reaction product N^1-acetylspermidine (see below) to be a more reliable indicator of increased SSAT enzyme activity in MIN/SSAT-tg mice.

Development of adenomatous polyps in the MIN/SSAT-tg mice was determined at 9 weeks of age over the full length of the small and large intestines, and compared with that in their nontransgenic MIN littermates. Total number of tumors in the small intestines of MIN mice (Fig. 1*B*) were similar to previously reported values (30). However, the MIN/SSAT-tg mice developed ~3-fold more tumors in the small intestine ($P < 0.01$), including ~2-fold increase in tumors <1 mm in diameter and a 4-fold increase in tumors >1 mm in diameter (Fig. 1*B*). Although tumor incidence was lower in colon than small intestine (Fig. 1*B*), all of the colonic polyps were >1 mm and the MIN/SSAT-tg mice contained about 6-fold more tumors than nontransgenic MIN mice ($P < 0.0001$). On average, tumor sizes in either the small intestine or the colon were not significantly different between MIN and MIN/SSAT-tg mice. These data indicate that the presence of the SSAT transgene potently enhances tumorigenesis in both the small intestine and colon of MIN mice.

Table 1. Genotypes of progeny resulting from crossing MIN females ($Apc^{Min/+}$) to SSAT-tg males ($Sat1^{tg/0}$)

Genotype	Observed*	Predicted
$Apc^{+/+}$	109 (37.7%)	72 (25%)
$Apc^{+/+}/Sat1^{tg/0}$	63 (21.8%)	72 (25%)
$Apc^{Min/+}$	95 (32.9%)	72 (25%)
$Apc^{Min/+}/Sat1^{tg/0}$	22 (7.6%)	72 (25%)

*Observed progeny distribution (percentage of total based on 289 mice).

SSAT overexpression is accompanied by compensatory increases in polyamine biosynthetic activity in MIN mice. To gain insight into the mechanisms underlying increased tumor development in MIN/SSAT-tg mice, we measured the activities of the two key polyamine biosynthetic enzymes ODC and SAMDC. Enzyme activities in normal mucosa and in tumors of the small intestine and colon were determined, and found to be dramatically different between MIN/SSAT-tg and MIN progeny. ODC levels in MIN/SSAT-tg mice were about 3- to 5-fold higher in normal mucosa of both the small intestine ($P < 0.0005$) and the colon ($P < 0.00001$) relative to the MIN mice (Fig. 2). Increases of 7- to 10-fold were observed in tumors of the small intestine ($P < 0.0005$) and the colon ($P < 0.003$; Fig. 2). Similarly, SAMDC activities in MIN/SSAT-tg mice were significantly increased relative to MIN mice in the normal mucosa of both the small intestine (i.e., ~20-fold; $P < 0.002$) and colon (i.e., >10-fold; $P < 0.01$). SAMDC in MIN/SSAT-tg tumors were also higher than MIN tumors in the small intestine (i.e., >40-fold; $P < 0.04$) and in the colon (i.e., >50-fold; $P < 0.001$; Fig. 2).

These results indicate that the presence of the SSAT transgene is associated with increases in both ODC and SAMDC activities in normal tissues and in polyps of the gastrointestinal tract. Thus, the increase in polyamine catabolic activity mediated by SSAT overexpression is metabolically offset by a large compensatory increase in biosynthetic activity. This finding, which is consistent with earlier characterization of various normal tissues of the SSAT transgenic mouse (19, 28), implies that metabolic flux through the polyamine metabolic pathway is heightened in both tumors and the intestinal epithelium of MIN/SSAT-tg mice.

Overexpression of SSAT in MIN mice differentially alters polyamine pools. To examine the effects of increased SSAT expression on polyamine pools, the concentrations of the SSAT product N^1-acetylspermidine, as well as the primary polyamines putrescine, spermidine, and spermine were measured and compared in MIN and MIN/SSAT-tg mice (Fig. 3). In normal small intestinal tissues, MIN/SSAT-tg mice exhibited a >30-fold increase in N^1-acetylspermidine levels ($P < 0.0002$), and an 18-fold increase in putrescine pools ($P < 0.00001$) relative to MIN tissues. By comparison, spermidine concentrations decreased by only 29% ($P < 0.0002$), whereas spermine levels were not significantly affected. Similar increases in N^1-acteylspermidine and putrescine were seen in the MIN/SSAT-tg normal colon, with no change in spermidine or spermine levels (Fig. 3).

Even larger increases in both N^1-acetylspermidine and putrescine levels were observed in tumors of MIN/SSAT-tg mice relative to MIN mice (Fig. 3). N^1-acetylspermidine levels were elevated by >70-fold in small intestinal tumors ($P < 0.01$), and by >200-fold in colonic tumors ($P < 0.02$). Putrescine concentrations were ~9-fold

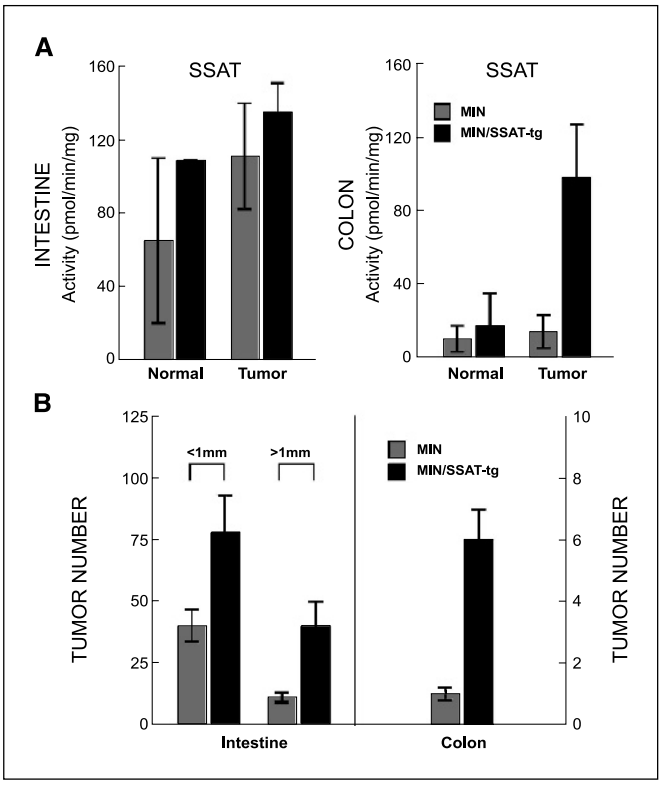

Figure 1. *A,* SSAT activity levels in intestinal tissues of MIN and MIN/SSAT-tg mice. Activities were measured in extracts of normal mucosa and adenomatous polyps (tumors) of the small intestine and colon from MIN mice (*gray columns*) and MIN/SSAT-tg mice (*black columns*). Values represent the averages of three to nine animals per group. *B,* tumor counts obtained from MIN (n = 14) and MIN/SSAT-tg (n = 16) mice were determined on the entire length of small intestine and colon. For the small intestine, tumors <1 mm in diameter and those >1 mm in diameter were counted separately (designated above the columns). All tumors arising in the colon were >1 mm.

higher in small intestinal polyps ($P < 0.0003$), and ~8-fold higher in colonic polyps ($P < 0.03$). As seen in normal tissues, tumor spermidine levels decreased by a modest 23% of MIN/SSAT-tg mice ($P < 0.02$), whereas spermine levels remained unchanged.

Overall, the results for normal tissues agree well with published data indicating that putrescine and N^1-acetylspermidine levels are dramatically higher in tissues of MIN/SSAT-tg mice as compared with normal MIN mice, whereas spermidine and spermine pools are essentially unchanged (28), presumably due to the compensatory increase in biosynthetic activity. The increase in putrescine is probably due to the combined effects of polyamine biosynthesis (resulting from high ODC and SAMDC levels) and back-conversion (due to SSAT overexpression). Expansion of the N^1-acetylspermidine pool is a strong indicator that SSAT is overproduced at the level of enzyme activity (28).

SSAT deficiency inhibits intestinal tumor development in MIN mice. The finding that overexpression of SSAT augments tumorigenesis in the MIN mouse model predicts that MIN mice lacking SSAT will exhibit reduced tumor development. To test this prediction, we used a SSAT-ko mouse that contains a targeted, inactivating insertion within the X-linked *Sat1* gene (29). SSAT-ko mice are viable, fertile, and show no obvious phenotype under the conditions of the current studies.

We crossed MIN males with *Sat1*$^{+/-}$ females, and observed that all expected genotypes segregated in a normal Mendelian fashion (data not shown). SSAT activities were examined in the small intestinal tumors from MIN/SSAT-ko progeny (all of which are males) and MIN progeny (Fig. 4*A*). The difference in total activity between MIN and MIN/SSAT-ko tumors was small and not statistically significant, due to low levels of basal SSAT activity, as well as the presence of nonspecific acetylating enzymes (35). Indirect evidence for loss of SSAT was apparent in a significant decrease in ODC activity, as noted below.

Tumor numbers were determined in the MIN/SSAT-ko mice, and compared with those in normal male MIN progeny. Total tumor counts in the small intestine were reduced by about 75% in MIN/SSAT-ko mice ($P < 0.02$); such a decrease was observed for both small (<1 mm diameter) and large (>1 mm diameter) tumors (Fig. 4*B*). Interestingly, there were no significant effects on the number or size of colonic tumors, despite the fact that overexpression of SSAT increased tumor number in this organ by ~6-fold (see Fig. 1).

ODC activity in intestinal tumors was significantly different between MIN/SSAT-ko and normal MIN mice ($P = 0.016$; Fig. 4*A*). Thus, loss of SSAT expression in the knock-out mice results in a 66% compensatory decrease in ODC activity. SAMDC activity was not measured due to the small size of the MIN/SSAT-ko tumor samples. Analysis of polyamine pools in small intestinal tumors of the two genotypes revealed modest changes in putrescine, spermidine, and spermine concentrations in MIN/SSAT-ko mice (Fig. 4*C*). Putrescine fell by 45% ($P = 0.017$), whereas the 18% increase in spermidine and the 6% decrease in spermine were not statistically significant. The SSAT product N^1-acetylspermidine was undetectable in tumors from either MIN or MIN/SSAT-ko mice (data not shown). The relative lack of change among the higher polyamines was somewhat unexpected because deletion of SSAT is expected to increase polyamine pools due to reduced catabolic activity (29). We attribute this lack of change to the decrease in ODC activity that accompanied loss of SSAT and thus, to decreased metabolic flux through the polyamine pathways. It is likely that this also accounts for the reduction in putrescine pools.

Tumor histology and loss of heterozygosity at the *Apc* locus in SSAT-overexpressing and in SSAT-deficient MIN mice. No discernible changes in gross morphology of tumors were noted in either MIN/SSAT-tg or MIN/SSAT-ko mice (data not shown). Tumor sections from both strains exhibited a typical adenomatous histology that was very similar to that found in MIN mice (data not shown).

Several studies have indicated that tumor development in *Apc*$^{Min/+}$ mice results from LOH at the *Apc* locus (20, 23, 36), leading to the loss of the wild-type *Apc* allele and a deficiency in expression of the full-length APC protein. To determine if LOH is the predominant mechanism of APC inactivation in mice with altered expression of SSAT, we isolated tumor epithelial cells from both MIN/SSAT-tg and MIN/SSAT-ko mice by laser capture microdissection, and assessed loss of the wild-type *Apc* allele in these cells.

The wild-type and *Min* alleles of the *Apc* gene differ by an A/T substitution at codon 850, resulting in gain/loss of a *Hin*dIII restriction site (23). *Hin*dIII digestion of a 155-bp PCR-generated fragment spanning this site results in 123 and 144 bp products, representing the wild-type and *Min* alleles, respectively. Both PCR fragments were evident in *Hin*dIII-digested DNA extracted from normal villus of MIN mice (Figs. 5*A* and *B*, both on lane 2). In contrast, epithelial cell DNA from small intestinal SSAT-tg tumors (Fig. 5*A*, lanes 3-15) exhibited the 144 bp *Hin*dIII fragment, with little evidence of the 123 bp fragment, indicating loss of the wild-type allele. Quantitation of band intensities showed that the ratio

of the wild-type to the *Min* allele was 0.80 ± 0.06 in DNA from normal villus and 0.25 ± 0.05 in DNA from adenoma epithelial cells ($P < 0.001$). The residual amount of the 123 bp wild-type band in some lanes is due to unavoidable contamination by infiltrating normal cells such as inflammatory cells, lymphocytes, and fibroblasts.

Very similar results were obtained upon analysis of MIN/SSAT-ko mice (Fig. 5*B*). DNA from normal villus exhibited both bands (lane 2), whereas that from microdissected tumor epithelial cells predominantly showed the *Min*-specific band. Thus, as in normal MIN mice, tumorigenesis in MIN/SSAT-tg and MIN/SSAT-ko mice is associated with loss of APC expression due to LOH at the *Apc* locus. Despite profound effects on tumorigenesis, genetic manipulation of SSAT expression does not change the underlying oncogenic mechanism, namely, APC loss during tumor initiation, indicating that SSAT contributes in some way to the process of LOH.

Discussion

The primary finding of this study is that variations in SSAT expression modulate intestinal tumorigenesis in the MIN mouse model. The ability of SSAT overexpression to increase intestinal polyps shows the tumorigenic potential of SSAT under exaggerated, although perhaps, nonphysiologic conditions. However, the observation that SSAT deficiency reduces intestinal polyps implies a significant role for the enzyme under basal conditions, a finding perhaps more relevant to understanding the actual role of SSAT in carcinogenesis. Similar to normal MIN mice, LOH at the *Apc* locus occurs in tumors of both the SSAT-overproducing as well as the SSAT-deficient MIN mice, suggesting that genetic manipulation of SSAT expression alters the frequency of LOH-type events that are involved in the initiation of tumor development.

Of additional significance to the current findings is the demonstration that SSAT-mediated effects are context-dependent, i.e., the impact of dysregulated SSAT expression varies among tumor types. We have recently shown that overexpression of SSAT in the TRAMP mouse model of prostate cancer markedly suppresses tumor outgrowth (19), an effect opposite to that of the present study. Thus, the impact of SSAT differs between the prostate and the gastrointestinal tract. Despite this disparity, the findings with both models strongly indicate a role for SSAT in tumor development, whereas at the same time reflecting the ambiguities associated with our current understanding of polyamine catabolism and its relationship to cell proliferation (4). There is no indication in our experience that SSAT-overproducing transgenic mice are more prone to developing spontaneous tumors in any tissue.[4]

A number of studies conducted over the past few years substantiate the complexity and context-dependency of SSAT and its role in tumorigenesis. Several reports, based on studies of cultured cells and animal models, are consistent with the notion that SSAT suppresses cell growth. For example, studies with polyamine analogues that potently induce SSAT indicate that apoptotic indices are increased when the enzyme is up-regulated, and are decreased when it is not (17). Conditional overexpression of SSAT causes growth inhibition in both MCF-7 breast carcinoma cells (12) and LNCaP prostate cancer cells (13). *In vivo* studies have shown that relative to normal mice, SSAT-overproducing transgenic mice are resistant to carcinogen-induced skin papilloma formation (37). As noted above, transgenic overexpression of SSAT in prostate cancer–predisposed TRAMP mice markedly reduces outgrowth of tumors (19). Taken as a whole, ample evidence indicates that SSAT exerts a decidedly negative effect on cell growth and tumor development.

In contrast to these findings, studies in other systems are consistent with the idea that SSAT stimulates, rather than inhibits, tumorigenesis. Enzyme levels are higher in breast tumors than in normal tissues, and correlate positively with tumor size (38). Gene expression profiling has identified SSAT mRNA as an up-regulated transcript in rectal tumors (39). Treatment of colon cancer cells with the chemopreventive agent resveratrol reduces levels of SSAT activity while causing growth arrest (40). Perhaps most convincingly, targeted overexpression of the enzyme in epidermal keratinocytes of mice increases the susceptibility to skin tumors in response to carcinogens (41). This is consistent with the present findings that SSAT overexpression promotes, whereas SSAT deficiency inhibits, tumor development in the MIN mouse.

In considering the mechanism by which SSAT modulates intestinal tumorigenesis in the MIN mouse model, we have taken into account the rather important observation that alterations in SSAT levels exert only minor effects on spermidine and spermine pools. It is well known that polyamine metabolism is highly dynamic and subject to compensatory responses designed to conserve intracellular polyamine pools (13, 19, 28, 29, 41, 42). Thus,

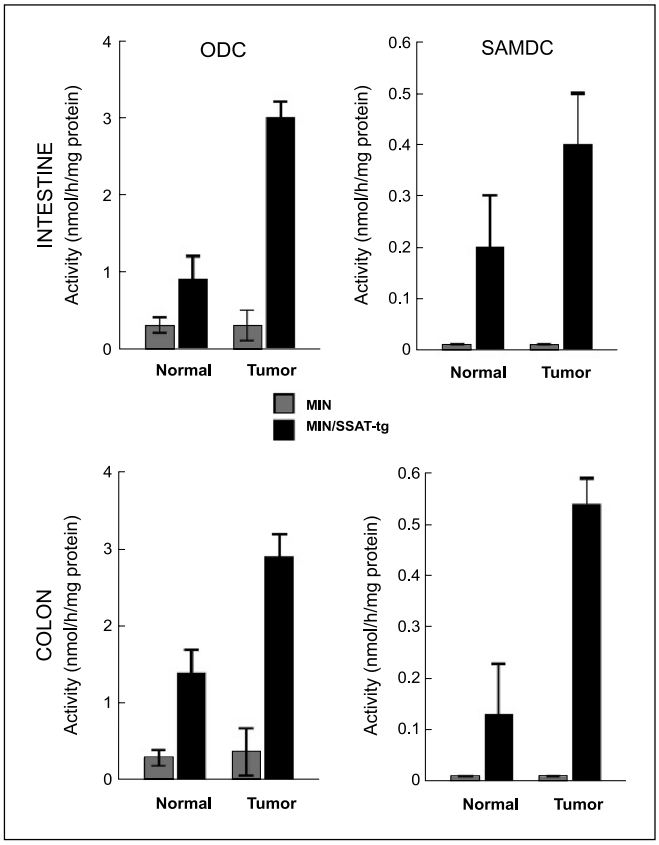

Figure 2. ODC and SAMDC activity levels in normal intestinal tissues and polyps of MIN and MIN/SSAT-tg mice. Enzyme activities were determined in normal mucosa and tumors of the small intestine and colon. Values for MIN/SSAT-tg mice (*black columns*) and MIN mice (*gray columns*) represent the average (± SD) of three to nine animals per group.

[4] Unpublished results.

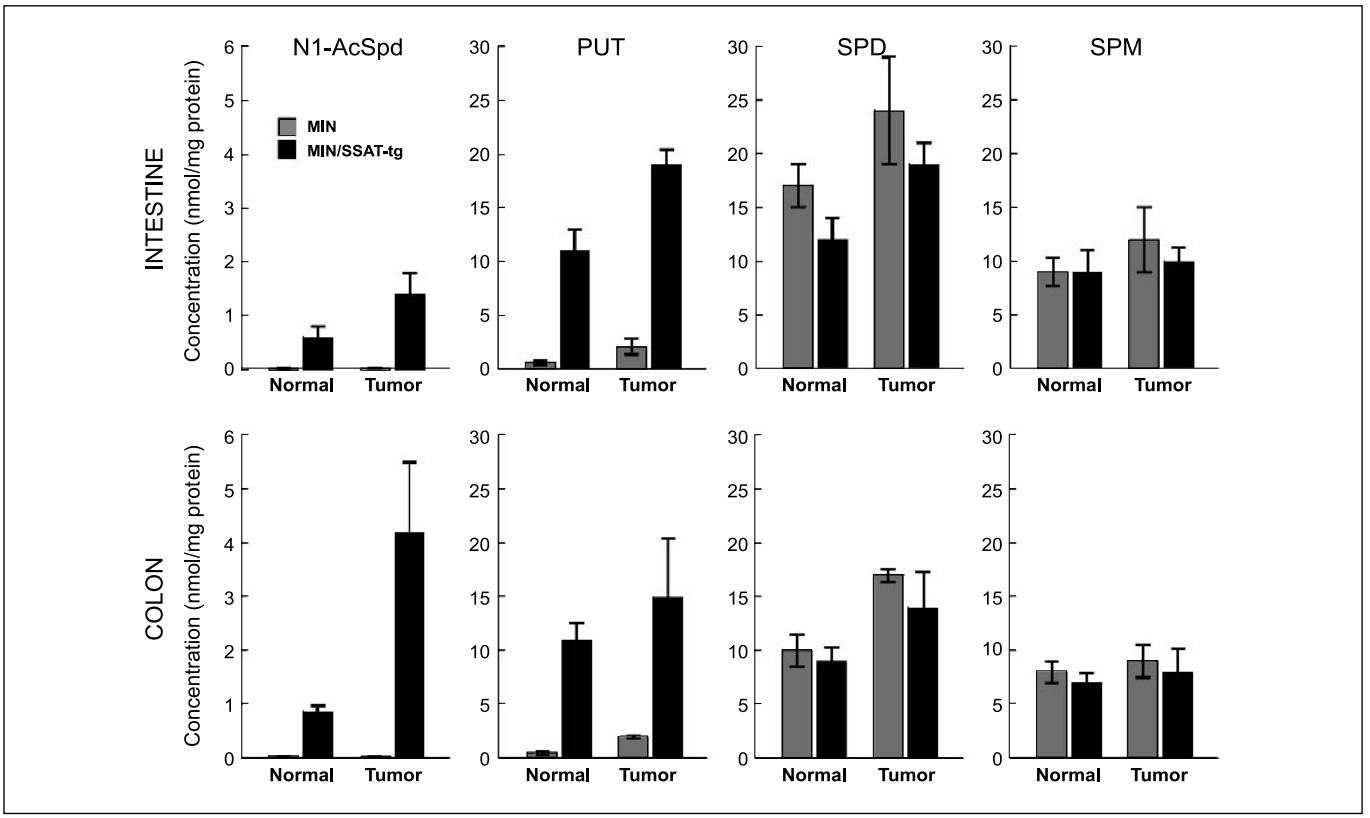

Figure 3. Polyamine pools in normal intestinal tissues and polyps of MIN and MIN/SSAT-tg mice. The concentrations of N^1-acetylspermidine, putrescine, spermidine, and spermine were determined for normal regions of small intestine and colon, and for polyps from both tissues. Values for MIN mice (*gray columns*) and MIN/SSAT-tg mice (*black columns*) represent averages of three to nine animals per group.

as seen here and elsewhere (13, 28), activation of polyamine catabolism at the level of SSAT gives rise to a compensatory increase in polyamine biosynthetic enzymes (i.e., ODC and SAMDC). We consider it unlikely that the relatively minor changes in spermidine and spermine pools seen in tumors of MIN/SSAT-tg and in MIN/SSAT-ko mice (Figs. 3 and 4) are responsible for altered tumorigenesis. Rather, we submit that changes in tumor development more likely arise from deregulated metabolic flux through the polyamine biosynthetic and/or catabolic pathways. This flux can be viewed as a metabolic ratchet (Fig. 6) driven by spermidine and spermine homeostasis. When SSAT is overexpressed as in transgenic mice, spermidine and spermine pools decrease, triggering a sustained increase in biosynthetic activity. This results in heightened metabolic flux and maintenance of polyamine pools which, in turn, permit continued polyamine oxidation. Changes in the flux can have dramatic effects on the concentrations of a number of metabolites. On the biosynthetic side, substrates such as ornithine, methionine, and *S*-adenosylmethionine are used, whereas products such as putrescine, methylthioadenosine and carbon dioxide are generated. On the catabolic side, substrates such as acetyl-CoA and FAD are used, whereas products and by-products such as putrescine, N^1-acetylspermidine, 3-acetamidopropanal, hydrogen peroxide, and $FADH_2$ are liberated (Fig. 6). The rate at which the metabolic ratchet turns determines how rapidly substrates are depleted and products are produced. We propose that at some point, either a substrate becomes rate-limiting or a product becomes toxic, causing a phenotypic change. It is interesting to note that the ratchet model also applies to the SSAT-ko mice where we showed that deletion of SSAT results in a lowering of ODC activity and polyamine pools (Fig. 4) and thus, a decrease in metabolic flux.

The metabolic ratchet model provides a useful explanation for the effects of SSAT on intestinal polyp formation, as observed in the present study. Although the particular metabolites mediating these responses are not yet known, we believe that certain oxidatively reactive by-products of polyamine catabolism may play a significant role. SSAT is rate-limiting in polyamine catabolism. When deregulated, the enzyme's activity gives rise to unlimited acetylated polyamines which are readily oxidized by polyamine oxidase to lower polyamines; hydrogen peroxide and aldehydes are released as by-products. Thus, when SSAT expression and polyamine catabolism are high, such as in MIN/SSAT-tg mice, a compensatory increase in polyamine biosynthesis heightens metabolic flux, giving rise to a sustained release of reactive by-products, an increased frequency of LOH events at the *Apc* locus, and thus, increased polyp formation. Conversely, when metabolic flux is low, such as in the MIN/SSAT-ko mice, there is minimal release of reactive by-products and thus, a much lower probability of LOH events and tumor formation. The correlative changes in LOH status at the *Apc* locus observed in normal MIN mice, as well as in MIN/SSAT-tg and MIN/SSAT-ko mice, is highly supportive of the above paradigm. The idea that the LOH may be due to increased DNA damage caused by reactive by-products of polyamine oxidase is quite consistent with several studies showing that MIN mice having deficiencies in DNA repair manifest similar increases in intestinal tumor development (43–46).

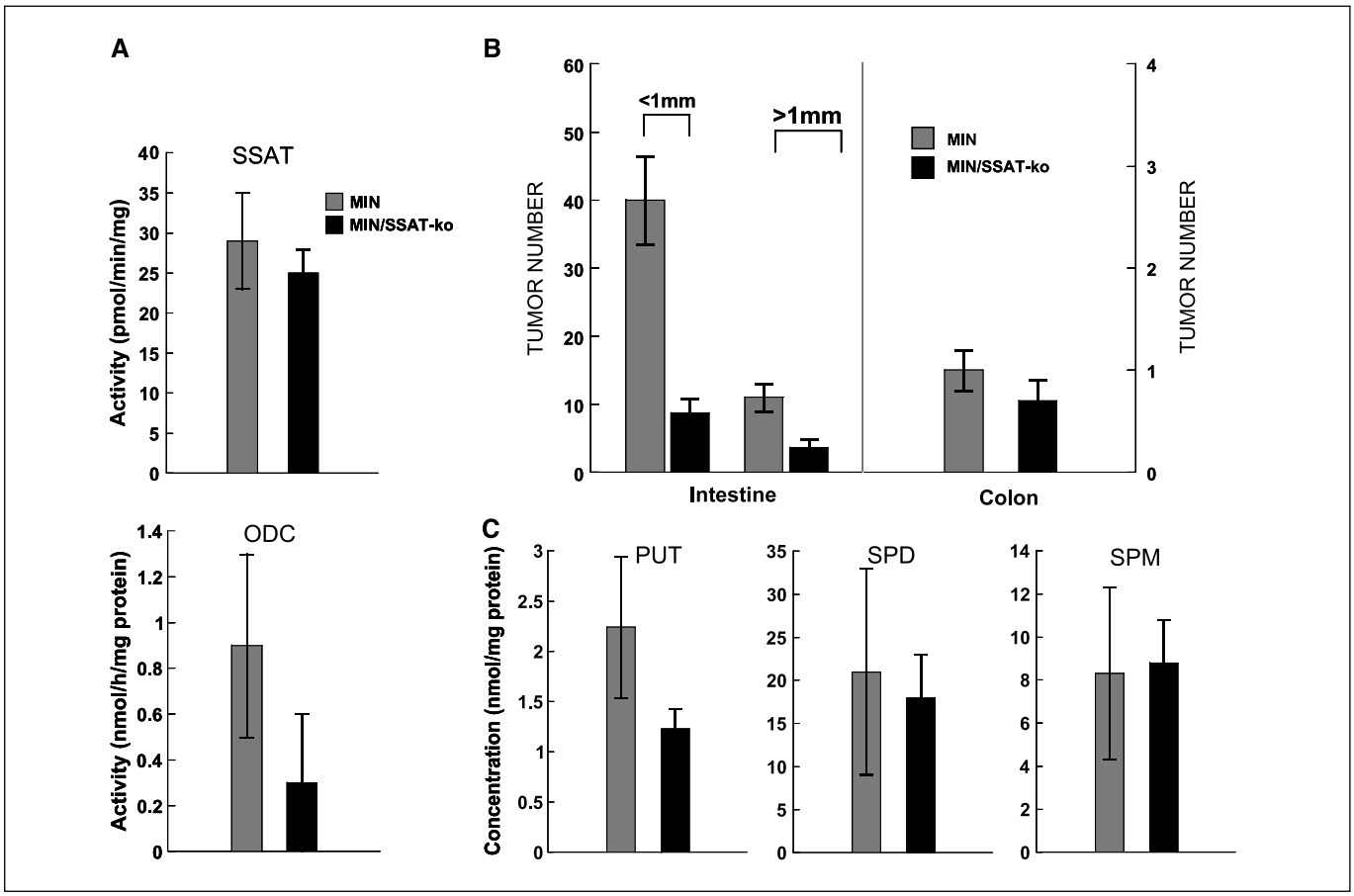

Figure 4. *A,* SSAT and ODC activity levels in small intestinal polyps of MIN/SSAT-ko mice. Activities were measured in tumor extracts and compared with those in normal MIN mice. Values for MIN/SSAT-ko mice (*black columns*) and MIN mice (*gray columns*) represent the averages of five to seven animals per group. The similar SSAT activity in MIN versus MIN/SSAT tumors is due to the low basal enzyme levels relative to nonspecific acetylating enzymes that are also detected in the assay. *B,* tumor numbers in SSAT-ko mice. Polyps were counted in the small intestine and the colon of MIN/SSAT-ko mice (n = 10, *black columns*), and compared with those found in MIN mice (n = 14, *gray columns*). For the small intestine, tumors <1 and >1 mm in diameter were counted separately (indicated above the columns). *C,* polyamine concentrations in small intestinal polyps of MIN/SSAT-ko mice. Polyamine pools were measured in tumor extracts of MIN/SSAT-ko mice (*black columns*) relative to MIN mice (*gray columns*). In all samples, N^1-acetylspermidine levels were below the level of detection (0.5 nmol/mg protein). Note that the scale of the y axis differs between polyamine graphs. Values represent the averages of seven to eight animals per group.

The consequences of altered metabolic flux through the polyamine pathways are obviously very different between the intestinal tract and the prostate of the mouse. SSAT suppression of prostate tumor growth has been associated both *in vitro* and *in vivo* with depletion of acetyl-CoA and/or *S*-adenosylmethionine pools (19). Although applicable to the TRAMP model, depleted acetyl-CoA pools and the attendant interference with fatty acid synthesis hardly seems relevant to tumorigenesis in the MIN

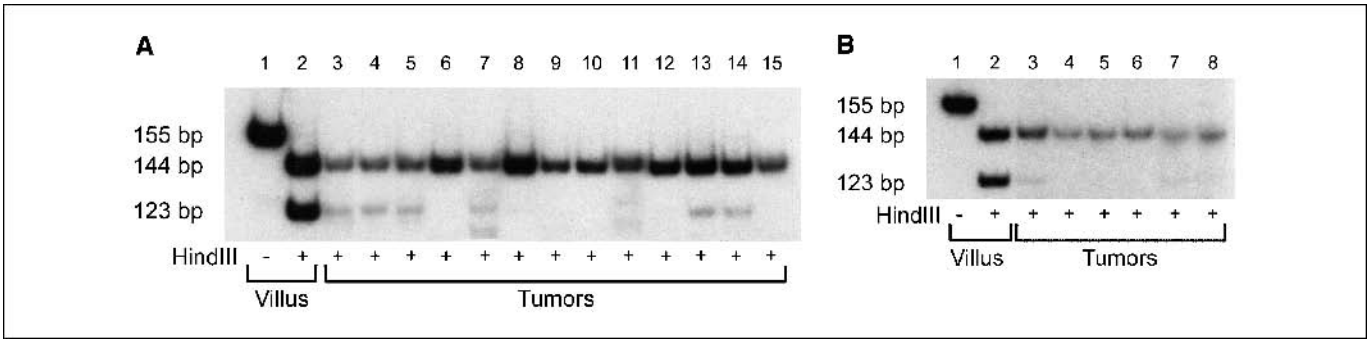

Figure 5. LOH at the *Apc* locus in intestinal tumors. Epithelial cells were isolated from tumor tissues and normal villus from MIN intestine by laser capture microdissection. DNA was extracted and the appropriate region within the *Apc* gene was amplified by PCR using radioactive nucleotide substrates; the amplified DNA was digested with *Hin*dIII, and observed by gel electrophoresis and autoradiography (see Materials and Methods for details). *A,* undigested DNA from normal MIN villus (*lane 1*), *Hin*dIII-digested DNA from normal MIN villus (*lane 2*), and *Hin*dIII-digested DNA from microdissected tumors of MIN/SSAT-tg mice (*lanes 3-15*). *B,* undigested DNA normal MIN villus (*lane 1*), *Hin*dIII-digested DNA from normal MIN villus (*lane 2*), and *Hin*dIII-digested DNA from microdissected MIN/SSAT-ko tumors (*lanes 3-8*). Sizes of the various DNA bands are shown (126 kb fragment represents wild-type allele, 144 kb fragment represents MIN allele).

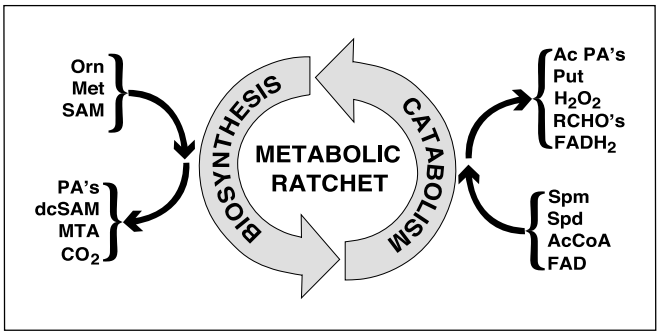

Figure 6. Metabolic ratchet model for polyamine homeostasis. Large arrows, the primary pathways for polyamine biosynthesis (*left*) and catabolism (*right*). Various metabolites are shown which are either substrates or products of these pathways. Substrates and precursors used in polyamine biosynthesis include ornithine (Orn), methionine (Met) and the SAMDC aminopropyl donor, *S*-adenosylmethionine (SAM), whereas substrates used in polyamine catabolism include spermidine (Spd), spermine (Spm), acetyl-CoA (AcCoA), and FAD. Compounds produced during polyamine biosynthesis include the natural polyamines (PA), the SAMDC by-product decarboxylated *S*-adenosylmethionine (dcSAM), the spermidine and spermine synthase by-product, methylthioadenosine (MTA) and the decarboxylase by-product, CO_2. Compounds produced during catabolism include the acetylated polyamines (AcPA), the polyamine oxidase product putrescine (Put) and the by-products hydrogen peroxide (H_2O_2), the aliphatic aldehyde 3-acetamidopropanal (RCHO), and $FADH_2$. In response to SSAT-induced decreases in spermidine and spermine, polyamine biosynthesis increases, giving rise to a sustained increase in metabolic flux. As flux through the pathway increases (such as that occurring in SSAT-tg mice), substrate utilization and product accumulation increase; conversely, as flux decreases, such as that seen in the SSAT-ko mice, substrate utilization and product accumulation decrease. The cellular response to alterations in flux depends upon the particular metabolites that change and how effectively the cell is able to react to that change. The direct correlation between SSAT expression levels and intestinal tumorigenesis suggests that a product of SSAT or a downstream enzyme such as polyamine oxidase is facilitating the tumorigenic process.

mouse because high fat content is known to be causally related to tumor development in the MIN mouse model (47); thus, depletion of acetyl-CoA would be expected to decrease rather than increase in tumorigenesis. Similarly, it is also unlikely that depletion of the methyl donor *S*-adenosylmethionine is relevant because it has been shown that reduction of hypermethylation suppresses, rather than promotes, polyp formation in the MIN mouse (48).

In further consideration of the disparity in SSAT effects between MIN and TRAMP mice, it must be realized that the consequences of altered flux through the polyamine pathway will depend upon (*a*) the nature of the metabolite effector, (*b*) how well the cell is prepared to respond to that metabolite, and (*c*) the overall metabolic milieu of the cell. All of these are likely to vary significantly between prostate epithelium and the intestinal mucosa. Because SSAT is systemically overexpressed in all cells and tissues of SSAT-tg mice, these same variables are also likely to differ in the stromal environment of tumor cells in the two tissues. The tumor stroma has been widely implicated in both tumorigenesis and drug responses (49), and could be a critical determinant of the SSAT effects.

Another contextual factor unique to these particular models is the driving cancer gene. Tumorigenesis in the MIN mouse is driven by a mutated *Apc* suppressor gene (20) and its downstream effectors, whereas that in the TRAMP mouse is driven by the SV40 large T antigen and its various target molecules (18). These are two entirely different and nonconverging pathways. For example, ODC, which is potently up-regulated when SSAT is overexpressed in both models, is transactivated by c-MYC (25), and thus, serves as an effector in the WNT signaling pathway that drives tumorigenesis in the MIN mouse (24). In contrast, ODC is not among the SV40-large T antigen targets of the TRAMP mouse.

Although daunting, the task of determining which of the above factors is most critical in determining tumor outcome is likely to shed new insights into the overall process of tumor development, the role of polyamine catabolism as a modulator of that process, and possible new strategies for cancer prevention or treatment. In this regard, the observation that by promoting metabolic flux, SSAT would seem to behave as a promoter of intestinal tumorigenesis, raises the interesting possibility that pharmacologic inhibitors of the enzyme or the downstream enzyme polyamine oxidase might be a useful targeted anticancer strategy. This notion is reinforced by the observation that within the context of the present experiments, the SSAT-ko mice exhibited no apparent phenotype suggesting that such an inhibitor of this enzyme, if specific, would have minimal host effects. Lastly, our findings tend to discount previous reports in which suppression of SSAT by activated Ki-ras has been implicated in intestinal tumorigenesis (50), or in which induction of SSAT by sulindac sulfone has been implicated in colorectal chemoprevention (10), at least in so far as these observations might apply to the MIN mouse model.

Acknowledgments

Received 1/24/2005; revised 3/10/2005; accepted 4/7/2005.

Grant support: NIH grants DK33886 (to F.G. Berger), CA222153 and CA76428 (to C.W. Porter); COBRE grant RR017698 (to F.G. Berger); and P30 CA16056 and Department of Defense grant PC020638 (to C.W. Porter).

The costs of publication of this article were defrayed in part by the payment of page charges. This article must therefore be hereby marked *advertisement* in accordance with 18 U.S.C. Section 1734 solely to indicate this fact.

References

1. Wallace HM, Fraser AV, Hughes A. A perspective of polyamine metabolism. Biochem J 2003;376:1–14.
2. Janne J, Alhonen L, Pietila M, Keinanen TA. Genetic approaches to the cellular functions of polyamines in mammals. Eur J Biochem 2004;271:877–94.
3. Gerner EW, Meyskens FL Jr. Polyamines and cancer: old molecules, new understanding. Nat Rev Cancer 2004; 4:781–92.
4. Seiler N. Catabolism of polyamines. Amino Acids 2004; 26:217–33.
5. Porter CW, Herrera-Ornelas L, Pera P, Petrelli NF, Mittelman A. Polyamine biosynthetic activity in normal and neoplastic human colorectal tissues. Cancer 1987; 60:1275–81.
6. Bachrach U, Wang YC, Tabib A. Polyamines: new cues in cellular signal transduction. News Physiol Sci 2001;16:106–9.
7. Wallace HM, Caslake R. Polyamines and colon cancer. Eur J Gastroenterol Hepatol 2001;13:1033–9.
8. Seiler N. Thirty years of polyamine-related approaches to cancer therapy. Retrospect and prospect. Part 1. Selective enzyme inhibitors. Curr Drug Targets 2003;4: 537–64.
9. Thomas T, Thomas TJ. Polyamine metabolism and cancer. J Cell Mol Med 2003;7:113–26.
10. Babbar N, Ignatenko NA, Casero RA Jr, Gerner EW. Cyclooxygenase-independent induction of apoptosis by sulindac sulfone is mediated by polyamines in colon cancer. J Biol Chem 2003;278:47762–75.
11. Fogel-Petrovic M, Shappell NW, Bergeron RJ, Porter CW. Polyamine and polyamine analog regulation of spermidine/spermine N^1-acetyltransferase in MALME-3M human melanoma cells. J Biol Chem 1993;268: 19118–25.
12. Vujcic S, Halmekyto M, Diegelman P, et al. Effects ofconditional overexpression of spermidine/spermine N^1-acetyltransferase on polyamine pool dynamics, cell growth, and sensitivity to polyamine analogs. J Biol Chem 2000;275:38319–28.
13. Kee K, Vujcic S, Merali S, et al. Metabolic and antiproliferative consequences of activated polyamine catabolism in LNCaP prostate carcinoma cells. J Biol Chem 2004;279:27050–8.
14. Shappell NW, Miller JT, Bergeron RJ, Porter CW. Differential effects of the spermine analog, N^1, N^{12}-bis(ethyl)-spermine, on polyamine metabolism and cell

growth in human melanoma cell lines and melanocytes. Anticancer Res 1992;12:1083–9.
15. Casero RA Jr, Celano P, Ervin SJ, Porter CW, Bergeron RJ, Libby PR. Differential induction of spermidine/spermine N^1-acetyltransferase in human lung cancer cells by the bis(ethyl)polyamine analogues. Cancer Res 1989;49:3829–33.
16. Ha HC, Woster PM, Yager JD, Casero RA Jr. The role of polyamine catabolism in polyamine analogue-induced programmed cell death. Proc Natl Acad Sci U S A 1997;94:11557–62.
17. Chen Y, Kramer DL, Jell J, Vujcic S, Porter CW. Small interfering RNA suppression of polyamine analog-induced spermidine/spermine N^1-acetyltransferase. Mol Pharmacol 2003;64:1153–9.
18. Greenberg NM, DeMayo F, Finegold MJ, et al. Prostate cancer in a transgenic mouse. Proc Natl Acad Sci U S A 1995;92:3439–43.
19. Kee K, Foster BA, Merali S, et al. Activated polyamine catabolism depletes acetyl-CoA pools and suppresses prostate tumor growth in TRAMP mice. J Biol Chem 2004;279:40076–83.
20. Su LK, Kinzler KW, Vogelstein B, et al. Multiple intestinal neoplasia caused by a mutation in the murine homolog of the APC gene. Science 1992;256:668–70.
21. Moser AR, Pitot HC, Dove WF. A dominant mutation that predisposes to multiple intestinal neoplasia in the mouse. Science 1990;247:322–4.
22. Fodde R, Smits R, Clevers H. APC, signal transduction and genetic instability in colorectal cancer. Nat Rev Cancer 2001;1:55–67.
23. Luongo C, Moser AR, Gledhill S, Dove WF. Loss of Apc+ in intestinal adenomas from Min mice. Cancer Res 1994;54:5947–52.
24. He TC, Sparks AB, Rago C, et al. Identification of c-MYC as a target of the APC pathway. Science 1998;281:1509–12.
25. Bello-Fernandez C, Packham G, Cleveland JL. The ornithine decarboxylase gene is a transcriptional target of c-Myc. Proc Natl Acad Sci U S A 1993;90:7804–8.
26. Erdman SH, Ignatenko NA, Powell MB, et al. APC-dependent changes in expression of genes influencing polyamine metabolism, and consequences for gastrointestinal carcinogenesis, in the Min mouse. Carcinogenesis 1999;20:1709–13.
27. Jacoby RF, Cole CE, Tutsch K, et al. Chemopreventive efficacy of combined piroxicam and difluoromethylornithine treatment of Apc mutant Min mouse adenomas, and selective toxicity against Apc mutant embryos. Cancer Res 2000;60:1864–70.
28. Pietila M, Alhonen L, Halmekyto M, Kanter P, Janne J, Porter CW. Activation of polyamine catabolism profoundly alters tissue polyamine pools and affects hair growth and female fertility in transgenic mice overexpressing spermidine/spermine N^1-acetyltransferase. J Biol Chem 1997;272:18746–51.
29. Niiranen K, Pietila M, Pirttila TJ, et al. Targeted disruption of spermidine/spermine N^1-acetyltransferase gene in mouse embryonic stem cells. Effects on polyamine homeostasis and sensitivity to polyamine analogues. J Biol Chem 2002;277:25323–8.
30. Tucker JM, Davis C, Kitchens ME, et al. Response to 5-fluorouracil chemotherapy is modified by dietary folic acid deficiency in Apc(Min/+) mice. Cancer Lett 2002;187:153–62.
31. Bernacki RJ, Oberman EJ, Seweryniak KE, Atwood A, Bergeron RJ, Porter CW. Preclinical antitumor efficacy of the polyamine analogue N^1,N^{11}-diethylnorspermine administered by multiple injection or continuous infusion. Clin Cancer Res 1995;1:847–57.
32. Kramer D, Mett H, Evans A, Regenass U, Diegelman P, Porter CW. Stable amplification of the *S*-adenosylmethionine decarboxylase gene in Chinese hamster ovary cells. J Biol Chem 1995;270:2124–32.
33. Yamada Y, Hata K, Hirose Y, et al. Microadenomatous lesions involving loss of Apc heterozygosity in the colon of adult Apc(Min/+) mice. Cancer Res 2002;62:6367–70.
34. Oshima M, Oshima H, Kitagawa K, Kobayashi M, Itakura C, Taketo M. Loss of Apc heterozygosity and abnormal tissue building in nascent intestinal polyps in mice carrying a truncated Apc gene. Proc Natl Acad Sci U S A 1995;92:4482–6.
35. Porter CW, Ganis B, Libby PR, Bergeron RJ. Correlations between polyamine analogue-induced increases in spermidine/spermine N^1-acetyltransferase activity, polyamine pool depletion, and growth inhibition in human melanoma cell lines. Cancer Res 1991;51:3715–20.
36. Levy DB, Smith KJ, Beazer-Barclay Y, Hamilton SR, Vogelstein B, Kinzler KW. Inactivation of both APC alleles in human and mouse tumors. Cancer Res 1994;54:5953–8.
37. Pietila M, Parkkinen JJ, Alhonen L, Janne J. Relation of skin polyamines to the hairless phenotype in transgenic mice overexpressing spermidine/spermine *N*-acetyltransferase. J Invest Dermatol 2001;116:801–5.
38. Wallace HM, Duthie J, Evans DM, Lamond S, Nicoll KM, Heys SD. Alterations in polyamine catabolic enzymes in human breast cancer tissue. Clin Cancer Res 2000;6:3657–61.
39. Clarke PA, George ML, Easdale S, et al. Molecular pharmacology of cancer therapy in human colorectal cancer by gene expression profiling. Cancer Res 2003;63:6855–63.
40. Wolter F, Turchanowa L, Stein J. Resveratrol-induced modification of polyamine metabolism is accompanied by induction of c-*Fos*. Carcinogenesis 2003;24:469–74.
41. Coleman CS, Pegg AE, Megosh LC, Guo Y, Sawicki JA, O'Brien TG. Targeted expression of spermidine/spermine N^1-acetyltransferase increases susceptibility to chemically induced skin carcinogenesis. Carcinogenesis 2002;23:359–64.
42. Halmekyto M, Alhonen L, Wahlfors J, Sinervirta R, Eloranta T, Janne J. Characterization of a transgenic mouse line over-expressing the human ornithine decarboxylase gene. Biochem J 1991;278:895–8.
43. Sieber OM, Howarth KM, Thirlwell C, et al. Myh deficiency enhances intestinal tumorigenesis in multiple intestinal neoplasia (ApcMin/+) mice. Cancer Res 2004;64:8876–81.
44. Shoemaker AR, Haigis KM, Baker SM, Dudley S, Liskay RM, Dove WF. Mlh1 deficiency enhances several phenotypes of Apc(Min)/+ mice. Oncogene 2000;19:2774–9.
45. Reitmair AH, Cai JC, Bjerknes M, et al. MSH2 deficiency contributes to accelerated APC-mediated intestinal tumorigenesis. Cancer Res 1996;56:2922–6.
46. Wong E, Yang K, Kuraguchi M, et al. Mbd4 inactivation increases C→T transition mutations and promotes gastrointestinal tumor formation. Proc Natl Acad Sci U S A 2002;99:14937–42.
47. Wasan HS, Novelli M, Bee J, Bodmer WF. Dietary fat influences on polyp phenotype in multiple intestinal neoplasia mice. Proc Natl Acad Sci U S A 1997;94:3308–13.
48. Eads CA, Nickel AE, Laird PW. Complete genetic suppression of polyp formation and reduction of CpG-island hypermethylation in Apc(Min/+) Dnmt1-hypomorphic Mice. Cancer Res 2002;62:1296–9.
49. Bhowmick NA, Neilson EG, Moses HL. Stromal fibroblasts in cancer initiation and progression. Nature 2004;432:332–7.
50. Ignatenko NA, Babbar N, Mehta D, Casero RA Jr, Gerner EW. Suppression of polyamine catabolism by activated Ki-ras in human colon cancer cells. Mol Carcinog 2004;39:91–102.